

**School of Chemistry Department of Inorganic and
Materials Chemistry**

**“Synthesis of Random and Block copolymers from terpene-
based and acrylate-based monomers”**

Beth Jordan Student ID: 14306758

Supervisors - Prof. Steve Howdle and Dr Vincenzo Taresco

Nottingham, 2021

Contents

I. Abstract	5
II. Acknowledgements	6
III. Declaration	7
IV. List of Abbreviations	8
V. List of figures	10
VI. List of tables	11
V.II List of Schemes	12
V.III COVID impact statement	13
1. Introduction	14
1.1 Polymers	14
1.2 Polymer structures	14
1.3 Methods of polymer synthesis.....	17
1.3.2 Living polymerisation techniques	19
1.3.3 RAFT polymerisation.....	20
1.4 Terpenes	22
1.5 Polymerisation Techniques.....	24
1.5.1 Heterogeneous Polymerisation	24
1.5.2 Homogeneous Polymerisation	25
1.6 Solvents for Polymerisation	25
1.6.1 Green Solvent Alternatives	26
1.7 Project Aims.....	27
2. Experimental.....	29
2.1 Materials.....	29
2.2 Polymer Analysis	29
2.2.1 Nuclear Magnetic Resonance Spectroscopy	29
2.2.2 Gel Permeation Chromatography.....	29
2.2.3 Differential Scanning Calorimetry.....	30
2.2.4 Dynamic mechanical analysis	30
2.3 Reactivity Ratio Calculations	31
2.4 Synthesis of tetrahydro-geraniol acrylate	32
2.5 Solution Polymerisations in toluene	33
2.5.1 Homopolymer synthesis of PMMA	33
2.5.2 Homopolymer synthesis of PTHGA.....	33
2.5.4 Random copolymer synthesis	34
2.5.6 Block copolymer synthesis	35
2.6. RAFT agents in 2-MeTHF	35

2.6.1 RAFT Agent Screening	35
2.6.2 UV/Vis analysis of RAFT agent solubility	36
2.6.3 RAFT Agents Screening	36
2.7 Solution Polymerisations in 2-MeTHF	36
2.7.1 High T _g Homopolymer Synthesis	36
2.7.2 THGA homopolymerisation in 2-MeTHF	37
2.7.3 Random copolymer synthesis	38
2.7.4 Synthesis of block copolymers	38
2.8.2 Reactivity ratio of THGA and IBMA	39
2.8.3 Reactivity ratio of THGA and α -pinene methacrylate	39
3. Results and Discussion	41
3.1 Synthesis of THGA	41
3.2 RAFT agent screening in Toluene	42
3.2.1 MMA homopolymers	42
3.2.2 THGA homopolymers	44
3.3 Random copolymer analysis	46
3.4 Reactivity Ratios of THGA and MMA in toluene	47
3.5 Block copolymer analysis	50
3.7 RAFT agent screening in 2-MeTHF	52
3.7.1 Initial screening	52
3.7.2 Investigation of Solubility of RAFT agents	54
3.7.3 Identifying the most important RAFT agent group	55
3.8 Homopolymerisation in 2-MeTHF	56
3.8.1 High T _g Homopolymers in 2-MeTHF	56
3.8.2 Homopolymerisation of THGA in 2-MeTHF	60
3.9 Random copolymers of High T _g monomers with butyl acrylate in 2-MeTHF	60
3.10 Block copolymers of High T _g monomers with butyl acrylate in 2-MeTHF	61
3.11 Fully terpene random copolymers in 2-MeTHF	63
3.12 The reactivity ratios of IBMA and THGA in 2-MeTHF	63
3.13 The reactivity ratios of α -PM and THGA in 2-MeTHF	65
3.14 Fully terpene block copolymers in 2-MeTHF	66
4. Conclusion	68
5. Future work	69
6. References	71
7. Appendix	77
7.1 NMR of THGA	77
7.2 NMR of PMMA	77

7.3 NMR of PTHGA	77
7.4 NMR of PMMA-<i>ran</i>-PTHGA.....	77
7.5 NMR of PIBMA	77
7.6 NMR of Pα-PM.....	77

I. Abstract

Due to the ever-growing need to reduce global carbon emissions, the need to replace traditionally petrochemically derived plastics has been growing exponentially. To solve this issue, research has been carried out on plant-based alternatives such as terpenes and terpenoids. Terpenes are a type of natural hydrocarbon which contains a carbon-carbon double bond which can be exploited for polymerisations. Many polymerisation reactions are also carried out in toxic and petrochemical based solvents, in order to reduce the environmental impact of these reactions, bio-based solvents have become a viable alternative.

This report describes the synthesis of terpene-based homopolymers and diblock copolymers using reversible addition-fragmentation chain-transfer (RAFT) polymerisation techniques in toluene and 2-MeTHF. These particular solvents were used as toluene is commonly used in solution polymerisations and 2-MeTHF is a bio-based alternative solvent. Control of polymerisation will be evaluated by altering the RAFT agent's structure. The synthesis of bioderived tetrahydrogeraniol acrylate (THGA) monomer is reported, with its use as a precursor to diblock and random copolymers with methyl methacrylate (MMA). The reactivity ratio of the random copolymer of MMA and THGA was investigated. In further reactions we investigated replacing MMA with other terpene-based monomers. Two different monomers were tested, isobornyl methacrylate and alpha-pinene methacrylate. Initially we tested these monomers with butyl acrylate to form random and diblock copolymers, before creating random and diblock copolymers with THGA. The reactivity ratios of both random copolymers with THGA were investigated.

I. Acknowledgements

Firstly, I would like to thank my supervisors, Professor Steve Howdle and Dr Vincenzo Taresco for giving me the opportunity to work within the research group and for their continued guidance and support throughout the year, both on an academic and personal level.

I would like to thank everyone in the B10 and B10a lab for making the time spent in the lab so enjoyable; I wish them all well in their future pursuits.

I would like to thank my family for supporting me throughout my university experience. You are always there for me when I need you. I would also like to thank my dog, although she cannot read. Thank you to my friends for the support, advice and believing in me when at times I did not believe in myself.

Finally, I would especially like to thank my day-to-day project demonstrators, Ana Pacheco, and Professor Fabricio Machado, for the enormous amount support, guidance, and patience throughout the year. This work would not have been possible without them, and I am grateful for all the knowledge they have passed on to me. I wish them both well in the future.

II. Declaration

I declare that the thesis is the result of my own work which has been mainly undertaken during my period of registration for this degree at The University of Nottingham. I have complied with the word limit for my degree.

Beth Amy Jordan

III. List of Abbreviations

α -PM alpha pinene methacrylate

AIBN 2,2-azobis(isobutyronitrile).

ATRP atom transfer radical polymerisation.

BA butyl acrylate

Cv coefficient of variance.

CPAB 4-Cyano-4-(phenylcarbonothioylthio)pentanoic acid

CPAD 4-cyano-4-[dodecylsulfanylthiocarbonylsulfyl] pentatonic acid

CPBD 4-cyano-2-propylbenzodithioate

CPDT 2-cyano-2-propyl dodecyl trithiocarbonate.

CRP conventional radical polymerisation

DCM dichloromethane.

DDMAT 2-(dodecylthiocarbonothioylthio)-2-methylpropanoic acid.

DP degree of polymerisation.

dRI differential refractive index.

DSC differential scanning calorimetry. **GPC** gel permeation chromatography. **IBMA** isobornyl methacrylate.

LAM least activated monomer

MAM most activated monomer.

Mn number averaged molecular weight.

Mw weight averaged molecular weight.

NMP nitroxide mediated living radical polymerisation.

NMR nuclear magnetic resonance.

P α PM poly(alpha-pinene methacrylate) **PTHGA** poly(tetrahydrogeraniol acrylate) **PIBMA** poly(isobornyl methacrylate).

PMMA poly(methyl methacrylate).

RAFT reversible addition-fragmentation chain-transfer.

RBF round-bottom flask.

SEC size exclusion chromatography.

T_g glass transition temperature.

T_m melting temperature.

THG tetrahydrogeraniol.

THGA tetrahydrogeraniol acrylate.

UV ultraviolet.

IV. List of figures

Introduction

Figure 1.1	The general molecular structure of a polymer	14
Figure 1.2	The four main types of copolymers: A) Random copolymer, B) Alternating copolymer, C) Block copolymer and D) Graft copolymer.	15
Figure 1.3	Schematic showing how molecular weight is affected by conversion for (a) step-growth polymerisation, (b) chain growth polymerisation, (c) living polymerisation	16
Figure 1.4	The general structure of a RAFT agent with a stabilising group (Z) and a leaving group (R).	19
Figure 1.5	the structure of a random copolymer consisting of 4-bromophenyl vinyl sulphide (BPVS) and N- vinylcarbazole (NVC).	22
Figure 1.6	The triblock copolymer structure of poly(styrene)- <i>b</i> -poly(isobutylene)- <i>b</i> -poly(styrene)	22
Figure 1.7	The structures of the terpenes that will be discussed in this document (A) alpha-pinene, (B) beta-pinene, (C) isobornyl methacrylate, (D) tetrahydro-geraniol.	23
Figure 1.8	The structures of tetrahydrogeraniol acrylate, butyl acrylate, ethyl acrylate, and 2-ethylhexyl acrylate.	24
Figure 1.9	Total and CO ₂ life cycle emission for 2-MeTHF (ecoMeTHF), THF, DCM, ethyl tert-butyl ether (ETBE), and a generic solvent (classical organic solvent).	28

Experimental

Figure 2.1	The labelled structure of THGA.	32
------------	---------------------------------	----

Results and Discussion

Figure 3.1	The three different RAFT agents used, (A) 2-(Dodecylthiocarbonothioylthio)-2-methylpropanoic acid(DDMAT), (B) 2-cyano-2-propyl dodecyl trithiocarbonate (CPDT), (C) 4-cyano-4-(phenylcarbonothioylthio) pentanoic acid (CPAB).	41
Figure 3.2	¹ H NMR of PMMA with (400 MHz, CDCl ₃), δ (ppm):	42
Figure 3.3	¹ H NMR of THGA (400 MHz, CDCl ₃).	43
Figure 3.4	¹ H NMR of PTHGA (400 MHz, CDCl ₃)	45
Figure 3.5	The ¹ H NMR of the 1:1 molar ratio PMMA- <i>ran</i> -PTHGA. (400 MHz, CDCl ₃)	46
Figure 3.6	The reactivity ratios of MMA and THGA. MMA is monomer 1 for this reactivity ratio. The blue circles indicate the experimental data collected and the red line shows the copolymer composition trend.	48
Figure 3.7	The difference between the structures of block, gradient, and random copolymers	49
Figure 3.8	The R ² value of the reactivity ratio model for MMA and THGA. The blue points are the Mayo-Lewis model prediction (predicted values) against the experimental data (observed values). The red line corresponds to the linear regression prediction. The blue dashed lines indicate the regression bands built with a 95% confidence level.	49
Figure 3.9	The GPC chromatogram of the PMMA- <i>b</i> -PTHGA copolymers (A) from BJ23 and (B) from BJ24.	51

Figure 3.10	(A) The DSC of PMMA- <i>b</i> -PTHGA from expt. BJ23, (B) The DSC of PMMA- <i>b</i> -PTHGA from expt. BJ24 identifying the two separate T_g s of the block copolymers.	52
Figure 3.11	the chromatograms from the GPC of (A) the polymerisation of MMA in 2-MeTHF with CPDT as the RAFT agent and (B) the polymerisation of MMA in 2-MeTHF with CPAB as the RAFT agent.	54
Figure 3.12	The structures of the RAFT agents (A) 4-cyano-4-[dodecylsulfanylthiocarbonylsulfyl] pentatonic acid (CPAD) and (B) 4-cyano-2-propyl benzodithioate (CPBD).	55
Figure 3.13	^1H NMR of PIBMA (400 MHz, CDCl_3)	57
Figure 3.14	^1H NMR of Pa-PM (400 MHz, CDCl_3)	58
Figure 3.15	The DMA of (A) PMMA, (B) PIBMA and (C) Pa-PM .	59
Figure 3.16	the labelled ^1H NMR of $\text{Pa-PM-}b\text{-PBA}$ (400 MHz, CDCl_3)	62
Figure 3.17	The reactivity ratio of IBMA and THGA	64
Figure 3.18	The reactivity ratio of $\alpha\text{-PM}$ and THGA. The blue circles indicate the experimental data collected and the red line shows the copolymer composition trend.	65
Figure 3.19	The R^2 values calculated for the reactivity ratios of $\alpha\text{-PM}$ and THGA. The blue points are the Mayo-Lewis model prediction (predicted values) against the experimental data (observed values). The red line corresponds to the linear regression prediction. The blue dashed lines indicate the regression bands built with a 95% confidence level	66
Figure 3.20	The GPC chromatograms for (A) PIMBA and PIMBA- <i>b</i> -PTHGA and (B) Pa-PM and $\text{Pa-PM-}b\text{-PTHGA}$ showing the increase in M_n for the block copolymers indicating the THGA has been successfully added.	67

V. List of tables

Experimental

Table 2.1	Reaction conditions of RAFT solution polymerisations of poly(methyl methacrylate). All reactions were carried out in toluene using 4.99g of monomer.	33
Table 2.2	Reaction conditions of RAFT solution polymerisations of poly(methyl methacrylate). All reactions were carried out in toluene using 1g of monomer	34
Table 2.3	Reaction conditions of RAFT solution random copolymerisation of methyl methacrylate and tetrahydro geraniol acrylate. All reactions were carried out in toluene	34
Table 2.4	Reaction conditions of RAFT polymerisation of methyl methacrylate and tetrahydro-geraniol acrylate to calculate the reactivity ratio of the two monomers.	35
Table 2.5	The molar amounts of PMMA, THGA and AIBN required for the block copolymerisation reactions to achieve the targeted PTHGA molecular weight.	35
Table 2.6	The different compositions of polymerisation solutions required to screen two RAFT agents in three different solvents.	35
Table 2.7	The different solutions required to test the solubility of the RAFT agent in two solvents	36
Table 2.8	The molar amounts of MMA, AIBN and RAFT used to investigate the polymerisation of MMA in 2- MeTHF using two different RAFT agents	36
Table 2.9	The molar amounts of the monomers, RAFT, and AIBN used to homopolymerisation of three different monomers	37
Table 2.10	The molar amounts of monomer, AIBN and RAFT used to produce random copolymers.	38
Table 2.11	The molar amounts of polymer, monomer and AIBN used to produce diblock copolymers.	38
Table 2.12	The molar amounts of monomers, RAFT and AIBN used to produce random copolymers	39
Table 2.13	Reaction conditions of RAFT polymerisation of isobornyl methacrylate and tetrahydro-geraniol acrylate to calculate the reactivity ratio of the two monomers.	39
Table 2.14	Reaction conditions of RAFT polymerisation of alpha-pinene methacrylate and tetrahydro-geraniol acrylate to calculate the reactivity ratio of the two monomers.	39
Table 2.15	The molar amounts of polymer, monomer, and AIBN used to produce fully-terpene based block copolymers.	40

Results and Discussion

Table 3.1	Results for the MMA homopolymerisation in toluene performed with three different RAFT agents	41
Table 3.2	The T_g of PMMA polymerised by three different RAFT agents	42
Table 3.3	Results of the homopolymerisation of THGA using three different types of RAFT agents.	44
Table 3.4	T_g of the homopolymers of PTHGA	45
Table 3.5	Results obtained for the random copolymers of PMMA- <i>ran</i> -PTHGA	46
Table 3.6	T_g values obtained via DSC for copolymers of PMMA- <i>ran</i> -PTHGA.	47

Table 3.7	Monomer compositions and polymer compositions of the random copolymers of MMA and THGA used for the reactivity ratio calculations	47
Table 3.8	The result of PMMA- <i>b</i> -PTHGA copolymers aiming at two different chain lengths of THGA	50
Table 3.9	The results from the RAFT screening using, two different RAFT agents and three solvents.	53
Table 3.10	The results of the UV at 350 nm for CPDT and 370 nm for CPAB	54
Table 3.11	The results of the polymerisation of MMA using two different RAFT agents, CPAD and CPBD.	55
Table 3.12	The results of the high T_g homopolymers	56
Table 3.13	T_g values for PMMA, PIBMA and P α -PM	58
Table 3.14	The conversion, actual target molecular weight and the target molecular weight and dispersity of copolymerisation of butyl acrylate with high T_g monomers in 2-MeTHF	60
Table 3.15	The DSC results for the random copolymers.	61
Table 3.16	The results of the block copolymers of a high T_g monomer with BA.	61
Table 3.17	The T_g of PMMA- <i>b</i> -PBA, PIBMA- <i>b</i> -PBA and P α -PM- <i>b</i> -PBA	62
Table 3.18	The results of the fully terpene-based random copolymers	63
Table 3.19	The results from the DSC of the fully-terpene based random copolymers.	63
Table 3.20	Monomer compositions and polymer compositions of the random copolymers of IBMA and THGA used for the reactivity ratio calculations	64
Table 3.21	Monomer compositions and polymer compositions of the random copolymers of α -PM and THGA used for the reactivity ratio calculations	65
Table 3.22	The results from the ^1H NMR and GPC of the fully-terpene block copolymers.	66
Table 3.23	The results from the DSC of the fully-terpene based block copolymers.	68

V.II List of Schemes

Introduction

Scheme 1.	The stages of CRP 1) initiation, 2) propagation, 3) chain transfer, 4) termination <i>via</i> a) disproportionation and b) combination	18
Scheme 2.	Proposed mechanism of reversible addition-fragmentation chain transfer (RAFT) polymerisation	20
Scheme 3.	General synthetic routes to monomers derived from renewable resources	24
Scheme 4.	shows geraniol hydrogenated to tetrahydro geraniol and then acrylated to tetrahydrogeraniol acrylate.	25
Scheme 5.	The manufacture of 2-MeTHF from Levulinic acid <i>via</i> two pathways.	27

Experimental

Scheme 6.	Generic schematic showing the synthesis of tetrahydrogeraniol acrylate from tetrahydrogeraniol.	32
Scheme 7.	The general scheme for the homopolymerisation of MMA	33
Scheme 8.	The general scheme for the homopolymerisation of THGA	33
Scheme 9.	The general scheme for the production of PMMA- <i>ran</i> -PTHGA.	34
Scheme 10.	The generic scheme for the homopolymerisation of isobornyl methacrylate	37
Scheme 11.	The generic scheme for the homopolymerisation of alpha-pinene methacrylate	37

III. COVID impact statement

As a result of the Covid-19 pandemic, I started in the lab later than planned, in November 2020 instead of September 2020, when I initially received a lab induction. The time available to me in the lab has been reduced in comparison to pre-Covid times because of an enforced maximum capacity of 8 people, significantly lower than the number of people needing to access the lab, and therefore impacting the amount of lab work I was able to complete.

In particular, the access to key facilities including NMR has been reduced, with a limited number of NMR runs per day, the focus of the project also shifted due to limited training opportunities on certain pieces of equipment, therefore starting to work on my final project in late January 2021.

1. Introduction

1.1 Polymers

A polymer is defined as a material consisting of large molecules or macromolecules. Polymers are made up of multiple repeating units known as monomers, joined by covalent bonds. For example, X is a monomer molecule, -X- is the repeat unit, and n is the number of repetitive units along the polymer chain also named as degree of polymerisation (DP), then the molecular structure of the polymer is represented by:

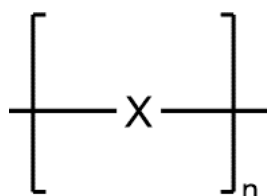


Figure 1.1 The general molecular structure of a polymer

Polymers are present in nature (*e.g.*, cellulose, starch, and natural rubber) in the form of different types of natural products (*e.g.*, wood, crustaceous shells, resins, etc.). Synthetic polymeric materials have been studied since the middle of the nineteenth century and today, the polymer industry has rapidly developed and is larger than the copper, steel, aluminium, and some other industries combined.¹ Both natural and synthetic polymers are remarkably involved in the comfort and facilitation of human life and are responsible for life itself, for medication,² nutrition, communication, transportation, irrigation, containers, and clothing. Synthetic and natural polymers can be used in the form of inorganic and organic polymers; coatings, elastomers, adhesives, blends, plastics, fibres, caulks, ceramics, and composites.³

1.2 Polymer structures

A homopolymer is a chain of one type of monomer chemically linked, whereas a copolymer can be chemically built of two or more types of monomer forming the same polymer chain. Copolymers are of four types: alternating, random (or statistic), block, and graft copolymers. The structures of these types of copolymers are shown in Figure 1.2. The copolymerisation term denotes the chemical process by which copolymers are synthesized.⁴

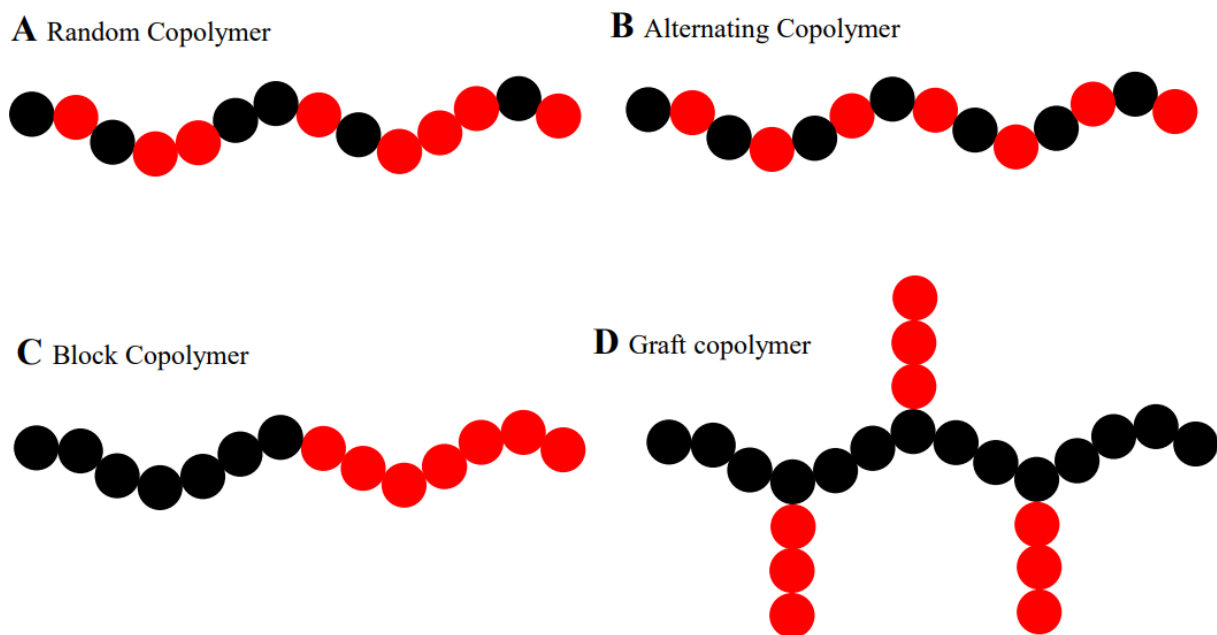


Figure 1.2 The four main types of copolymers: **A)** Random copolymer, **B)** Alternating copolymer, **C)** Block copolymer and **D)** Graft copolymer.

Alternating copolymers consist of two types of monomer in alternating arrangement; random copolymers have monomer units arranged randomly in the polymer. Block copolymers have blocks of one type of monomer linked with blocks of other monomers, diblock copolymers have two subunits whilst a triblock copolymer is made up of three different subunits. Graft copolymers are made of polymer chains of one type of monomer grafted onto another polymer chain of a different monomer.⁵

1.3 Methods of polymer synthesis

Polymerisations can be characterised by the mechanism that the polymer chain grows by. There are two main types of polymerisations: chain growth and step growth:

- In chain growth polymerisations, vinyl monomers are sequentially linked together *via* activation of the double bond using ions, radical attack, or by co-ordination with a metal complex.⁶
- Step growth polymerisation refers to a type of polymerisation mechanism in which bi-functional or multifunctional monomers react to form first dimers, then trimers, longer oligomers, and eventually long chain polymers. Due to the nature of the polymerisation mechanism, a high conversion of the reaction is required to achieve high molecular weight.⁷

Living polymerisation is characterised as a type of chain growth polymerisation. In an ideal case, there are mechanistically only two steps, initiation and propagation in a living polymerisation. Initiation is followed by propagation if the monomer is present in the polymerisation system, and addition of a new monomer (or a second monomer) leads to further propagation. There are no chain breaking reactions, such as termination or chain transfer, and after consumption of the initiating species, only propagation occurs.⁸ This is desirable because it offers precision and control in macromolecular synthesis.⁹ This is important since many of the novel or useful properties of polymers result from their microstructure and molecular weight. Advantages of this method also include predetermined molecular weight, control over end-groups and narrow dispersity (\bar{D}).¹⁰ Due to molecular weight and dispersity being less controlled in non-living polymerisations, living polymerisation is desirable for materials design. In addition, living polymerisation is a popular method for synthesising a specific type of block copolymer since the polymer can be synthesized in stages, each stage containing a different monomer sequence with a specific molecular weight target. The molecular weight of the polymer is affected by the increasing conversion of the polymerisation, this is shown by Figure 1.3.

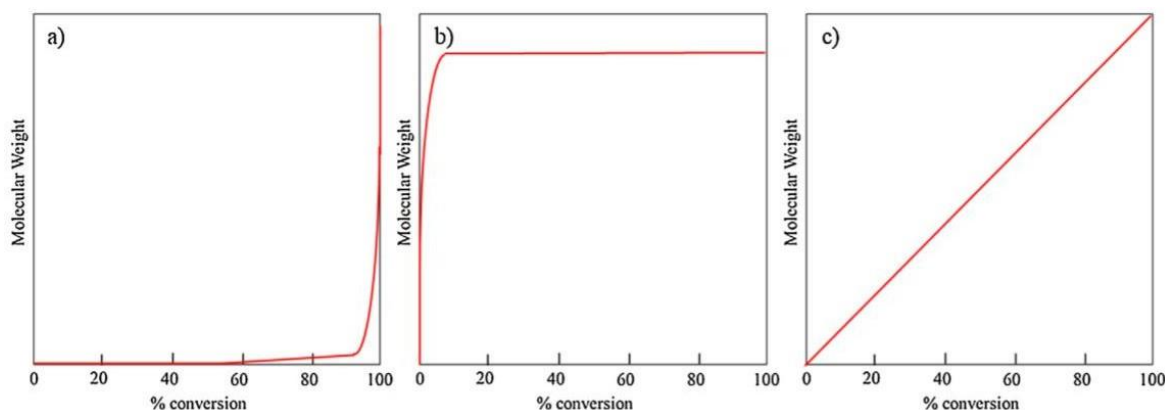


Figure 1.3 Schematic showing how molecular weight is affected by conversion for (a) step-growth polymerisation, (b) chain growth polymerisation, (c) living polymerisation.¹¹

1.3.1 Polymer Molecular Weight

Polymer average molecular weight arises from a molecular weight distribution rather than a specific number because polymerisations produce a variety of different chain lengths.¹² Weight-average molecular weight (M_w) and number-average molecular weight (M_n) are two ways we can characterise the polymer molecular weight. Polymer M_w is defined by Equation 1.

$$M_w = \sum_{i=1}^N \omega_i M W_i \quad (1)$$

Here, ω_i is the weight fraction of polymer chains having a molecular weight of $M W_i$. The absolute M_w is typically measured by light scattering experiments. When light passes through a liquid polymer-solvent solution, it is scattered by the individual polymer molecules suspended in the solution. The degree of scattering arises from the molecule size and, thus, molecular weight distribution can be mathematically resolved from

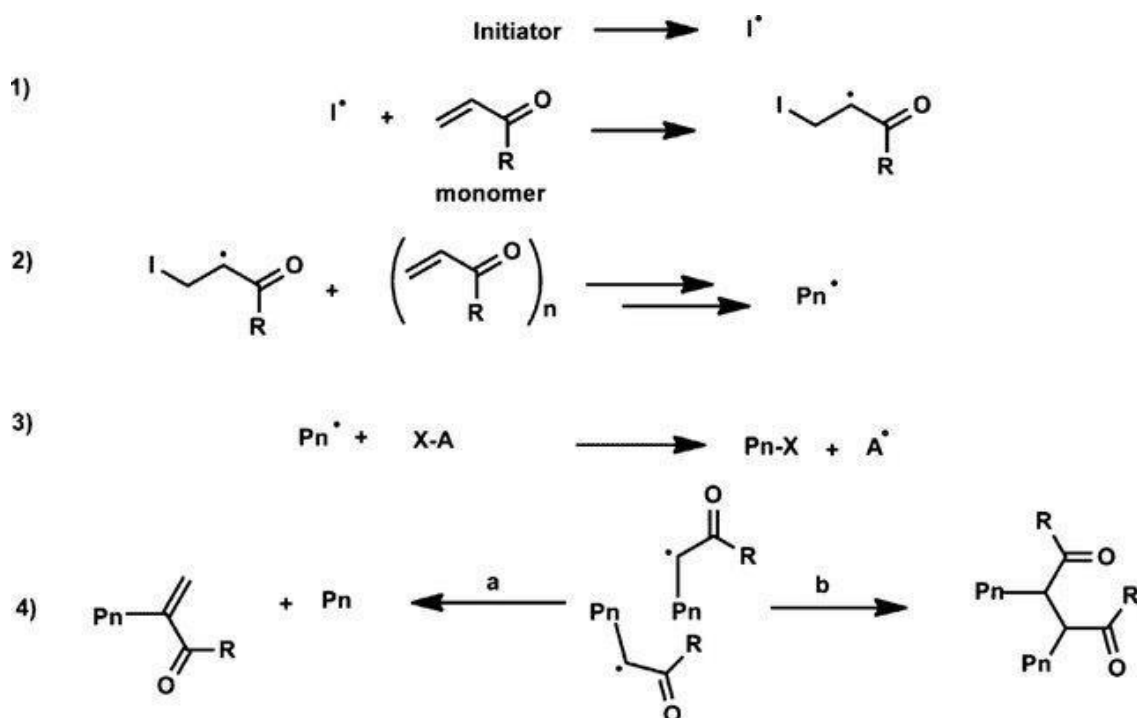
the total scattering created by the sample.¹² M_n is an average based on the number of polymer chains in a sample and is defined as follows (equation 2).

$$M_n = \sum_{i=1}^N X_i MW_i \quad (2)$$

In Equation 4, MW_i refers to the molecular weight of each individual polymer chain and X_i refers to the mole fraction of each chain length included in the summation. This number average means that each chain, regardless of its molecular weight, contributes equally to the reported M_n . Dispersity (\bar{D}) can be calculated by the ratio of M_w to M_n . \bar{D} has a value equal to or greater than 1, but as the polymer chains approach uniform chainlength, \bar{D} approaches unity (1).¹³ A successful living polymerisation has a \bar{D} of 1.02–1.10. Step-growth polymerisation reactions typically yield \bar{D} value of around 2.0 and chain-growth polymerisation yield \bar{D} values in the range of 1.5–20, depending on the chain-breaking reactions and/or the nature of the propagating reactive centers.¹⁴

1.3.2 Conventional Radical Polymerisation

Conventional radical polymerisation (CRP), also known as free radical polymerisation, is a method of polymerisation, by which a polymer is formed by the successive addition of free-radical building blocks. Free radicals can be formed by several different mechanisms, usually involving separate initiator molecules. Following its generation, the initiating free radical adds monomer units, thereby growing the polymer chain, thus it is categorised as a type of chain-growth polymerisation.¹⁵ The relatively non-specific nature of conventional radical chemical interactions makes this as one of the most versatile forms of polymerisation available and allows facile reactions of polymeric free-radical chain ends and other chemicals or substrates.¹⁶ The stages of CRP are shown in scheme 1.



Scheme 1. The stages of CRP 1) initiation, 2) propagation, 3) chain transfer, 4) termination *via* a) disproportionation and b) combination.¹⁷

However, this type of polymerisation has many disadvantages, for example, CRP does not allow for complex polymer architectures to be produced, such as block and graft copolymers.¹⁸ Additionally, CRP also has poor control over the final molecular weight of the polymer.¹⁸ The poor control of the molecular weight of the final polymer leads to difficulties in determining the final properties of the polymer.¹⁹ This stimulated research to develop living polymerisation techniques.

1.3.3 Living polymerisation techniques

As a radical polymerisation cannot be a truly living process, due to unavoidable bimolecular termination and chain transfer, this polymerisation technique is known as reversible-deactivation radical polymerisation (RDRP). A successful RDRP has fast and reversible activation/deactivation of propagating chains. There are three types of RDRP: deactivation by catalysed reversible coupling, deactivation by spontaneous reversible coupling and deactivation by degenerative transfer. In any RDRP processes, the radicals can propagate with the propagation rate constant (k_p), by addition of a few monomer units before the deactivation reaction occurs to regenerate the dormant species. k_p is defined as $-d[M]/dt = k_p[M][M^\bullet]$, where $[M]$ is the monomer concentration, $[M^\bullet]$ corresponds to the concentration of monomer terminated radical units, and dt is the change in time. Concurrently, two radicals may react with each other to form dead chains with the termination rate constant (k_t), which is defined as $-d[M^\bullet]/dt = 2k_t[M^\bullet]^2$. The rates of propagation and termination between two radicals are not influenced by the mechanism of deactivation or the catalyst used in the system. Thus, it is possible to estimate how fast a RDRP can be conducted with preserved chain end functionality.

RDRP polymerisation includes techniques such as, atom transfer radical polymerisation (ATRP), nitroxide-mediated polymerisation (NMP), and reversible addition-fragmentation chain transfer (RAFT) polymerisation. RAFT polymerisation has grown in popularity due to its simplicity and that RAFT polymerisation is very tolerant of different functionality in the monomer and solvent, including aqueous solutions.²⁰ This wide range of compatibility provides the ability to synthesise a wide range of narrow polydispersity polymers containing end or side chain functionality in a one-step process without any need for protection or deprotection.²¹ This can be

used to advantage in the synthesis of block polymers and other products of more complex architecture. RAFT polymerisation has also been effectively carried out over a wide temperature range.

1.3.4 RAFT polymerisation

RAFT polymerisation is a type of RDRP, this type of polymerisation can be classed as a 'living' polymerisation despite some termination reactions occurring.²² The molecular weight of the polymer grows linearly with increasing conversion (Fig. 1.5), unlike conventional radical polymerisation. The addition of a suitable RAFT agent to a polymerisation reaction allows a greater amount of control over the molecular weight and the dispersion of the chain lengths (\bar{D}). RAFT agents are thiocarbonylthio based compounds (Fig. 1.6) which comprises of a stabilising group (Z) and a leaving group (R).²

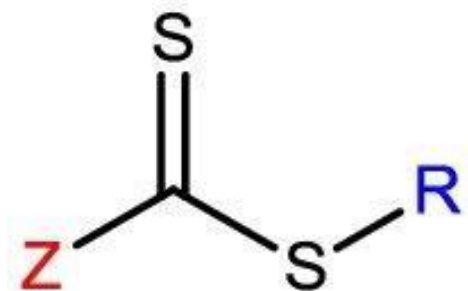
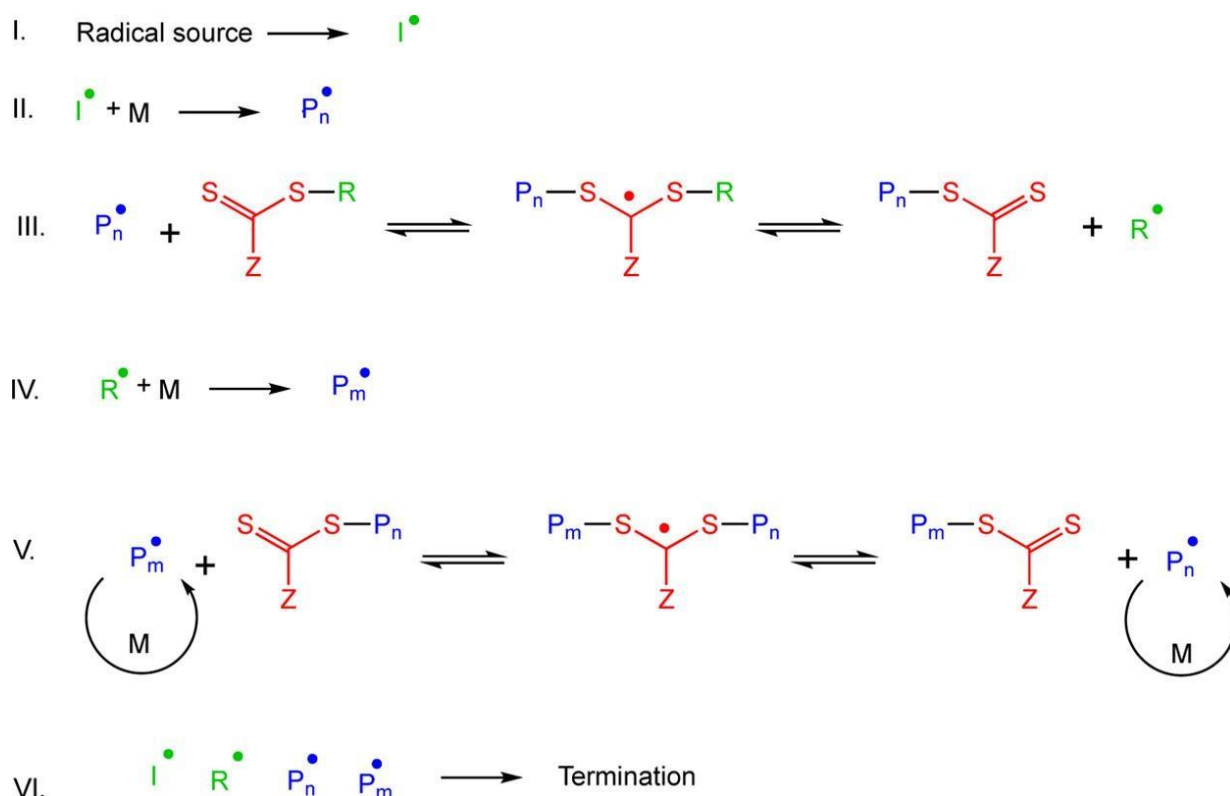


Figure 1.4 The general structure of a RAFT agent with a stabilising group (Z) and a leaving group (R).²

The propagating polymer, P_n^\bullet , initiated by primary radicals, generated from the thermal decomposition of AIBN, interacts with the monomer (M) (II) as shown in scheme 2. The propagation polymer P_n^\bullet reacts with the RAFT agent, attaching the RAFT agent to the growing polymer chain (III), forming an intermediate species (dormant dithioester species).²³ The R group fragments out and is now a radical species that can grow a second polymer chain, P_m^\bullet (IV) and a RAFT agent. This new chain P_m^\bullet is then captured by the RAFT agent (V), which leads to the main equilibrium step, established between the addition and fragmentation of propagating polymer chains (P_m^\bullet and P_n^\bullet) from the RAFT intermediate. As the capture of the chain by the dithioester group is fast and reversible, most chains are in the dormant dithioester form at any one time. This is what reduces the probability of a termination event. The exchange of chains on the RAFT agent continues until all monomer is consumed, meaning all chains grow at a similar rate and have narrow dispersities. Some pathways result in a dead chain, such as the bimolecular combination of R^\bullet and P^\bullet (VI), although provided that the RAFT agent efficiency is high enough, these combination reactions usually make an insignificant contribution.²⁴ Most the chains do not terminate in this way and as they carry a terminal RAFT group (Z group), which allows them to be further reacted with another monomer and so being able to create different polymer architectures such as block copolymers.²⁵



Scheme 2. Proposed mechanism of reversible addition-fragmentation chain transfer (RAFT) polymerisation, adapted from S. Perrier.²³

RAFT agents are selectively reactive, therefore only some types of RAFT agents will be effective with aspecific monomer. When choosing a RAFT agent, it is important to consider the reactivity of the C=S bond relative to the C=C bond of the monomer. For the RAFT agent to be an effective chain transfer agent, the C=S bond must be more reactive than the monomer C=C bond. The C=S bond strength can be tuned by varying the Z group and the R group. The Z group is responsible for the reactivity of the RAFT agent, whilst the R group is responsible for the initiation of monomers to form new chains. Two classes of monomers exist, most activated monomers (MAMs) and least activated monomers (LAMs). MAMs, which have the double bond conjugated to an aromatic ring, carbonyl group or nitrile group and form relatively stable radicals due to electronic and steric stabilisation gained from substituent groups. Therefore, the Z group must stabilise the radical intermediate and favour addition at the C=S bond. LAMs contain a double bond adjacent to oxygen, nitrogen, halogen, sulphur lone pairs, or saturated carbons.²³

For RAFT polymerisation, the degree of polymerisation (DP) depends on the ratio of monomer to RAFT rather than monomer to initiator ratio, as it is with CRP. The number average molecular weight of the polymer can be predicted using Equation 3:

$$M_n = \left(X \frac{[\text{Monomer}]}{[\text{RAFT}]} M_{w \text{ Monomer}} \right) + M_{w \text{ RAFT}} \quad (3)$$

Where [Monomer] and [RAFT] are the initial monomer and RAFT agent concentrations, $M_{w \text{ monomer}}$ and $M_{w \text{ RAFT}}$ are the molar masses of monomer and RAFT agent, and X is the monomer conversion.²⁶

In RAFT, the number fraction of living chains at the end of the polymerisation decreases with increasing target DP, because at a given concentration of radical source the number of dead chains is constant independently of other parameters, including targeted DP. The lower the targeted DP (typically calculated from the $[M]_0/[RAFT]_0$); the higher is the concentration of RAFT agent, thus the higher is the absolute number of living chains.²³ Therefore, RAFT is an ideal technique for the synthesis of low molecular weights oligomers of

controlled molecular weights. Control over low molecular weight polymers is an advantage of RAFT over other RDRP systems for which, due to the persistent radical effect, control tends to increase with increasing conversion and thus increasing molecular weight.^{27,28}

1.4 Polymer thermal properties

The glass transition temperature (T_g) is an important property, as it is the temperature at which the polymer changes from a brittle-glassy state to viscous or rubbery state. Materials that have a higher T_g usually exhibit less molecular mobility at a given temperature ($T < T_g$), which correlates with better physical and chemical stability (*i.e.*, such materials are often less prone to chemical degradation and have a lower tendency to crystallize than corresponding polymers with lower T_g values, *e.g.*, where is frequently correlated with moisture $T \approx T_g$). Combining two or more monomers together can affect the properties of the final polymer. Combining two or more monomers with a different T_g in a random or alternating monomer structure, can change the T_g of the resulting copolymer.²⁹ This is caused by the polymer structure being changed. For example, the introduction of monomer units that occupy a larger space reduces the intermolecular forces between the polymer chains, therefore lowering the T_g . The T_g value of the random copolymer can be calculated using several mathematical equations, the most commonly used is the Flory-Fox and the Gordon-Taylor equation.³⁰ The Flory-Fox equation relates the number-average molecular weight, M_n , to, T_g . this is shown by (equation 4).

$$T_g = T_{g,\infty} - \frac{k}{M_n} \quad (4)$$

$T_{g,\infty}$ is the maximum glass transition temperature that can be achieved at a theoretical infinite molecular weight and K is an empirical parameter that is related to the free volume present in the polymer sample. It is this concept of “free volume” that is observed by the Flory-Fox equation.³¹

Free volume in a polymer can be defined as the volume of the total mass, that is not occupied by polymer chains themselves. The higher the amount of free volume that a polymer chain has, the easier it is for the chain to move and achieve different physical conformations. Free volume decreases upon cooling from the rubbery state until the glass transition temperature at which point it reaches some critical minimum value and molecular rearrangement is effectively “frozen” out, so the polymer chains lack sufficient free volume to achieve different physical conformations.⁸ This ability to achieve different physical conformations is called segmental mobility.³² Random copolymers can be shown by the notation PA-*ran*-PB, with A and B being different monomers, an example of a random copolymer is shown in Figure 1.3.

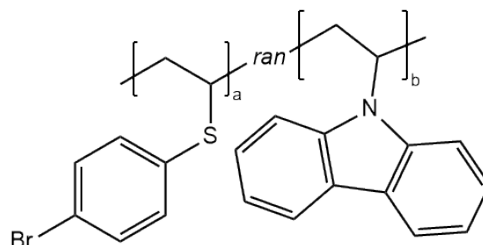


Figure 1.5 the structure of a random copolymer consisting of 4-bromophenyl vinyl sulphide (BPVS) and N-vinylcarbazole (NVC). Adapted from Lo et al.³³

In block copolymers, by combining two or more monomers with a different T_g , the polymer can exhibit phase separation.³⁴ Due to the repulsive interactions between the chemically different blocks, they can phase separate. However, the fact that these blocks are linked covalently prevents macroscopic separation of the block. As a result of these two competing tendencies, block copolymers self-assemble to form various ordered phases.³⁵ Depending on intrinsic immiscibility (or lack of compatibility), block copolymers can exhibit two separate T_g values corresponding to the two parent homopolymer blocks.⁶ However this can only be seen if the two blocks are incompatible enough.³⁶ A monomer with a high T_g can be referred to as a ‘hard’ block whilst a monomer with a lower T_g is a ‘soft’ block. The most common method to determine the phase obtained at a given temperature (and pressure) is to apply the Flory-Huggins equation.³⁷ This depends on the interactions between the blocks and the architecture of the block copolymer molecule (total number of monomers per chain, N , and the volume fraction of one of the blocks, ϕ).³⁸ The Flory-Huggins theory describes the steric interferences among polymers (Equation 5).³⁹

$$\Delta G_m = RT(n_1 \ln \phi_1 + n_2 \ln \phi_2 + n_1 \phi_1 \chi_{12}) \quad (5)$$

Where R is the gas constant, T is the absolute temperature, ϕ_i is the volume fraction of the component i , n_i is the number of moles of component i , and χ_{ij} is the interaction parameter between components i and j . Block copolymers can be denoted with PA-*b*-PB, with A and B being different blocks of monomers, the structure of a block copolymer is shown in figure 1.4.

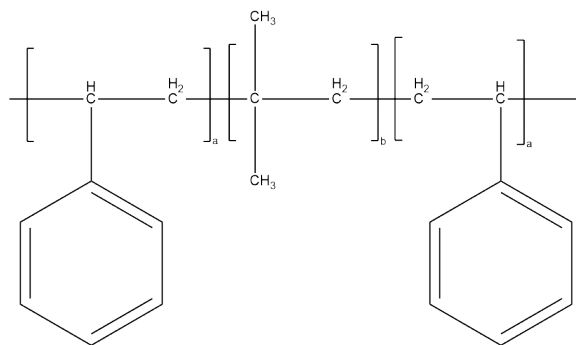


Figure 1.6 The triblock copolymer structure of poly(styrene)-*b*-poly(isobutylene)-*b*-poly(styrene). Adapted from Fittipaldi et al.⁴⁰

1.5 Terpenes

Environmental concerns and long-term strategic planning encourage the search for bio-sourced raw materials for polymer production that reduce the current reliance on polymers from fossil-fuel-based sources.⁴¹ Therefore, the development of polymers from renewable resources, such as biomass, is becoming a prominent area of interest for industry and academia.⁴² Methods to extract small molecules from biomass include fermentation of carbohydrates, chemical transformation of natural polymers (*e.g.* cellulose, lignin) and directly extracting molecules from natural resources (*e.g.* plant oils and terpenes).⁴³

Terpenes are typically derived from citrus fruits and wood waste and are characteristically comprised of varying numbers of isoprene units.⁴⁴ These unsaturated hydrocarbons are produced predominantly by plants, particularly conifers, these compounds number approximately 30,000. Terpenoids are terpenes that have been modified with (usually oxygen-containing) functional groups.⁴⁵ The terms terpenes and terpenoids are used interchangeably. Both have strong and often pleasant odours, which may protect their hosts or attract pollinators.⁴⁶ The inventory of terpenes and terpenoids is estimated at 55,000 chemical entities. The structures of the terpenes mentioned in this document are shown in figure 1.7.

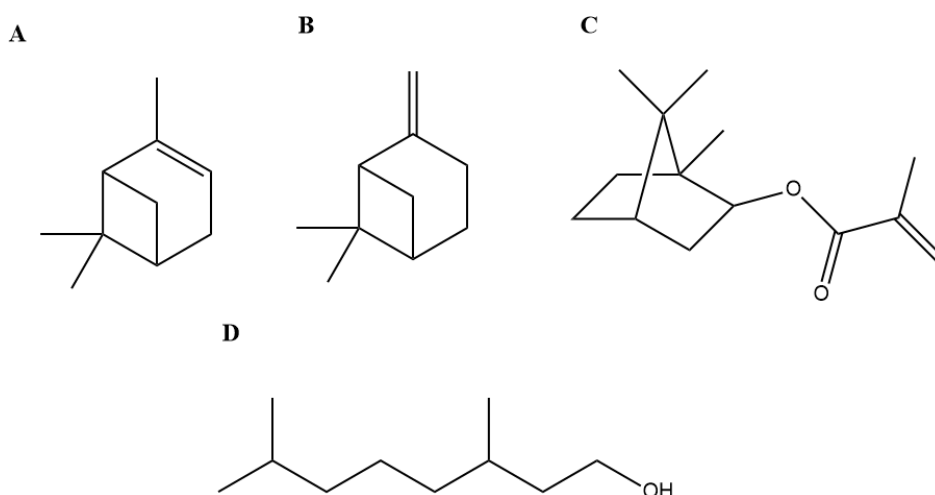
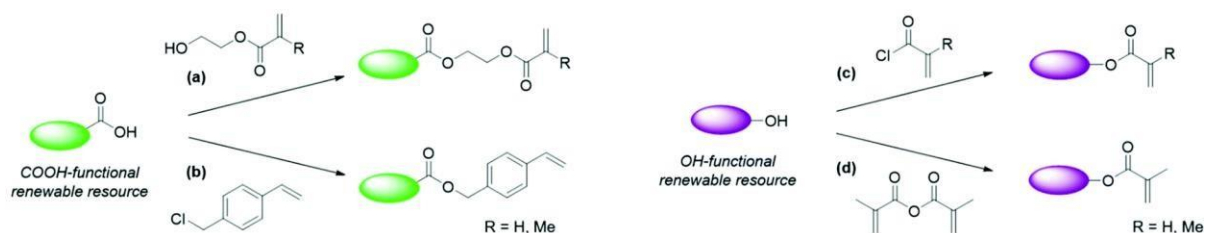


Figure 1.7 The structures of the terpenes that will be discussed in this document (A) α -pinene, (B) β -pinene, (C) isobornyl methacrylate, (D) tetrahydro-geraniol.

Terpenes have become of interest for replacing monomers from fossil fuels due to the presence of multiple unsaturated carbon bonds in these naturally occurring molecules, such as limonene.^{47,48} However, due to the polymerisation of terpene monomers being less successful than their copolymerisation with petroleum-based monomers, this typically yields lower incorporation of bio-sourced monomers than petroleum-based monomers.^{49,50} The high performance of plastics derived from fossil fuels is the outcome of many years of intensive research and commercial-scale optimisation.⁵¹ Therefore it remains a challenge to design terpene-based polymers with similar performances and cost as petroleum-based polymers.^{41,52,53} To improve the incorporation of terpene-based monomers into plastics, a vinyl bond is extremely useful, however in most cases a polymerisable vinyl monomer cannot be directly extracted, therefore producing such a monomer requires chemical modification.⁵⁴ A convenient approach to achieve this was introduced by Wilbon *et al.*,⁴⁴ where monomers bearing an acrylate moiety were prepared by esterification of pendant hydroxyl and acid groups. This allowed higher incorporation of the terpene-based materials into polymer matrices. Some examples of synthetic routes most used to prepare monomers from renewable resources are highlighted in Scheme 3, these synthetic routes can also be utilised in the production of terpene-based monomers, a terpene which has been modified can be referred to as a terpenoid.



Scheme 3. General synthetic routes to monomers derived from renewable resources. Adapted from F. Hatton.⁵⁴ Carboxylic acid-functional renewable resources have been modified to give polymerisable monomers using (a) N, N'-dicyclohexylcarbodiimide (DCC) and 4-dimethylamino pyridine (DMAP) mediated esterification,^{55,56} or (b) esterification using a halogenated compound mediated by 1,1,3,3-tetramethylguanidine (TMG).⁵⁷ Alcohol-functional renewable resources can be reacted with (c) acryloyl or methacryloyl chloride in the presence of triethylamine (TEA),^{58,59} or (d) methacrylic anhydride with DMAP as a catalyst.^{60,61}

Howdle *et al.*⁶² utilised cyclic terpenes including β -pinene to prepare (meth)acrylate-based monomers *via* oxidation and subsequent esterification of the hydroxyl groups. The free radical polymerisation of those monomers resulted in high monomer conversions (> 95 %), yielding polymers with T_g up to about 100°C. The bio-based (meth)acrylic polymers displayed interesting thermal properties, with T_g ranging from room temperature to in excess of 120 °C.

Terpene and terpenoid molecules can be used to replace monomers from petroleum sources, for example tetrahydrogeraniol acrylate (THGA) can be used as a substitute for widely used acrylates such as butyl acrylate ($T_g = -54^\circ\text{C}$), ethyl acrylate ($T_g = -20^\circ\text{C}$) and 2-ethylhexyl acrylate ($T_g = -85^\circ\text{C}$) monomers,⁶³ due to its low glass transition temperature ($T_g = -46^\circ\text{C}$).³⁴ The structures of these monomers is shown in figure 1.8.

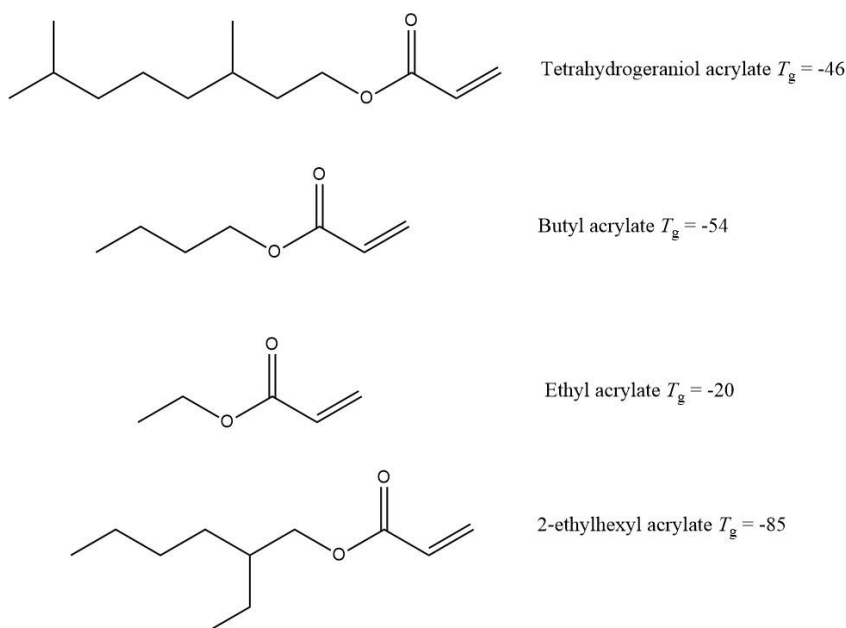
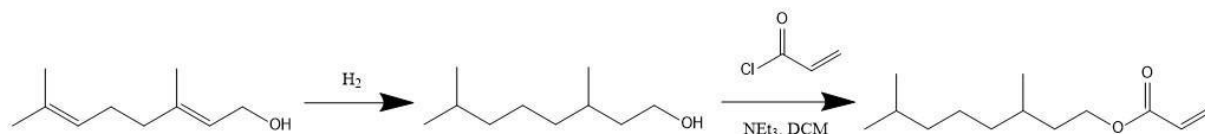


Figure 1.8 The structures of tetrahydrogeraniol acrylate, butyl acrylate, ethyl acrylate, and 2-ethylhexyl acrylate.

THGA is sourced from geraniums, where the oil is used to produce geraniol. This is then hydrogenated, and finally undergoes an acrylation reaction, as shown in Figure 1.8.⁶⁴ This reaction places a carbon double bond into the molecule, and therefore can be used for polymerisations easily. However, this reaction is completed using toxic acryloyl and methacryloyl chloride, to improve the renewability of this process, these reagents can be substituted with acrylic and methacrylic acid; both of which are commercially available from renewable sources. Propyl phosphonic anhydride (T3P®)⁶⁵ was also used to promote ester coupling between terpene alcohols and acrylic acid. This reagent gives an environmentally benign water-soluble triphosphate by-product; considerably more sustainable than chloride in any waste stream.⁶²



Scheme 4. shows geraniol hydrogenated to tetrahydro geraniol and then acrylated to tetrahydrogeraniol acrylate.

Another common source of terpene molecules is from pine sap, these include monomers such as alpha and beta pinene, and isobornyl methacrylate (IBMA). IBMA can be synthesised from camphene via reactions with the appropriate acrylic or methacrylic acid.⁶⁶ Camphene itself can be derived from α -pinene.⁶⁷ High T_g values were observed for poly(α -pinene methacrylate) in the range of 85–142 °C because of increased polymer backbone stiffening (greater conformational barriers) versus polyacrylate analogues. Poly(β -pinene methacrylate) showed a lower T_g (115°C) compared to poly(pinene methacrylate) with similar molecular weights presumably because of the added flexibility and increased free-volume imposed by the methylene spacer.⁶⁸ Isobornyl methacrylate has a hydrophobic bulky bicyclic isobornyl group that improves thermal stability when copolymerised; it can impart a high T_g to the copolymer (poly(IBMA) = 110–200°C).^{69–72} Thus, such sustainable feedstocks can lead to polymers that are not necessarily drop-in replacements for other polymer such as poly(methyl methacrylate), PMMA ($T_g \approx 105^\circ\text{C}$) but the higher T_g of polymers such as poly(IBMA) and poly(α -pinene methacrylate) enables applications toward engineering thermoplastics.⁷⁰

1.6 Polymerisation Techniques

Different polymerisation techniques are applied to obtain polymers with unique properties suitable for various applications. Polymerisations can be classed as either a homogeneous or heterogeneous process. Homogeneous polymerisations can be carried out in solution (with solvent) or in bulk (without solvent). Heterogeneous polymerisations can form polymer micro or nanoparticles if a dispersed liquid phase in which the monomer/polymer is insoluble is suitable selected.⁷¹

1.6.1 Heterogeneous Polymerisation

Heterogeneous techniques involve the formation of a polymer which is insoluble in the continuous phase, meaning that the polymerisation occurs independently in the dispersed phase.⁷³ This is shown to increase the rate of polymerisation compared to homogeneous techniques.²⁴ Heterogeneous polymerisation techniques are typically divided into four categories: emulsion, suspension, precipitation, and dispersion.^{74–77} These techniques have fundamental differences in their polymerisation protocol and thus the form of the final polymer product produced.

The molecular weight of polymer produced in an emulsion polymerisation is normally of an order of magnitude greater than that in a similar homogeneous free-radical polymerisation.⁷⁸ This is due to segregation (compartmentalisation) of propagating chains into nanoscale particles, coupled with generation of radicals in the continuous aqueous phase along with a desirable micellar nucleation and a consequent increase in the radical lifetime. Due to this, it is possible to achieve high rates of polymerisation and to produce high molecular weight polymer in the same polymerisation.⁷⁹

Suspension polymerisation has monomer droplets with dissolved initiator and are commonly dispersed in water. As the polymerisation progresses, the droplets are transformed into viscous monomer–polymer particles that become rigid, spherical polymer particles of size 50–500 μm .⁸⁰ The concentration of polymer is typically 30–50% in the fully converted suspension. The viscosity of the suspension is determined by the dispersed phase and, therefore, remains constant throughout the reaction and thus, temperature control is not difficult. To avoid coalescence and agglomeration of the dispersion of monomer droplets/polymer particles, surface-active stabilising agents are added into the dispersion and significant agitation is applied. The control of particle size distribution (PSD) normally performed by proper manipulation of the suspending agent (stabiliser) concentration and stirring speed may be in general a complex issue and can cause problems when scaling-up the process.⁸⁰

Precipitation polymerisation is realized by single preparative step and belongs to high yield polymerisation method. This type of polymerisation is used to obtain uniform and spherical particles (diameters typically less than 1 μm), but large

amount of template is required. Precipitation polymerisation is a surfactant-free method, which involves polymerisation of monomers in dilute solutions (without overlap and coalescence), and resultant polymer particles will precipitate from the solution. Particle growth predominantly occurs by entropic precipitation of nanogel (seed) particles followed by continuous capture of oligomers from solution. This method of polymerisation requires a large amount of solvent.⁸¹

Dispersion polymerisation is another type of heterogeneous polymerisation, and, unlike emulsion and suspension polymerisations, the monomer is soluble in the continuous phase, resulting in dispersed polymer particles. The continuous phase usually consists of water and alcohol (such as methanol or ethanol). Upon initiation, the polymerisation starts in the continuous phase and the oligomers formed are precipitated and aggregated to form particles which are then stabilized by a non-ionic surfactant such as poly(vinyl pyrrolidone). Due to the short nucleation step, monodispersed particles in the size range 1–5 μm are formed.⁸² Particle size is controlled by several parameters such as the type and concentration of the surfactant, the solids content, the initiator concentration, and the solvent used.⁶ Many dispersion polymerisation methods have been described in the literature for production of polymer particles made from styrene and acrylate-based monomers. The solvents used range from highly polar alcohols to very apolar hydrocarbons.⁸³

1.6.2 Homogeneous Polymerisation

Homogenous polymerisations can be divided into two categories, solution and in bulk. Solvent polymerisations are carried out in a single phase, in which monomer, initiator, and resulting polymer are all soluble. This is commonly in an organic solvent, such as toluene.⁸⁴ Bulk polymerisation is solventless, and thus the phase in which the polymerisation occurs is the monomer itself. Bulk polymerisation produces the highest purity polymers,⁸⁵ however, problems occur with the viscosity of this polymerisation technique due to auto-acceleration and heat transfer issues. This polymerisation technique is currently rarely used in commercial manufacture.⁸⁶

Solution polymerisation is used to solve the issues with bulk polymerisation. Due to the solvent lowering the viscosity of the reaction, thus aiding in heat transfer, and reducing auto-acceleration. This method of polymerisation requires an appropriate solvent to be selected, as both the monomer and polymer needs to be soluble, as well as the solvent having an appropriate boiling point. The choice of solvent and concentration of solvent can also affect the propagation rate of the polymerisation,⁸⁷ due to the formation of complexes of propagating radicals with aromatic solvents, such as benzene.⁸⁸ The workup of this polymerisation technique usually involves precipitating the final polymer in a solvent in which the polymer is insoluble.

1.7 Solvents for Polymerisation

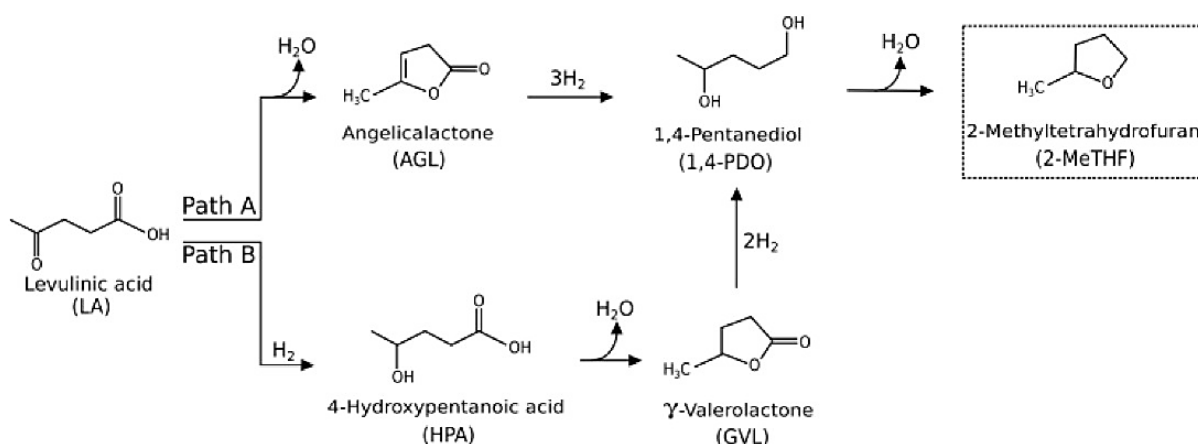
Petrochemical solvents such as dichloromethane (DCM) and tetrahydrofuran (THF) are generally chosen for a variety of polymerisation processes because they are relatively inexpensive. These conventional solvents dissolve a wide range of monomers and the resulting polymer products, making them ideal solvents for homogeneous polymerisations.⁸⁹

Other solvents used include hexane and toluene,⁹⁰ however these solvents are also produced from petrochemical sources and are thus non-renewable. The European regulation concerning the 'Registration, Evaluation, Authorisation and Restriction of Chemicals' (REACH) has introduced restrictions on toluene, chloroform and DCM with specific conditions.⁹¹ REACH is now affecting the import and usage of a wide range of chemicals in Europe.⁹² Therefore bio-based solvents have grown in popularity.⁹³ Another type of solvent used for polymerisation is an ionic liquid; an organic salts or mixtures of salts that is a fluid at room or near room temperature. The essential property of ionic liquids is their zero-vapour pressure therefore they are considered as potential solvents for clean chemical processes. Ionic liquids can be used for both heterogeneous and homogeneous polymerisations as some organic compounds are immiscible with some ionic liquids.⁹⁴ However, as polymers are non-volatile, polymerisation in ionic liquids may require the use of organic solvents to isolate the polymer, therefore the advantage of using this environmentally friendly reaction medium is partly lost.⁹⁴

1.6.1 Green Solvent Alternatives

Several criteria should be fulfilled to call a solvent 'green'. It should be bio-based, non-toxic, biodegradable, and recyclable.⁹⁵ Most bio-based solvents are made from sugar, corn, or beet. They are chosen primarily owing to their ability to replace oil-based solvents and are as safe and as effective as the traditional options. Green solvents do not release toxic by-products and volatile organic compounds (VOC) during manufacturing.⁹⁶ Owing to their high boiling point, low toxicity, and low miscibility, many green solvents have become popular in recent years. These solvents are mainly used for coatings, paints, printing inks, personal care products, cosmetics, sealants, and pharmaceuticals, and therefore, sustainable solvents suppliers see the demand for bio-based solvents growing exponentially.⁹⁷

2-Methyl tetrahydrofuran (2-MeTHF) is an aprotic ether solvent that can be used as an alternative bio-based solvent for tetrahydrofuran (THF) however, this solvent is still problematic because of its high flammability.⁹⁸ While being a strong Lewis base, like THF, it is only partially miscible with water.⁹⁹ An attractive feature of 2-MeTHF is that it is derived from renewable resources. There are two paths for the production of 2-MeTHF from Levulinic acid (Scheme 5).¹⁰⁰ Initial studies have shown 2-MeTHF to have lower toxicity, and it has been approved for pharmaceutical chemical processes.¹⁰¹ It can be synthesised from xylose and glucose, both of which are derived from biomass *via* other feedstock intermediates such as levulinic acid and furfural.¹⁰²



Scheme 5. The manufacture of 2-MeTHF from Levulinic acid *via* two pathways. Adapted from Licursi *et al.*¹⁰⁰

Khoo *et al.* performed a detailed life cycle analysis (LCA) to produce bio-derived 2-MeTHF from three biomass sources (corn stover, sugar cane bagasse, and rice straw).^{103,104} The LCA investigated the environmental implications, such as land usage emissions (such as eutrophication) and global warming potential (from CO₂, methane, and NO_x emissions),

and the total energy of production (per kilogram of 2- MeTHF). The LCA results showed that the energy usage and environmental damage caused by crop production far outweighed that of biomass processing. These results show how solvent sustainability also depends on feedstock cultivation.

The energy consumption for the processing of 2-MeTHF was calculated to be ~ 0.2 MJ/kg, which is significantly lower than the processing of THF, which is 111 MJ/kg.¹⁰⁵ Manufacturing 2-MeTHF from furfural, which may be derived from many agricultural wastes, has been calculated to reduce solvent emissions by 97% relative to non-renewable THF production (Figure 1.10).

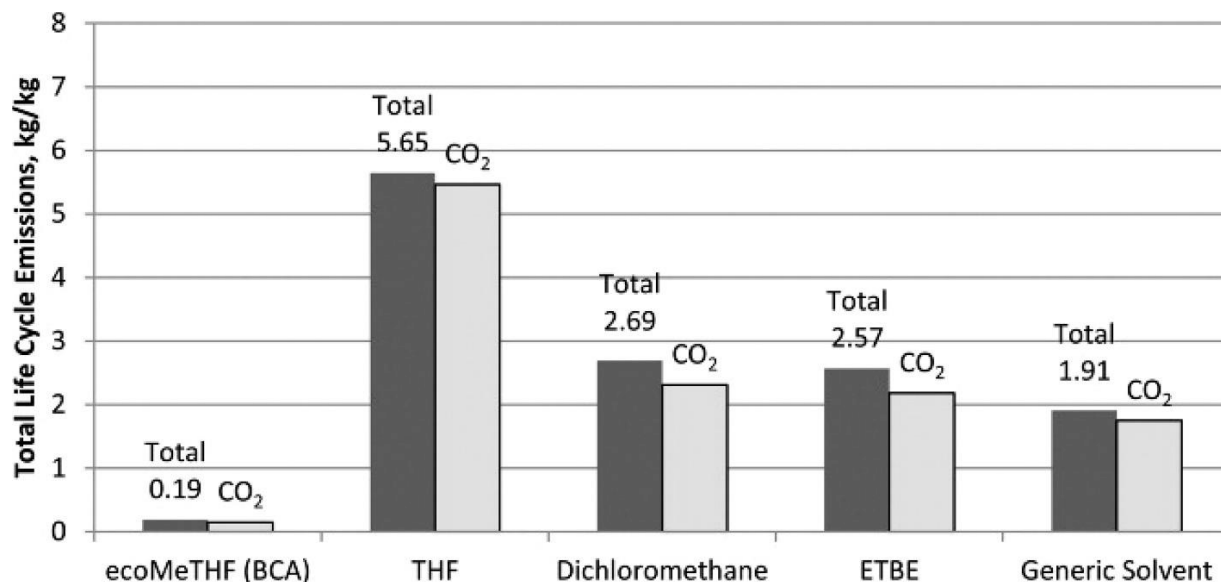


Figure 1.9 Total and CO₂ life cycle emission for 2-MeTHF (ecoMeTHF), THF, DCM, ethyl tert-butyl ether (ETBE), and a generic solvent (classical organic solvent). Adapted from C. Clarke *et al.*¹⁰⁶

2-MeTHF has been successfully demonstrated as an effective reaction solvent for multiple types of polymerisations such as ring-opening polymerisation (ROP), enzymatic ring-opening polymerisation (eROP), CRP, and RAFT polymerisations as both a single process and in tandem. These polymerisations showed that multiple types of monomers are applicable for polymerisation in 2-MeTHF such as lactide, caprolactone, block copolymers macroinitiators, and hybrid methacrylate-ester macroinitiators.⁸⁹ This solvent has also been used successfully with ethyl lactate acrylate (ELA), which is derived from biological sources. Therefore demonstrating 2-MeTHF as an excellent bio-based solvent for polymerisations.¹⁰⁷

1.8 Project Aims.

The aim of this project is to produce novel random and block copolymers containing the green low T_g monomer, THGA. This monomer has been combined with methyl methacrylate (MMA), IBMA and alpha-pinene methacrylate (α -PM), to create 'hard'-'soft' diblock copolymers as well as random copolymers.

To the best of our knowledge, little has been published on the polymerisation of THGA alone or as a copolymer. In general, bio-based monomers of lower T_g are less studied than their high T_g counterparts. In order to study the polymerisation of this monomer when used to form random and block copolymers, MMA was chosen as a model monomer. MMA was selected as it is a well-known monomer in the literature and various papers have been published about the polymerisation of MMA. Random and 'hard'-'soft' diblock copolymers of MMA and THGA will be produced, and the thermal properties of these polymers investigated. The reactivity ratio of MMA and THGA will then be studied to calculate the reactivity of THGA in random copolymers.

The next stage in our use of THGA is to replace the petrochemical-based MMA with a terpene-based high T_g monomer, such as IBMA and α -PM. The thermal properties of these homopolymers will then be studied and compared to MMA to

ensure these monomers provide a suitable alternative to MMA. These monomers will be then combined with butyl acrylate to investigate whether random and block copolymers can be produced. Butyl acrylate will first be used as a model monomer in comparison to THGA, as butyl acrylate has a similar T_g to THGA. In order to make this polymerisation as environmentally sustainable as possible, an alternative solvent will be tested and compared to toluene, which is a common solvent for solution polymerisations. 2-MeTHF was chosen as an alternative solvent, because it can be produced from a biological source and has similar properties to other solvents for polymerisations such as toluene and THF.

The final step of the project is to successfully combine THGA (low T_g monomer) with the terpene-based high T_g monomers, IBMA and α -PM, into random and 'hard'-'soft' diblock copolymers. These polymers will then have their thermal properties determined, allowing for suitable applications of these polymers to be determined. The reactivity ratios of THGA and IBMA as well as THGA and α -PM will be calculated to determine the reactivity of the terpene-based random copolymers.

2. Experimental

2.1 Materials

MMA was purchased from ProSciTech (99%) and was filtered through aluminium oxide to remove the stabiliser before polymerisation. All other chemicals were used as received. Dimethyl-octanol (tetrahydro-geraniol or THG), Azobis(isobutyronitrile) (AIBN), dichloromethane (DCM), all RAFT agents including: 2-(Dodecylthiocarbonothioylthio)-2-methylpropanoic acid (DDMAT), 2-cyano-2-propyl dodecyl trithiocarbonate (CPDT), 4-cyano-4-(phenylcarbothioylthio)pentatonic acid (CPAB), 4-cyano-4-[dodecylsulfanythiocarbonylsulfonyl] pentatonic acid (CPAD) and 4-cyano-2-propylbenzodithioate (CPBD) were purchased from Sigma Aldrich (98% (HPLC)). Toluene, tetrahydrofuran (THF) (HPLC grade), 2-methyl tetrahydrofuran (2-MeTHF), deuterated chloroform (CDCl_3), triethylamine and methanol were all purchased from Fischer Scientific.

2.2 Polymer Analysis

All polymers produced during this work were characterised initially by Nuclear Magnetic Resonance (NMR) spectroscopy and Gel Permeation Chromatography (GPC). Further characterisation on samples was carried out using Differential Scanning Calorimetry (DSC) and Dynamic mechanical analysis (DMA) to analyse the thermal properties of the polymer samples.

2.2.1 Nuclear Magnetic Resonance Spectroscopy

Samples were analysed by ^1H NMR spectroscopy to calculate the percentage conversion of monomer to polymer (Equation 6). All samples were dissolved in deuterated chloroform (CDCl_3) and analysed using a Bruker 400 Ultrashield (400 MHz Spectrometer). Chemical shifts are reported in parts per million (ppm) using tetramethylsilane (TMS) as the standard.

$$\text{Conversion} = \frac{\text{Integral}(1_{\text{Polymer}})}{\text{Integral}(1_{\text{Monomer}} + 1_{\text{Polymer}})} \quad (6)$$

2.2.2 Gel Permeation Chromatography

Gel Permeation Chromatography (GPC) is used as an analytical technique to obtain information on the molecular weight distribution of polymers. The technique separates samples based on the molecular size of polymer coils, with larger chains eluting first, and smaller chains later. This is due to smaller polymers taking a longer pathway through the porous column. Larger polymers are too big to fit inside the pores, and so pass through the column at a faster rate. Molecular weight parameters of polymer samples were measured relative to PMMA standards by GPC using an Agilent Infinity 1260 GPC in conjunction with a Wyatt Differential refractive index (dRI) detector, a multi-angle light scattering (MALS) detector, and a UV detector sensitive at $\lambda=305$ nm, all operating in a THF mobile phase at 40°C at a flow rate of 1 mL min^{-1} . This enabled the M_n , M_w , and \bar{M}_w/\bar{M}_n values for the polymers to be determined. All polymers do not interact with solvents in the same way thus there is a deviation from the reported figure if the polymer being analysed is not the same as the one in the calibration standards. The UV detector is used to assess whether the RAFT agent, which absorbs in the 305 nm region, is attached to the polymer chains or not. This is useful in determining the polymerisation pathway taken during the reaction. During this work, a mixed-D ($3\text{ }\mu\text{m}$ pores) column was used.

2.2.3 Differential Scanning Calorimetry

Thermal analysis of polymer samples is important as information about the thermal and oxidative stability, lifetime, and shelf-life under certain conditions can be determined. DSC is a thermoanalytical technique that measures the difference in the amount of heat required to vary the temperature of the polymer sample and a reference. The Tzero® sample pan has a well-defined heat capacity over the range of temperatures used in the instrument. This allows metrics such as T_g to be determined. The T_g is observed as a change in the heat capacity of the polymer and is not an exothermic or endothermic process.

DSC measurements were taken using a TA Instruments Q2000, with a purge environment of N_2 gas. Measurements were taken between $-90\text{ }^{\circ}\text{C}$ and $250\text{ }^{\circ}\text{C}$ at a heating or cooling rate of $10\text{ }^{\circ}\text{C min}^{-1}$, with cooling regulated by a sealed refrigerant system, the sample size was targeted as between 3-5 mg. An empty Tzero®pan and lid were used as a reference.

2.2.4 Dynamic mechanical analysis

Dynamic mechanical analysis (DMA) is a technique used to study and characterise a materials viscoelastic behaviour. A sinusoidal stress is applied and the strain in the material is measured, the complex modulus can then be determined. The temperature of the sample or the frequency of the stress are often varied, leading to variations in the complex modulus; this approach can be used to locate the glass transition temperature of the material, as well as to identify transitions corresponding to other molecular motions.

Measurements were performed on a Triton Technologies DMA using the powder pocket accessories. For each measurement, the sample ($40\text{ mg} \pm 5\text{ mg}$) was weighed into a powder pocket. Samples were measured at 1 and 10 Hz. In single cantilever bending geometry between $20 - 200\text{ }^{\circ}\text{C}$ for known high T_g polymers, The value of T_g was taken as the peak of the tan delta ($\tan \delta$) curve.

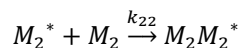
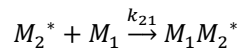
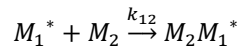
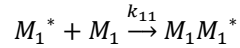
2.2.5 UV/Vis analysis.

Ultraviolet-visible (UV/Vis) spectrophotometry is a technique used to measure light absorbance across the ultraviolet and visible ranges of the electromagnetic spectrum. The absorbance of radiation in the UV-Vis range causes atomic excitation however, before an atom can change excitation states, it must absorb sufficient level of radiation for electrons to move into higher molecular orbits. Shorter bandgaps typically correlate to absorption of shorter wavelengths of light. The energy required for molecules to undergo these transitions, therefore, are electrochemically-specific. A UV-Vis spectrophotometer can use this principle to quantify the analytes in a sample based on their absorption characteristics.

The Uv/Vis analysis was performed using an Epoch 2 spectrometer that was measured between 300-700 nm with a step of 10nm. This was carried out by first running a spectrum of only the solvent which was, then compared to the spectrum of the solution that wanted to be studied. This analysis was carried out using a cuvette with approximately 3.5 mL of each sample used.

2.3 Reactivity Ratio Calculations

The reactivity ratio calculations were performed using the Mayo-Lewis equation (the terminal model), this describes the distribution of monomers in a copolymer.¹⁰⁸ Taking into consideration a monomer mix of two components M_1 and M_2 and the four different propagation reactions that can take place at the reactive chain end terminating in either monomer (M^*) with their reaction rate constants : k.



The reactivity ratios can be defined as:

$$r_1 = \frac{k_{11}}{k_{12}} \quad (7)$$

$$r_2 = \frac{k_{21}}{k_{22}} \quad (8)$$

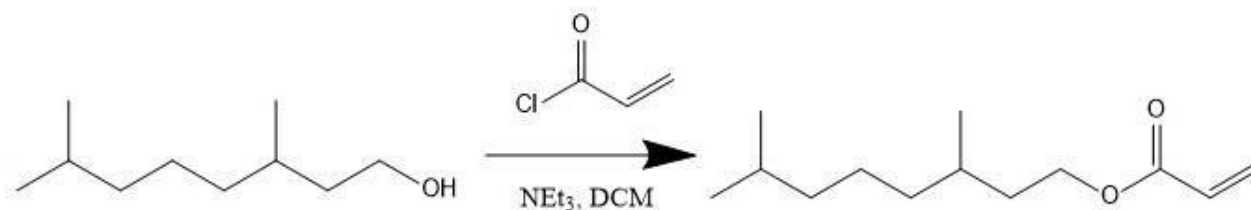
The copolymer equation can be written as:

$$F_1 = 1 - F_2 = \frac{r_1 f_1^2 + f_1 f_2}{r_1 f_1^2 + 2f_1 f_2 + r_2 f_2} \quad (9)$$

Where F is the mole fraction of each monomer in the copolymer and f is the mole fraction of each monomer in the feed. The value of f is between 0 and 1.0. Calculation of reactivity ratios generally involves carrying out several polymerisations at varying monomer ratios. The copolymer composition was analysed with proton nuclear magnetic resonance. The polymerisations are carried out at low conversions, so monomer concentrations can be assumed to be constant (ca. 10%) and are consumed preferentially in the propagation reactions. With all the other parameters in the copolymer equation known (Equation 9), r_1 and r_2 can be found.

The Mayo-Lewis method uses a form of the copolymer equation relating r_1 and r_2 to monomer concentrations and copolymer compositions. For each set of different monomer/copolymer compositions, r_1 and values were estimated through a nonlinear least square estimation procedure by using the Levenberg-Marquardt algorithm. All the reactivity ratio calculations and graphs were produced using python.

2.4 Synthesis of tetrahydro-geraniol acrylate



Scheme 6. Generic schematic showing the synthesis of tetrahydrogeraniol acrylate from tetrahydrogeraniol.

Tetrahydro geraniol (THG) (19.0 g, 0.120 mol), triethylamine (12.2 g, 0.120 mol), and dichloromethane (DCM) (360 mL) were combined. The mixture was placed in an ice bath and left to stir for 2 h. Subsequently, acryloyl chloride (14.5 mL, 16.2 g, 0.179 mol) was added dropwise *via* a dropping funnel. Upon complete addition, the mixture was left to stir for 30 min in the ice bath and for 24 hours at ambient temperature. After, the mixture was filtered and washed several times with brine and deionized water. The volatiles were removed by rotary evaporation to yield a pale yellow transparent viscous liquid (45% conversion). The scheme of the polymerisation (scheme 6). The monomer was characterised by ¹H and ¹³C NMR, using the labelled structure (figure 2.2).

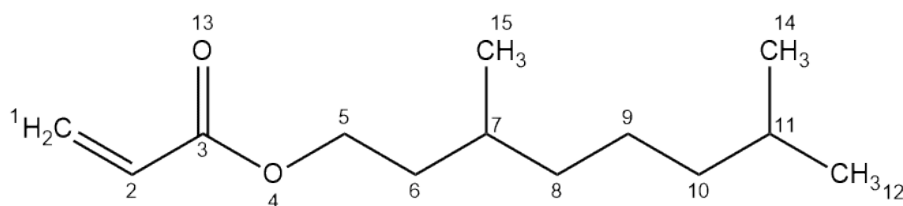
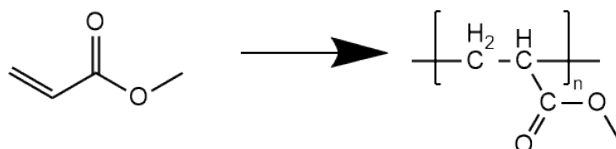


Figure 2.1 The labelled structure of THGA.

2.5 Solution Polymerisations in toluene

2.5.1 Homopolymer synthesis of PMMA

The scheme of the homopolymerisation of MMA (scheme 7) is shown below.



Scheme 7. The general scheme for the homopolymerisation of MMA

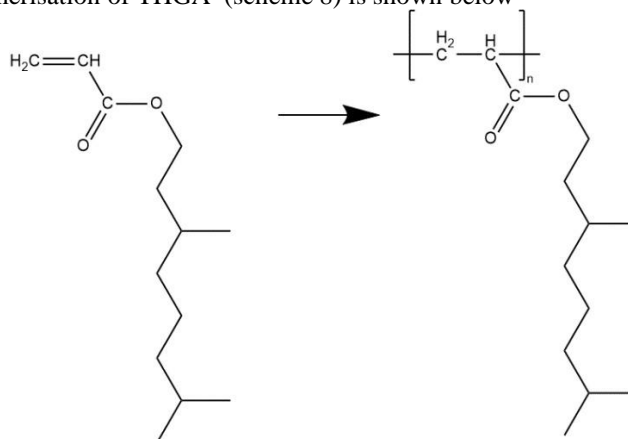
AIBN (0.017 mmol), RAFT agent (0.083 mmol), MMA (49.9 mmol) and 5 mL of toluene were combined with a magnetic stirrer into a sample vial, which was then sealed and degassed under argon for 30 minutes. The tube was then heated to 65°C in an oil bath and agitated by magnetic stirring. After 24 hours, the vessel was cooled and the polymer was precipitated from solution in a 10-fold volume of methanol, filtered and dried in vacuum. Analysis was carried out using ¹H NMR to determine conversion using equation 6 as shown in 2.2.1. GPC, and DSC were also used to determine molecular weight, polydispersity and the *T_g* of the polymer. A chain length of 600 units was targeted. Scheme 7 shows the polymerisation scheme. The molar amounts used for the polymerisations of MMA is shown in table 2.1.

Table 2.1 Reaction conditions of RAFT solution polymerisations of poly(methyl methacrylate). All reactions were carried out in toluene using 4.99g of monomer.

RAFT agent	[M]:[RAFT]:[I]	Target <i>M_n</i>
DDMAT	600:5:1	60000
CPDT	600:5:1	60000
CPAB	600:5:1	60000

2.5.2 Homopolymer synthesis of PTHGA

The scheme of the homopolymerisation of THGA (scheme 8) is shown below



Scheme 8. the general scheme for the homopolymerisation of THGA

AIBN (0.017 mmol), RAFT agent (0.083 mmol), THGA (5.076 mmol) and 5 mL of toluene were combined with a magnetic stirrer into a sample vial, which was then sealed and degassed under argon for 30 minutes. The tube was then heated to 65°C in an oil bath and agitated by magnetic stirring. Analysis was carried out using ¹H NMR to determine conversion using equation 6 as shown in 2.2.1. GPC, and DSC were also used to determine molecular weight, polydispersity and the *T_g* of the polymer. A chain length of 300 units of THGA was targeted. The molar amounts of reagents used for the polymerisation is shown in table 2.2.

Table 2.4 Reaction conditions of RAFT polymerisation of methyl methacrylate and tetrahydro-geraniol acrylate to calculate the reactivity ratio of the two monomers.

THGA: MMA	THGA (mmols)	MMA (mmols)	AIBN (mmols)	RAFT agent (mmols)
9:1	4.569	0.507	0.012	0.087
8:2	4.061	1.015	0.012	0.087
7:3	3.553	1.523	0.012	0.087
6:4	3.046	2.030	0.012	0.087
5:5	2.538	2.538	0.012	0.087
4:6	2.030	3.046	0.012	0.087
3:7	1.523	3.553	0.012	0.087
2:8	1.015	4.061	0.012	0.087
1:9	0.507	4.569	0.012	0.087

2.5.5 Block copolymer synthesis

AIBN, PMMA, THGA and 5 mL of toluene were combined in different monomer ratios as shown in table 2.5 with a magnetic stirrer into a sample vial, which was then sealed and degassed under argon for 30 minutes. The sample was then heated to 65 °C in an oil bath and agitated by magnetic stirring. After 24 hours, the vessel was cooled and the polymer was precipitated from solution in a 10-fold volume of methanol, filtered and dried in vacuum. Analysis was carried out using ¹H NMR to determine conversion using equation 6 as shown in 2.2.1. GPC, and DSC were also used to determine molecular weight, polydispersity and the T_g of the polymer.

Table 2.5 The molar amounts of PMMA, THGA and AIBN required for the block copolymerisation reactions to achieve the targeted PTHGA molecular weight.

PMMA (mols)	THGA (mols)	AIBN (mmols)	Targeted PTHGA M_n
0.005	0.005	0.017	30000
0.005	0.015	0.026	15000

2.6. RAFT agents in 2-MeTHF

2.6.1 RAFT Agent Screening

AIBN (0.017 mmol), RAFT agent (0.083 mmol), MMA (0.01 mol) and 5 mL of solvent, see table 2.6, were combined with a magnetic stirrer into a sample vial, which was then sealed and degassed under argon for 30 minutes. The tube was then heated to 65°C in an oil bath and agitated by magnetic stirring. After 24 hours, the vessel was cooled, and analysis was carried out using ¹H NMR to determine conversion using equation 6 as shown in 2.2.1. GPC, and DSC were also used to determine molecular weight, polydispersity and the T_g of the polymer.

Table 2.6 The different compositions of polymerisation solutions required to screen two RAFT agents in three different solvents.

Solvent	RAFT agent	MMA (mols)	Targeted M_n
2-MeTHF	CPDT	0.01	34500
Toluene	CPDT	0.01	34500
THF	CPDT	0.01	34500
2-MeTHF	CPAB	0.01	33300
Toluene	CPAB	0.01	33300
THF	CPAB	0.01	33300

2.6.2 UV/Vis analysis of RAFT agent solubility

AIBN (0.001 g), RAFT agent (0.01 g) and 5 mL of solvent were combined into a sample vial, and a UV/Vis spectrum of each solution was taken, after 24 hours another UV/Vis spectrum was taken. The compositions of the solutions are shown in Table 2.7.

Table 2.7 The different solutions required to test the solubility of the RAFT agent in two solvents.

Solvent	RAFT agent	AIBN (mmols)	RAFT (mmols)
2-MeTHF	CPDT	0.006	0.03
toluene	CPDT	0.006	0.03
2-MeTHF	CPAB	0.006	0.03
toluene	CPAB	0.006	0.03

2.6.2 RAFT Agents Screening.

AIBN (0.017 mmol), RAFT (0.083 mmol), MMA (0.01 mol) and 5 mL of solvent, see table 2.9, were combined with a magnetic stirrer into a sample vial, which was then sealed and degassed under argon for 30 minutes. The tube was then heated to 65°C in an oil bath and agitated by magnetic stirring. After 24 hours, the vessel was cooled, and Analysis was carried out using ¹H NMR to determine conversion using equation 6 as shown in 2.2.1. GPC was also used to determine the molecular weight and polydispersity of the polymer.

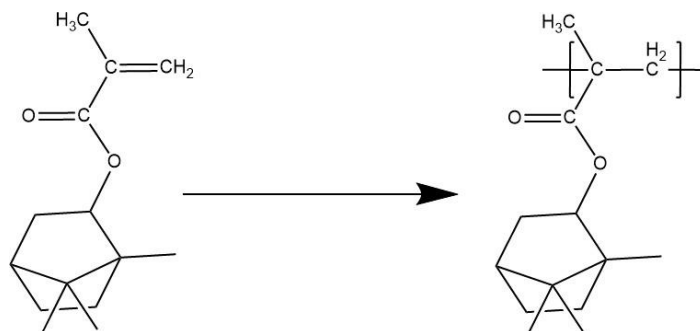
Table 2.9 The molar amounts of MMA, AIBN and RAFT used to investigate the polymerisation of MMA in 2- MeTHF using two different RAFT agents.

RAFT agent	MMA moles	AIBN mols	RAFT mols	Targeted M_n
4-cyano-4-[dodecylsulfanylthiocarbonylsulfyl]pentanoic acid	0.01	0.017	0.083	28000
4-cyano-2-propyl benzodithioate	0.01	0.017	0.083	22000

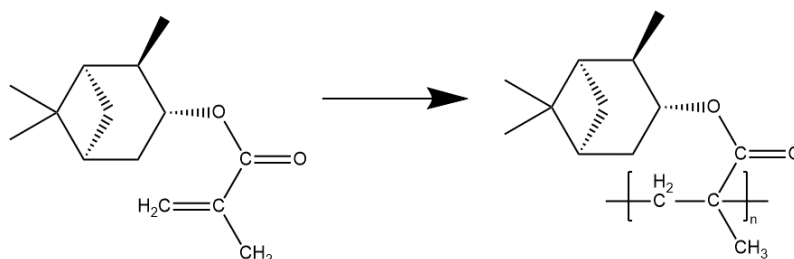
2.7 Solution Polymerisations in 2-MeTHF

2.7.1 High T_g Homopolymer Synthesis

The schemes of the polymerisations of isobornyl methacrylate (scheme 10) and alpha-pinene methacrylate (scheme 11) are shown below.



Scheme 10. The generic scheme for the homopolymerisation of isobornyl methacrylate



Scheme 11. The generic scheme for the homopolymerisation of alpha-pinene methacrylate

AIBN, CPAB, the selected monomer and 5 mL of 2-MeTHF were combined with a magnetic stirrer into a sample vial, which was then sealed and degassed under argon for 30 minutes. The tube was then heated to 65°C in an oil bath and agitated by magnetic stirring. After 24 hours, the vessel was cooled and the polymer was precipitated from solution in a 10-fold volume of methanol, filtered and dried in vacuum. Analysis was carried out using ^1H NMR to determine conversion using equation 6 as shown in 2.2.1. GPC, and DSC were also used to determine molecular weight, polydispersity and the T_g of the polymer.. Table 2.10 shows the molar amounts used for each homopolymerisation.

Table 2.10 The molar amounts of the monomers, RAFT, and AIBN used to homopolymerisation of three different monomers.

Monomer	Monomer(mmols)	RAFT (mmols)	AIBN (mmols)	[M]:[RAFT]:[I]	Targeted M_n
MMA	15	0.070	0.012	1200:6:1	21000
Isobornyl methacrylate	6.8	0.035	0.006	1100:6:1	43000
α -Pinene methacrylate	11	0.035	0.006	1800:6:1	42000

2.7.2 THGA homopolymerisation in 2-MeTHF

AIBN (0.017 mmol), CPDT (0.083 mmol), THGA (49.9 mmol) and 5 mL of 2-MeTHF were combined with a magnetic stirrer into a sample vial, which was then sealed and degassed under argon for 30 minutes. The tube was then heated to 65°C in an oil bath and agitated by magnetic stirring. After 24 hours, the vessel was cooled and the polymer was precipitated from solution in a 10-fold volume of methanol, filtered and dried in vacuum. Analysis was carried out using ¹H NMR to determine conversion using equation 6 as shown in 2.2.1. GPC, and DSC were also used to determine molecular weight, polydispersity and the T_g of the polymer.

2.7.3 Random copolymer synthesis

AIBN (0.006 mmol), CPDT (0.03 mmol), butyl acrylate, and the selected monomer, see Table 2.11 with 5 mL of 2-MeTHF were combined with a magnetic stirrer into a sample vial, which was then sealed and degassed under argon for 30 minutes. The tube was then heated to 65 °C in an oil bath and agitated by magnetic stirring. After 24 hours, the vessel was cooled and the polymer was precipitated from solution in a 10-fold volume of methanol, filtered and dried in vacuum. Analysis was carried out using ¹H NMR to determine conversion using equation 6 as shown in 2.2.1. GPC, and DSC were also used to determine molecular weight, polydispersity and the T_g of the polymer.

Table 2.11 The molar amounts of monomer, AIBN and RAFT used to produce random copolymers.

Monomer	Monomer(mols)	Butyl acrylate (mols)	RAFT (mmols)	AIBN (mmols)	Targeted M_n
MMA	0.0117	0.0117	0.03	0.006	88000
Isobornyl methacrylate	0.0059	0.0117	0.03	0.006	58000
α -Pinene methacrylate	0.0059	0.00595	0.03	0.006	46000

2.7.4 Synthesis of block copolymers

The homopolymers created in 2.4.1 were combined in a 1:1 molar ratio with butyl acrylate, AIBN and 5 mL of 2-MeTHF (table 2.12 with a magnetic stirrer into a sample vial, which was then sealed and degassed under argon for 30 minutes. The sample was then heated to 65 °C in an oil bath and agitated by magnetic stirring. After 24 hours, the vessel was cooled and the polymer was precipitated from solution in a 10-fold volume of methanol, filtered and dried in vacuum. Analysis was carried out using ¹H NMR to determine conversion using equation 6 as shown in 2.2.1. GPC, and DSC were also used to determine molecular weight, polydispersity and the T_g of the polymer.

Table 2.12 The molar amounts of polymer, monomer and AIBN used to produce diblock copolymers.

Polymer	Butyl acrylate (mols)	AIBN (mmols)	Targeted M_n of butyl acrylate block
MMA	0.001	0.003	8000
Isobornyl methacrylate	0.001	0.003	8000
α -Pinene methacrylate	0.001	0.003	8000

2.8 Fully Terpene-Based Copolymers.

2.8.1 Random copolymers

AIBN (0.006 mmol), CPAB (0.03 mmol), butyl acrylate, and the selected monomer, 5 mL of 2-MeTHF were combined in a 1:1 molar ratio for the monomers (table 2.13) with a magnetic stirrer into a sample vial, which was then sealed and degassed under argon for 30 minutes. The tube was then heated to 65 °C in an oil bath and agitated by magnetic stirring. After 24 hours, the vessel was cooled and the polymer was precipitated from solution in a 10-fold volume of methanol, filtered and dried in vacuum. Analysis was carried out using ^1H NMR to determine conversion using equation 6 as shown in 2.2.1. GPC, and DSC were also used to determine molecular weight, polydispersity and the T_g of the polymer.

Table 2.13 The molar amounts of monomers, RAFT and AIBN used to produce random copolymers.

High T_g monomer	High T_g monomer (mols)	THGA (mols)	AIBN (mmols)	RAFT (mmols)	Targeted M_n
Isobornyl methacrylate	0.0058	0.0058	0.006	0.03	64000
Alpha-pinene methacrylate	0.0029	0.0029	0.006	0.03	32000

2.8.2 Reactivity ratio of THGA and IBMA

AIBN (0.017 mmol), RAFT (0.084 mmol), THGA, IBMA and 5 mL of 2-MeTHF were combined with a magnetic stirrer into a sample vial, which was then sealed and degassed under argon for 30 minutes. The monomers were combined in differing compositions (table 2.14). The tube was then heated to 65°C in an oil bath and agitated by magnetic stirring. After 2 hours hydroquinone was added to act as a radical scavenger to stop the reaction and a ^1H NMR sample was taken to determine conversion.

Table 2.14 Reaction conditions of RAFT polymerisation of isobornyl methacrylate and tetrahydro-geraniol acrylate to calculate the reactivity ratio of the two monomers.

THGA: MMA	THGA (mmols)	IBMA (mmols)	AIBN (mmols)	RAFT (mmols)	agent
9:1	4.569	0.507	0.012	0.087	
8:2	4.061	1.015	0.012	0.087	
7:3	3.553	1.523	0.012	0.087	
6:4	3.046	2.030	0.012	0.087	
5:5	2.538	2.538	0.012	0.087	
4:6	2.030	3.046	0.012	0.087	
3:7	1.523	3.553	0.012	0.087	
2:8	1.015	4.061	0.012	0.087	
1:9	0.507	4.569	0.012	0.087	

2.8.3 Reactivity ratio of THGA and α -pinene methacrylate

AIBN (0.017 mmol), RAFT (0.084 mmol), THGA, α -PM and 5 mL of 2-MeTHF were combined with a magnetic stirrer into a sample vial, which was then sealed and degassed under argon for 30 minutes. The monomers were combined in differing compositions (table 2.15). The tube was then heated to 65°C in an oil bath and agitated by magnetic stirring. After 2 hours hydroquinone was added to act as a radical scavenger to stop the reaction and a ^1H NMR sample was taken to determine conversion.

Table 2.15 Reaction conditions of RAFT polymerisation of alpha-pinene methacrylate and tetrahydro-geraniol acrylate to calculate the reactivity ratio of the two monomers.

THGA: MMA	THGA (mmols)	α -PM (mmols)	AIBN (mmols)	RAFT agent (mmols)
9:1	4.569	0.507	0.012	0.087
8:2	4.061	1.015	0.012	0.087
7:3	3.553	1.523	0.012	0.087
6:4	3.046	2.030	0.012	0.087
5:5	2.538	2.538	0.012	0.087
4:6	2.030	3.046	0.012	0.087
3:7	1.523	3.553	0.012	0.087
2:8	1.015	4.061	0.012	0.087
1:9	0.507	4.569	0.012	0.087

2.8.4 Block Copolymers

The homopolymers of PIBMA and α -PM were created using the same method as 2.4.2. These homopolymers, once dried were combined with THGA to target a second block of 80 units. The polymer, THGA, AIBN (0.006 mmols) and 5 mL of 2- MeTHF (table 2.16) with a magnetic stirrer into a sample vial, which was then sealed and degassed under argon for 30 minutes. The sample was then heated to 65 °C in an oil bath and agitated by magnetic stirring. After 24 hours, the vessel was cooled and the polymer was precipitated from solution in a 10-fold volume of methanol, filtered and dried in vacuum. Analysis was carried out using ^1H NMR to determine conversion using equation 6 as shown in 2.2.1. GPC, and DSC were also used to determine molecular weight, polydispersity and the T_g of the polymer.

Table 2.16 The molar amounts of polymer, monomer, and AIBN used to produce fully-terpene based block copolymers.

High T_g monomer	THGA (mols)	AIBN (mmols)	Targeted M_n of THGA block
Isobornyl methacrylate	0.0025	0.006	16000
Alpha-pinenemethacrylate	0.0025	0.006	16000

3. Results and Discussion

RAFT agent screening in Toluene

The first stage of this experimental work required the screening of multiple RAFT agents to identify the RAFT agent that was most suitable for the further polymerisations required. MAM's molecules, such as MMA, produce relatively more stabilized radicals owing to the electronic stabilisation from their substituent, often coupled with steric factors, and therefore require a Z-group that will help with the stabilisation of the intermediate radical to favour radical addition on the C=S. Therefore, trithiocarbonates (Z = S-alkyl) or dithiobenzoates (Z = Ph) RAFT agents are typically selected to control the polymerisation of methacrylates and acrylates.²³ Therefore, the RAFT agents selected to screen included, two trithiocarbonates and a dithiobenzoate, the structures of these RAFT agents are shown in figure 3.2.

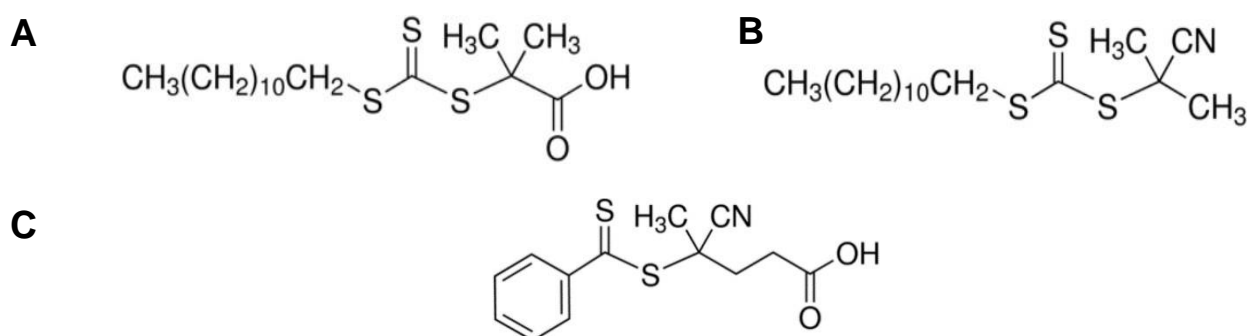


Figure 3.1 The three different RAFT agents used, (A) 2-(Dodecylthiocarbonothioylthio)-2-methylpropanoic acid (DDMAT), (B) 2-cyano-2-propyl dodecyl trithiocarbonate (CPDT), (C) 4-cyano-4-(phenylcarbonothioylthio) pentanoic acid (CPAB).

3.1.1 MMA homopolymers

Homopolymerisations of MMA were carried out using three different RAFT agents (figure 3.2) to control the polymerisation. These polymerisations are shown in table 3.1. The RAFT solution polymerisations in toluene were performed using AIBN as an initiator with a RAFT AGENT: AIBN ratio of 5: 1. The results confirm the inability of DDMAT to control MMA polymerisation, leading to PMMA chains with a broad molecular-weight dispersity ($\bar{D} = 1.70$) and an M_n that does not match the expected theoretical value. DDMAT (Figure 3.2 A) has a tertiary alkyl -R reinitiating group, which has been reported to be a good RAFT AGENT for acrylates, but not applicable for methacrylates.¹⁰⁹ It has been well documented that DDMAT gives essentially no control over polymerisation of methacrylates in solution, this has been demonstrated by the large difference between theoretical and experimental molecular weight and high dispersity for the homopolymerisation of MMA with DDMAT.¹¹⁰

Table 3.1. Results for the MMA homopolymerisation in toluene performed with three different RAFT agents

Expt.	RAFT agent	Conv. ^a (%)	$M_{n, th}^b$	M_n^c	\bar{D}^c
BJ08	DDMAT	60.0	36000	46000	1.70
BJ09	CPDT	50.0	30000	30000	1.19
BJ10	CPAB	50.0	30000	21000	1.07

^a Conversion calculated from ¹H NMR.

^b Theoretical M_n calculated relative to RAFT AGENT and monomer concentration, relative to the actual conversion and given in kg mol⁻¹.

^c \bar{D} and M_n (in kg mol⁻¹) obtained by THF-SEC with RI detector against PMMA standards. (Molar ratio RAFT agent/AIBN 5:1, 65 °C, 300 rpm stirring rate, 5 mL of toluene)

CPDT and DDMAT are trithiocarbonate RAFT agents. Trithiocarbonates have the advantage of being more hydrolytically stable than dithiobenzoates,¹¹¹ such as CPAB, and also cause less inhibition of polymerisations.¹¹² It is known that with appropriate R and Z groups that both dithiobenzoates and trithiocarbonates can provide good control to methacrylates.⁷³ However, the choice of the R group is critical in the case of methacrylates, with the most effective RAFT agent carrying a strongly stabilized R reinitiating group such as a tertiary cyanoalkyl or a cumyl. Therefore, as CPDT gave the best control over molecular weight, this RAFT agent was selected as the most applicable RAFT agent (Table 3.1) to complete further polymerisations.

The polymerisation was monitored by ¹H NMR. The two peak signals located at 6.18 ppm and 5.63 ppm of the ¹H NMR of PMMA show the presence of vinyl whereas the peak signal around 3.83 ppm indicates the presence of methoxy protons. The successful polymerisation of MMA can be identified by the peak at 3.68 ppm.¹¹³ The ¹H NMR of PMMA is shown in figure 3.3.

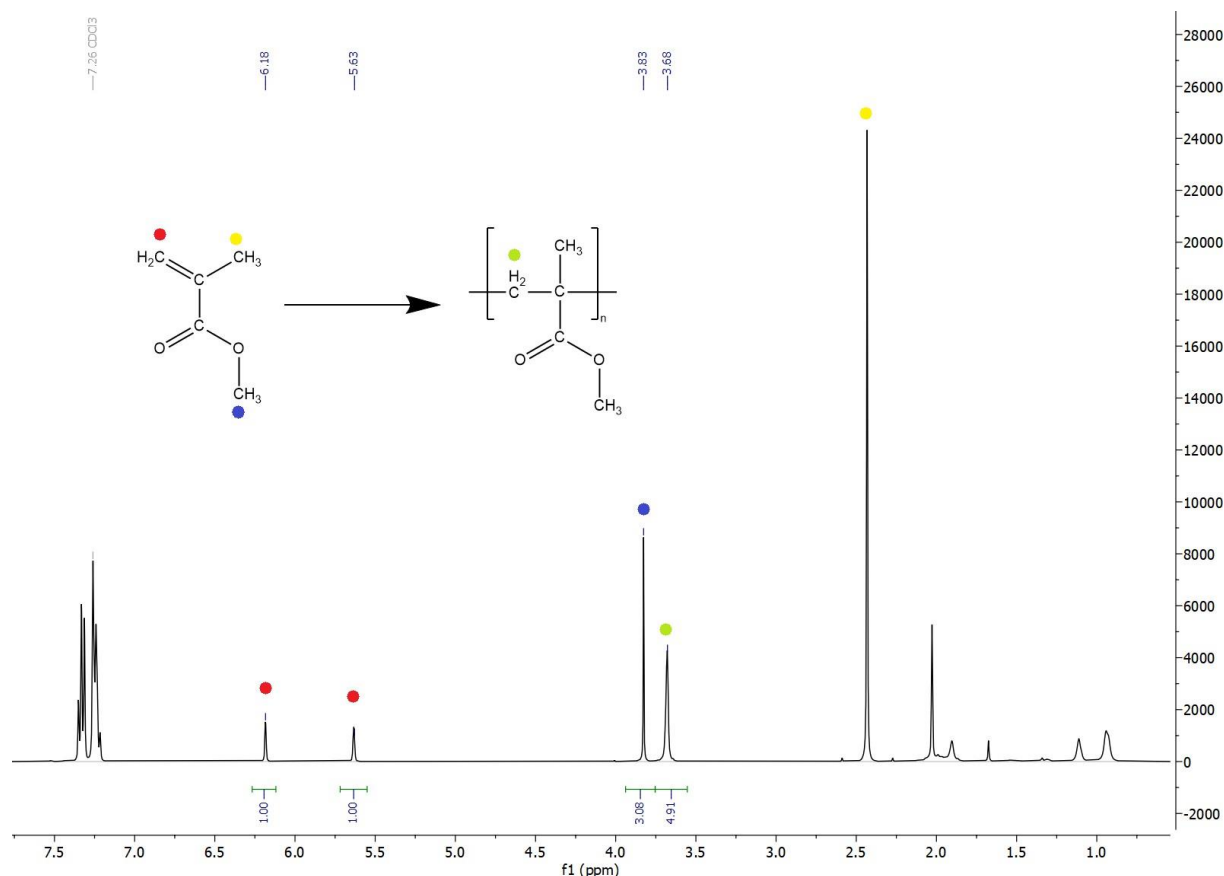


Figure 3.2 ¹H NMR of PMMA with (400 MHz, CDCl₃), δ (ppm): - Appendix 7.2

Thermal analysis was also carried out on the PMMA produced to ensure that the RAFT polymerisation did not affect the *T_g* of the PMMA polymer, these results are shown in Table 3.2. The *T_g* values are determined as the inflexion points from the DSC curves which signify a change in heat capacity. In the temperature range analysed, there is no *T_m* (melting temperature) detected meaning PMMA is an amorphous polymer, as expected.¹¹⁴

Table 3.2 The *T_g* of PMMA polymerised by three different RAFT agents.

RAFT agent	<i>T_g</i>	<i>M_n</i>
DDMAT	123.66	46000
CPDT	103.79	30000
CPAB	106.74	21000

^d *T_g* calculated by DSC, with a heating rate of 10°C per minute, heating range of 0-200°C

The DSC data shows that the T_g of the two polymers made using CPDT and CPAB had very similar T_g . The T_g value obtained for these polymers are also very similar to the literature value of 105°C for ca. 20,000-30,000 M_n .¹¹⁵ The PMMA produced using DDMAT had a higher T_g , this is likely due to the longer chain length of the PMMA (46,000).¹¹⁶

3.1 Synthesis of THGA

The presence of the hydroxyl group on the renewable starting material THGA was utilised to incorporate an acrylic functionality (Figure 1.2). The preparation of the monomer was carried out by acylation with acryloyl chloride on a relatively large scale, to produce a theoretical yield of 25g of THGA, to screen the potential of this new class of renewable biobased monomer derived from side products of the paper industry. More sustainable approaches to the same molecule are currently under study, however these methods were not used due to the extra steps required to produce the T3P® catalyst. The success of the reaction was then confirmed by ^1H and ^{13}C NMR (Figure 3.1), showing the presence of the reactive vinyl bonds ($\delta = 5.8\text{--}6.5$ ppm). The small peak at $\delta = 5.4$ ppm indicates residual DCM, which is used as the solvent for the synthesis of THGA. The peaks at between 3.4-1.9 ppm is likely due to impurities caused by side reactions in the acrylation of the THG.¹¹⁷ The overall conversion of this reaction was 45%, with impurities calculated as 10% in addition to the overall weight of the THGA.

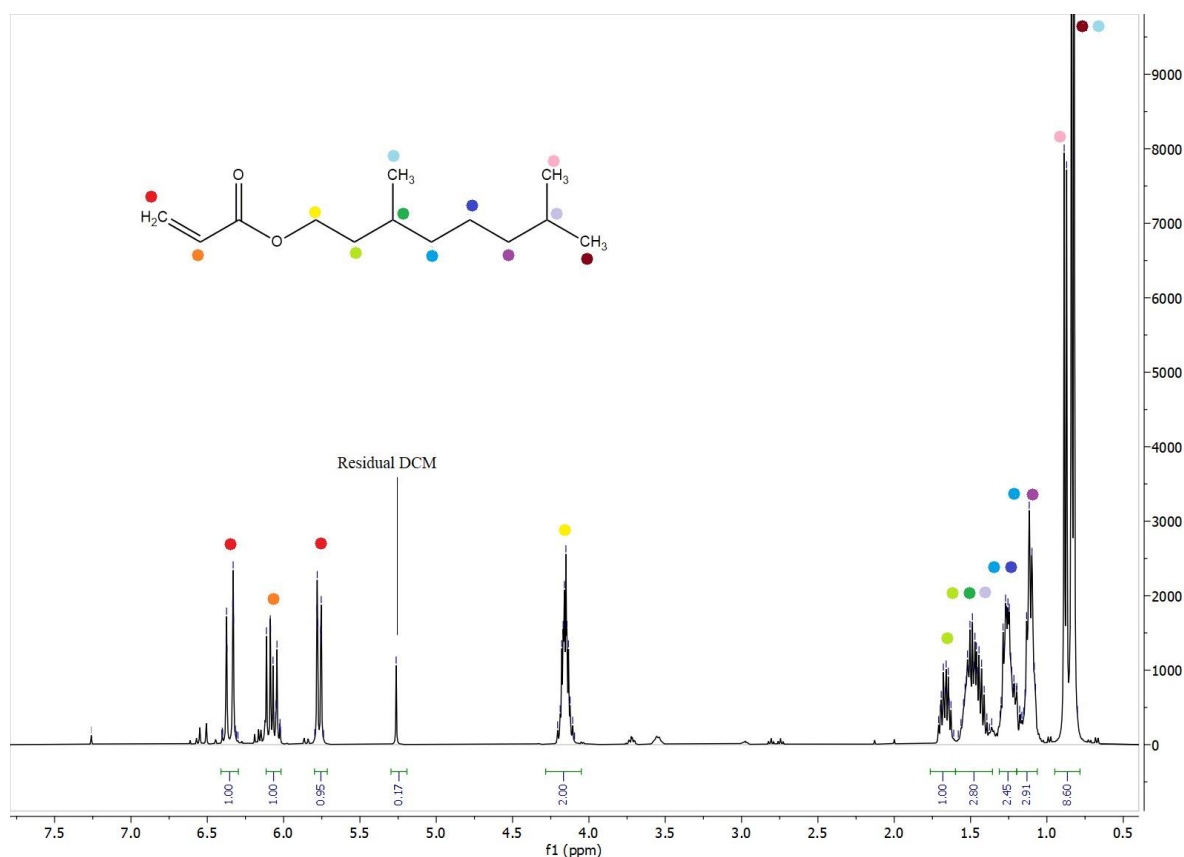


Figure 3.3 ^1H NMR of THGA (400 MHz, CDCl_3). – Appendix 7.1

3.2.2 THGA homopolymers

THGA was also polymerised using the same RAFT agents, DDMAT, CPDT and CPAB, as for MMA homopolymerisation. THGA has an acrylate functional group therefore it is also a MAM like MMA, and the same types of RAFT agent are expected to be able to successfully polymerise THGA. The results of the RAFT homopolymerisation of THGA (table 3.3.)

Table 3.3. results of the homopolymerisation of THGA using three different types of RAFT agents.

Expt.	RAFT agent	Conv ^e (%)	$M_{n,th}^f$	M_n^g	D^g
BJ11	DDMAT	70.0	6300	5800	2.49
BJ12	CPDT	66.0	6000	6100	1.31
BJ13	CPAB	66.0	6000	8000	1.28

The dispersity of PTHGA is larger than that of PMMA, this is likely due to branching of the PTHGA polymers, this has been noted previously with PTHGA,³⁴ and other terpene-based polymers.^{118,119} The branching might be due to the occurrence of undesired chain transfer to solvent reactions, as well as chain transfer to polymer reactions, which introduces the presence of midchain radical (MCRs). Both intramolecular (also referred to as backbiting) and intermolecular chain transfer reactions are relatively common in acrylic polymerisation, with intra- molecular transfer being the predominant pathway.¹²⁰ The presence of MCRs in the polymer chains can yield the formation of branches and/or the formation of macromonomers (bearing ω -vinyl functionalities) and initiating radicals through β -scission.¹²¹ The polymerisation of THGA with CPDT and CPAB showed a better dispersity than with DDMAT. Although DDMAT has previously been reported as a good RAFT agent in the polymerisation of butyl acrylate.¹²² Furthermore, as DDMAT is an incompatible RAFT agent with MMA, this RAFT agent was discarded for future polymerisations. CPDT showed the most accurate molecular weight when compared with the targeted molecular weight and as CPDT also showed good control over the polymerisation of MMA in toluene, this RAFT agent was used in the copolymerisations of THGA and MMA. The ¹H NMR of PTHGA (figure 3.4) shows evidence of polymerisation. The polymerisation is indicated by the ¹H NMR peak at 4.21 ppm.

^e Conversion calculated from ¹H NMR.

^fTheoretical M_n calculated relative to RAFT agent and monomer concentration, relative to the actual conversion and given in kg mol⁻¹.

^g D and M_n (in kg mol⁻¹) obtained by THF-SEC with RI detector against PMMA standards. (Molar ratio RAFT AGENT/AIBN 5:1, 65 °C, 300 rpm stirring rate, 5 mL of toluene)

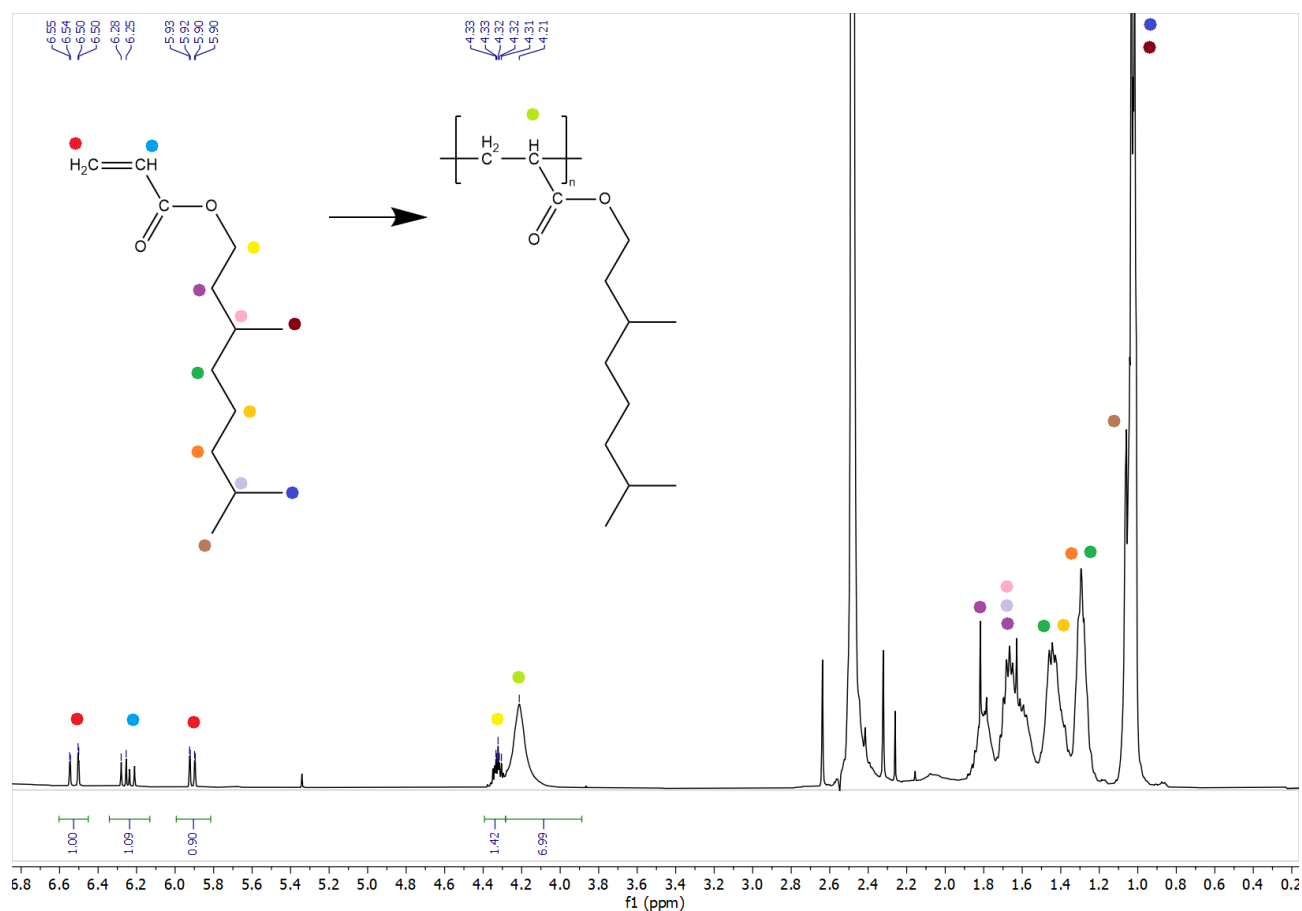


Figure 3.4 ^1H NMR of PTHGA (400 MHz, CDCl_3) – Appendix 7.3

Thermal analysis of PTHGA was carried out using DSC, (table 4). PTHGA synthesised in presence of DDMAT was not analysed due to an error with precipitation which caused not enough sample to remain to analyse. The T_g of PTHGA was lower than the literature value of -46°C .¹²³ This is likely due to the short chain length caused by the branching of the polymer. The higher the amount of chain ends in high branching systems contribute more to the free volumes in the branched THGA polymer, and so therefore has a less closely packed structure than a polymer which has a more closely packed structure. Therefore, it may be assumed that this static property, which reflects the difference of free volumes in polymer systems with different degrees of branching, manifests the reason for the observed dependence of T_g on the degree of branching of the polymer systems.¹²⁴

Table 3.4. T_g of the homopolymers of PTHGA.

RAFT agent	T_g
CPDT	-63.28
CPAB	-62.01

^h T_g determined by DSC, heating rate of 10°C with a heating range of $-90 - 100^\circ\text{C}$

3.3 Random copolymer analysis

To investigate the properties of THGA when in a random copolymer, three random copolymers of MMA and THGA were produced using different molar ratios of 1:1, 3:1 and 1:3. CPDT was used as the RAFT agent for the random copolymerisations as it was shown to be compatible with both monomers. Random copolymers of MMA and THGA were produced in varying monomer compositions (table 5).

Table 3.5. results obtained for the random copolymers of PMMA-*ran*-PTHGA.

Expt.	MMA: THGA molar ratio	MMA conv. ⁱ (%)	THGA conv. ⁱ (%)	$M_{n,th}^j$	M_n^k	\bar{D}^k
BJ15	1:1	91	38	38000	50000	1.31
BJ16	3:1	81	23	40000	42000	1.24
BJ17	1:3	88	40	31000	43000	1.29

The NMR of the random copolymers (figure 3.5) shows the successful polymerisation of MMA can be identified by the peak at 3.68ppm. The NMR also shows that THGA has been successfully polymerised by the presence of the broad peak at around 4.16ppm.

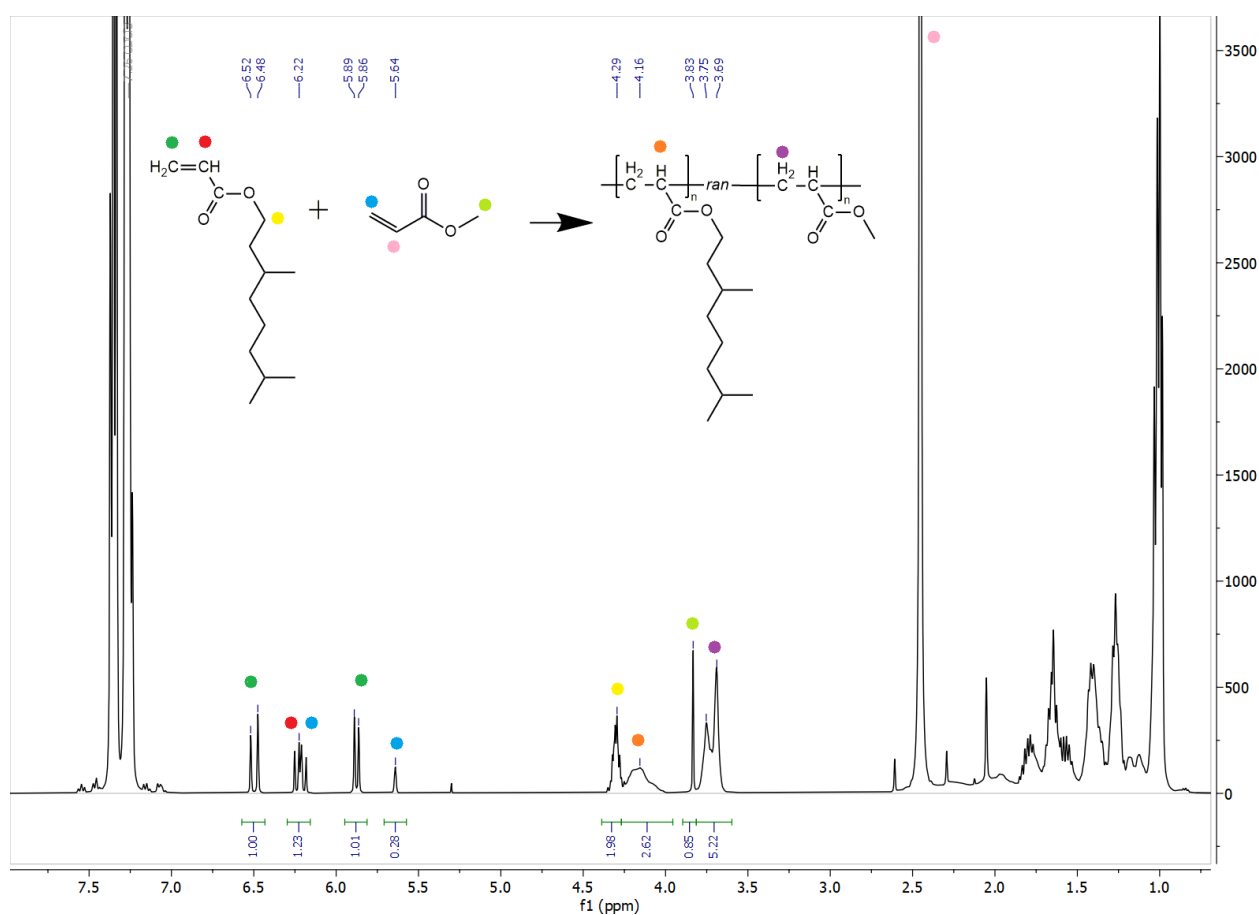


Figure 3.5 The ^1H NMR of the 1:1 molar ratio PMMA-*ran*-PTHGA. (400 MHz, CDCl_3) – Appendix 7.4

The high conversion of MMA but the lower conversion of THGA after 24 hours indicates a difference in the reactivity of the two monomers, this will be further investigated in section 3.4. These copolymers showed a

ⁱ Conversion calculated from ¹H NMR.

^jTheoretical M_n calculated relative to RAFT AGENT and monomer concentration, relative to the actual conversion and given in kg mol⁻¹.

^k \bar{D} and M_n (in kg mol⁻¹) obtained by THF-SEC with RI detector against PMMA standards. (Molar ratio RAFT agent/AIBN 5:1, 65 °C, 300 rpm stirring rate, 5 mL of toluene)

higher dispersity than the homopolymers of MMA, therefore the difference is likely due to the presence of the THGA monomer, however, a dispersity value below 1.3 can still be considered a successful RAFT polymerisation.²³

Thermal analysis of these polymers was carried out by DSC (table 3.6) to find the T_g of the random copolymers and to ensure that a successful copolymerisation has occurred. The T_g value depends on the monomer composition of the polymer.

Table 3.6. T_g values obtained via DSC for copolymers of PMMA-*ran*-PTHGA.

Molar ratio of MMA: THGA	Percentage of MMA in copolymer (%)	T_g^1
1:1	70.5	-24
3:1	77.9	38
1:3	68.8	16

All the random copolymers produced exhibited one T_g and are therefore consistent with other random copolymers produced and therefore shows that the polymer consists of both monomers.¹²⁵ The lower-than-expected T_g of the 1:1 molar ratio random copolymer could have been caused by some solvent remaining within the polymer. The ability to tune the T_g of the random copolymer is an advantage as it allows the terpene-based THGA to be incorporated into a wider range of applications than if the THGA was only used as a homopolymer.

3.4 Reactivity Ratios of THGA and MMA in toluene

The low conversion of THGA when compared to MMA in the random copolymers, prompted investigation of the reactivity ratios of these monomers. To perform these calculations, the random polymerisation of MMA and THGA was studied at varying monomer compositions, these polymerisations were performed with CPDT as the RAFT agent and with toluene as the solvent. The reaction was aimed at low conversion (ca. 10%) to study the propagation step of the polymerisation. The monomer composition and conversions are shown in table 3.7. The reactivity ratio is a measure of the tendency for a comonomer to show a preference for insertion into a growing chain in which the last inserted unit was the same, rather than the other comonomer.¹²⁶

Table 3.7. monomer compositions and polymer compositions of the random copolymers of MMA and THGA used for the reactivity ratio calculations.

MMA ratio	THGA ratio	MMA conv. ^m (%)	THGA conv. ^m (%)	Composition of MMA in polymer. ⁿ (%)
0.1	0.9	0.917	2.166	29.75%
0.2	0.8	11.364	1.010	54.86%
0.3	0.7	1.923	1.818	51.40%
0.4	0.6	2.941	1.961	60.00%
0.5	0.5	2.597	0.990	72.40%
0.6	0.4	4.624	0.971	82.65%
0.7	0.3	4.985	0.952	83.96%
0.8	0.2	12.647	1.887	87.02%
0.9	0.1	10.917	0.935	92.11%

¹ T_g (°C) obtained from DSC with heating range of -90 to 200°C with a heating rate of 10°C min⁻¹m Conversion calculated from ¹H NMR.

ⁿ Composition determined by percentage of MMA present in random copolymer. Calculated by ¹H NMR.

Using the terminal model and the Mayo-Lewis equation (9), allowed the preference of one monomer to react over the other to be compared. These calculations were performed using Python.

$$F_1 = 1 - F_2 = \frac{r_1 f_1^2 + f_1 f_2}{r_1 f_1^2 + 2 f_1 f_2 + r_2 f_2} \quad (9)$$

where r_1 and r_2 are the reactivity ratios, f_1 and f_2 are the mole fractions of monomers 1 and 2 in the monomer feed and F_1 is the mole fraction of units from monomer 1 in the copolymer. Due to the anomalous result for $f_1=0.2$, this value was excluded from the calculations. The values calculated for the reactivity ratio of MMA and THGA are shown (figure 3.6).

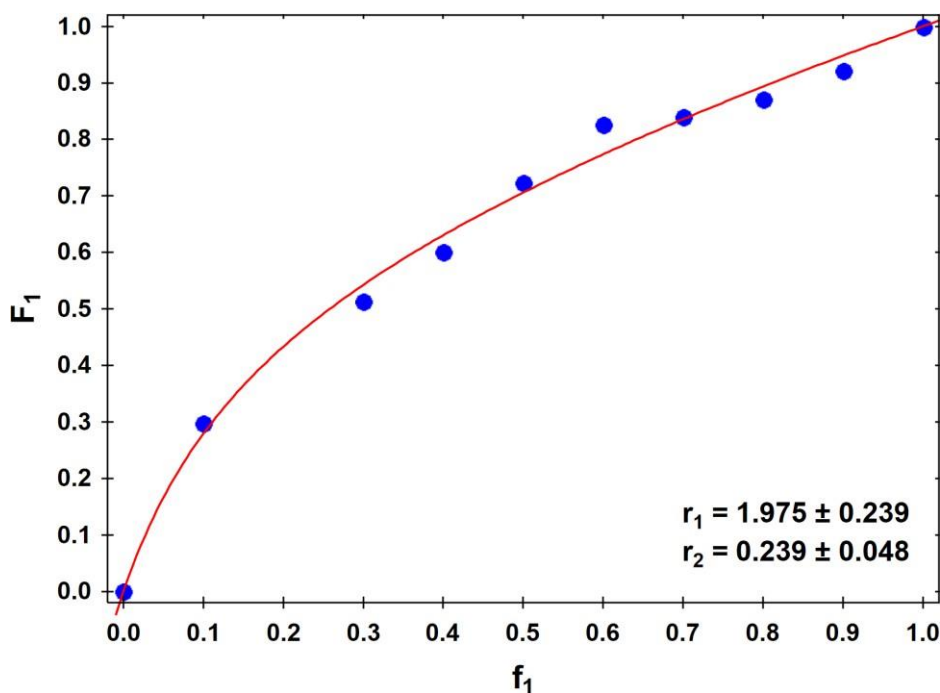


Figure 3.6 The reactivity ratios of MMA and THGA. MMA is monomer 1 for this reactivity ratio. The blue circles indicate the experimental data collected and the red line shows the copolymer composition trend.

As the value of r_1 is above 1 and the value of r_2 is below 1, this shows that the random copolymer has compositional drift. This is where one monomer, in this case, MMA, is incorporated faster into the polymer than the other monomer, THGA. When the first monomer is used up, more segments of the second monomer are added. The variation of the monomer feed and the difference in the reactivity ratio, results in the difference in the rates of incorporation of the monomer. Therefore, changes in the instantaneous composition arising from these variations are reflected along the chains. This leads to the formation of gradient copolymers.¹²⁷ This contrasts with block copolymers, which have no change in composition until the crossover from one block to the other, and random copolymers, which have no continuous change in instantaneous composition (figure 3.7). To achieve this continuous change in instantaneous composition, all chains must be initiated simultaneously and must survive until the end of the polymerisation. Therefore, a living (ionic) or controlled/living radical polymerisation technique must be employed, as the significant presence of chain-breaking reactions would lead to heterogeneity in composition as well as in molecular weight.¹²⁸

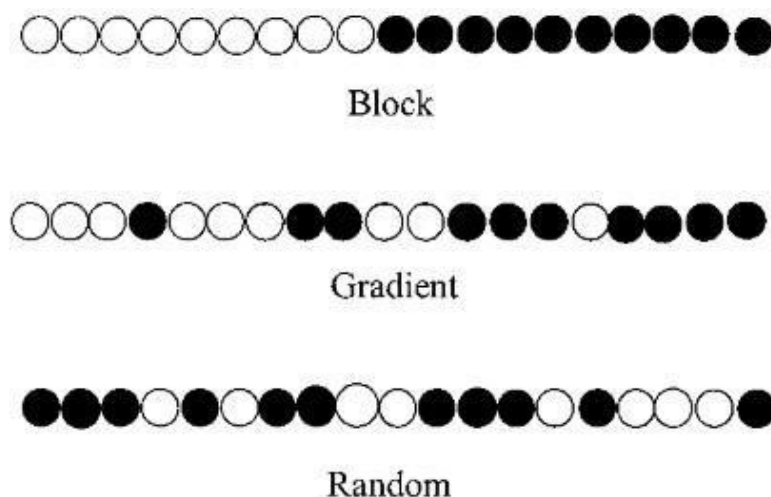


Figure 3.7 The difference between the structures of block, gradient, and random copolymers

This polymerisation has been produced in a batch system, using RAFT polymerisation, therefore, the gradient is produced spontaneously due to the feed composition drift that occurs during the reaction. The strength of the gradient is dictated only by the reactivity ratios of the monomer pair and initial monomer feed and cannot be further controlled.¹²⁸ This is known as a spontaneous gradient copolymer. The R^2 value (figure 3.8), also known as the coefficient of determination, shows the proportion of the variance in the dependent variable that is predictable from the independent variable.¹²⁹ R^2 is used as a measure of goodness of fit and as a measure of precision in predictions for the general linear model.¹³⁰ An R^2 close to 1 implies an almost perfect relationship between the model and the data, whereas an R^2 close to 0 implies that just fitting the mean is equivalent to the model fitted.¹³¹

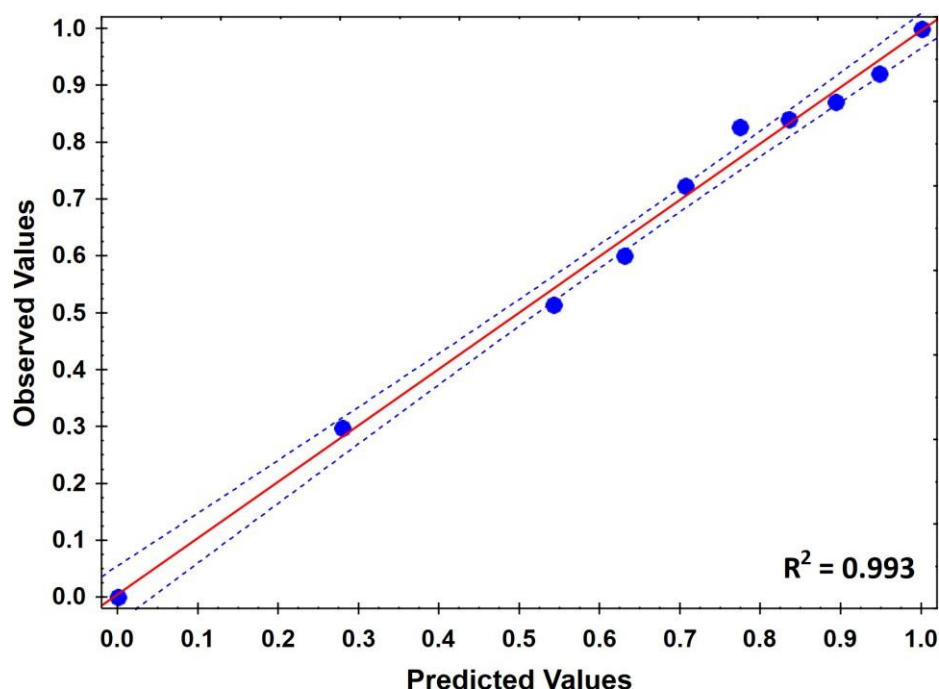


Figure 3.8 The R^2 value of the reactivity ratio model for MMA and THGA. The blue points are the Mayo-Lewis model prediction (predicted values) against the experimental data (observed values). The red line corresponds to the linear regression prediction. The blue dashed lines indicate the regression bands built with a 95% confidence level.

The reactivity ratio of MMA ($r_M = 1.975$) to THGA ($r_T = 0.239$) is comparable to the reactivity ratio of MMA (r_M) to butyl acrylate (r_B), $r_M = 2.17$ and $r_B = 0.42$.¹²⁷ The similarity between the two ratios supports that THGA can be used as a terpene alternative to butyl acrylate, as THGA reacts similarly to butyl acrylate when producing random copolymers with MMA. Therefore, THGA can be used as a replacement for butyl acrylate when used in random copolymers.

3.5 Block copolymer analysis

Block copolymers of MMA and THGA were produced, aiming at two different chain lengths of the ‘soft’THGA block. block copolymers are produced, because their final morphologies can usually be finely controlled and even predicted by the molecular parameters, such as the molecular weight, the length of each block and the chemical nature of blocks. The results of the production of MMA and THGA block copolymers are shown in table 3.8. PMMA was used to produce the block copolymers which had been previously synthesised in 3.2.1, with an M_w of 30000.

Table 3.8. The result of PMMA-*b*-PTHGA copolymers aiming at two different chain lengths of THGA.

Expt.	THGA conv. ^o (%)	Targeted PTHGA chain length ^p	$M_{n,th}$ ^q	M_n ^r	\bar{D} ^r	T_g
BJ23	86	30000	60000	25000	1.56	-51°C, 126°C
BJ24	91	15000	45000	65000	1.73	-50°C, 115°C

Large dispersity and difference between targeted chain length and actual chain length were noticed when adding the soft THGA block due to the branching of the THGA molecules. The GPC of these polymers ensured that an extension had occurred instead of two different polymerisations (figure 3.9) this is shown by the increase in M_n between the homopolymer and block copolymer indicated by the reduction in elution time for higher M_n polymers. The addition of the THGA block is also confirmed due to the GPC only having one peak and so all polymers eluted at the same time. However, the GPC chromatogram of BJ23 indicates that some homopolymer of PTHGA has formed, giving a small secondary peak (figure 3.9 A). The M_n of the block copolymers also increased from the homopolymers, and so this confirmed that the THGA block had been added to the PMMA homopolymer. The dispersity is higher for the lower amount of THGA added to the MMA block, this may be due to an increase in branching due to the lower molar concentration of THGA. This effect has been previously reported with the production of styrene-THGA-styrene triblock copolymers, to reduce the branching of the THGA molecules, the molar concentration of the THGA to solvent must be above 3.6 mol L⁻¹.³⁴

^o Conversion calculated from ¹H NMR.

^p Theoretical M_n calculated relative to RAFT AGENT and monomer concentration, relative to the actual conversion and given in kg mol⁻¹.

^q Theoretical M_n calculated by the sum of the M_n of the PMMA and theoretical M_n of the PTHGA block

^r \bar{D} and M_n (in kg mol⁻¹) obtained by THF-SEC with RI detector against PMMA standards. (Molar ratio RAFT agent/AIBN 5:1, 65 °C, 300 rpm stirring rate, 5 mL of toluene)

^s T_g (°C) obtained from DSC with heating range of -90 to 200°C with a heating rate of 10°C min⁻¹

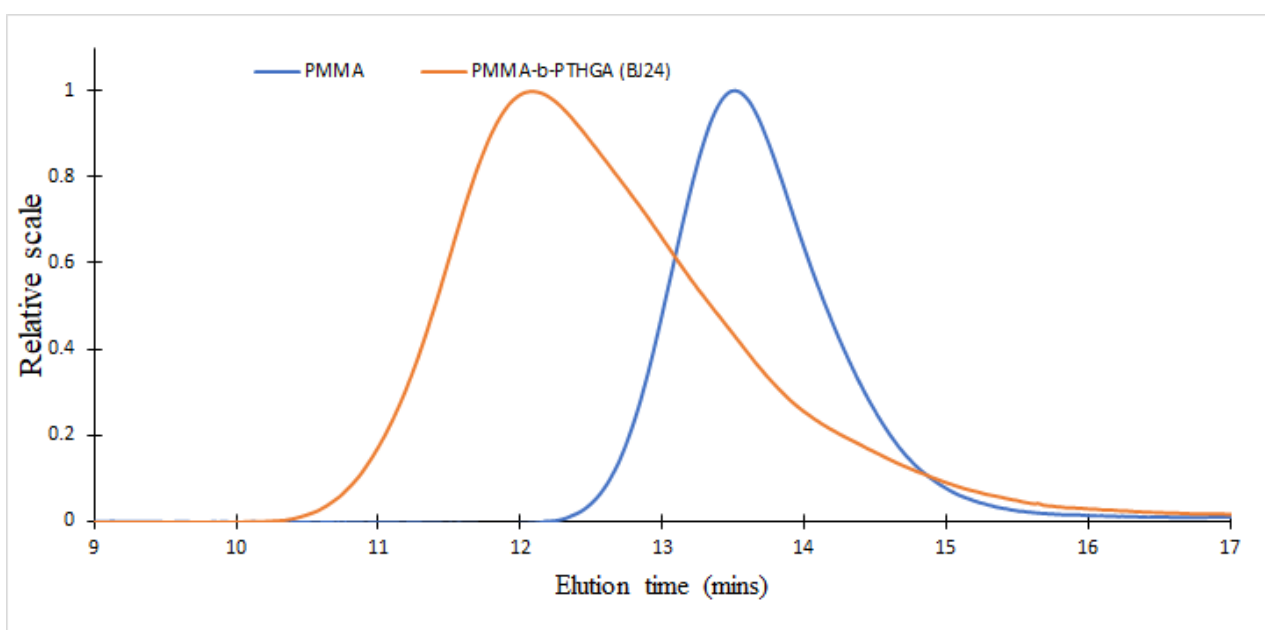
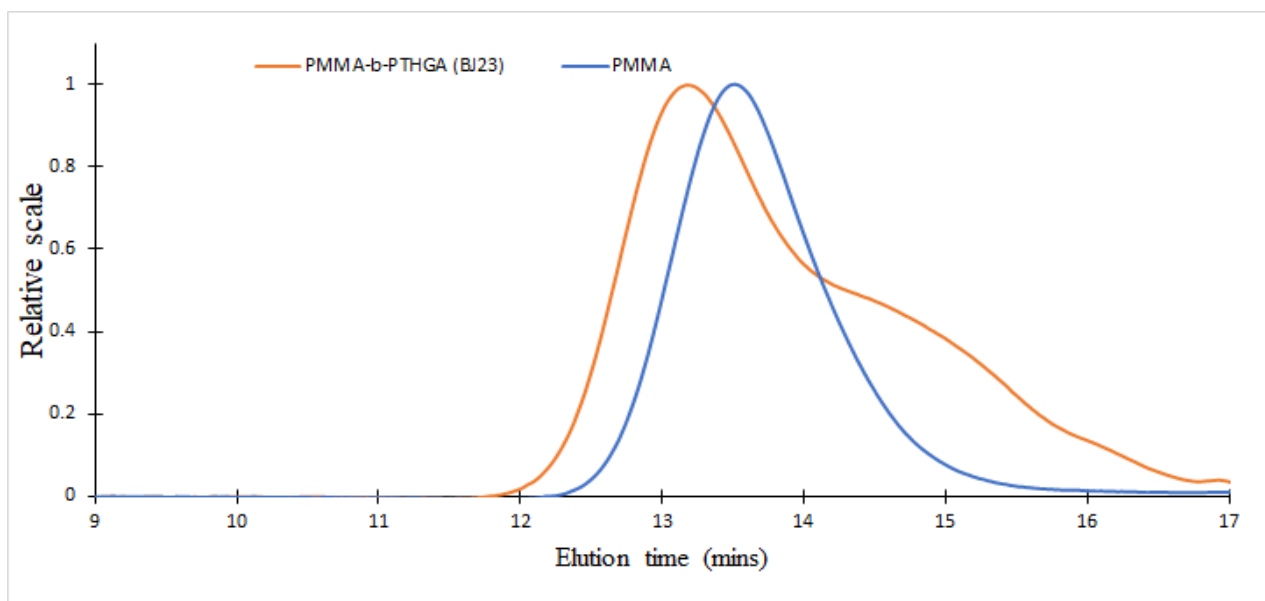


Figure 3.9 The GPC chromatogram of the PMMA-*b*-PTHGA copolymers (A) from BJ23 and (B) from BJ24.

The block copolymers were analysed by DSC (Figure 3.10). For the block copolymers, there were two T_g s and this shows the existence of different domains of PMMA block and PTHGA block. Although block copolymers have been successfully produced, due to the large dispersity, possibly due to the branching of the PTHGA block and the difference between target and actual molecular weight, further optimisation is required. However, due to time constraints, this could not be achieved during this project.

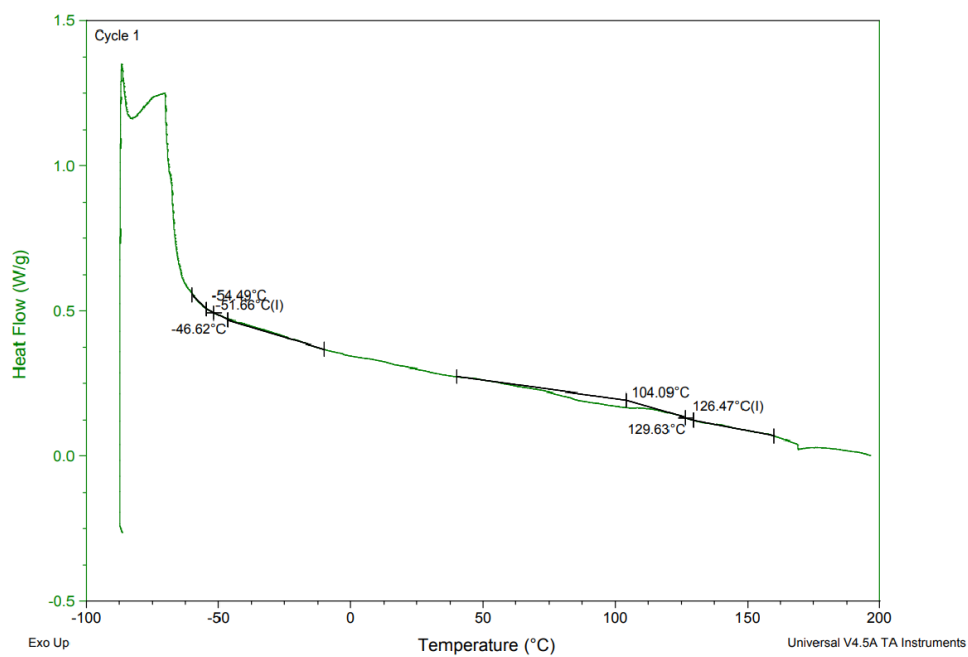
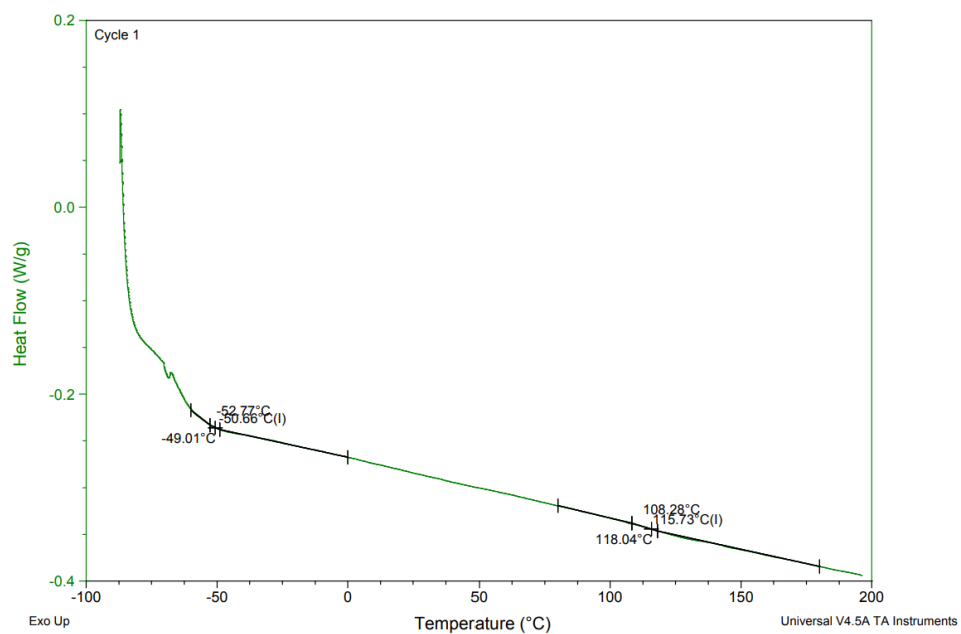
A**B**

Figure 3.10 (A) The DSC of PMMA-*b*-PTHGA from expt. BJ23, (B) The DSC of PMMA-*b*-PTHGA from expt. BJ24 identifying the two separate T_g s of the block copolymers.

3.7 RAFT agent screening in 2-MeTHF

3.7.1 Initial screening

2-MeTHF has a relatively high boiling point (80°C) and showed a good dissolution ability for all the adopted reagents. This allowed different polymerisation strategies to be carried out directly in 2-MeTHF, without further alterations.⁸⁹ To ensure that RAFT polymerisation had good control in 2-MeTHF, two different RAFT agents CPDT and CPAB, were used to polymerise MMA in three different solvents: toluene, THF and 2-MeTHF (Table 3.9). These RAFT agents had been previously shown to have good control over the polymerisation of MMA in toluene. THF was chosen to act as a petrochemical comparison to 2-MeTHF, as THF and 2-MeTHF have similar structures and polarity and therefore a similar reactivity.¹³²

Table 3.9 The results from the RAFT screening using, two different RAFT agents and three solvents.

Solvent	RAFT agent	Conv. [†] (%)	$M_{n, th}^u$	M_n^v	\bar{D}^v
2-MeTHF	CPDT	60	20700	130000	8.34
Toluene	CPDT	42	14500	23000	1.46
THF	CPDT	60	20700	22000	1.40
2-MeTHF	CPAB	34	11300	11000	1.13
Toluene	CPAB	44	14500	11000	1.10
THF	CPAB	52	17300	20000	1.60

The data gathered from the GPC showed that whilst CPDT gave better conversion overall, when used in 2-MeTHF, this RAFT agent gave very poor control of the polymer molecular weight dispersity. This shows that CPDT has poor RAFT control in 2-MeTHF. However, in 2-MeTHF, CPAB gave very good control over the polymerisation of MMA, as the M_n from the GPC was very close to the targeted molecular weight as well as having a good dispersity value. The dispersity value for CPAB in 2-MeTHF is also very similar to the dispersity value for CPAB in toluene, therefore it is a good RAFT agent in both solvents.

The GPC chromatogram of CPDT in 2-MeTHF showed a bimodal molecular weight distribution (Figure 3.11 A). and the UV peak did not completely overlap with the bimodal dRI peak. The broad, non-symmetrical dRI trace, indicates loss of control during the reaction due to polymer chains propagating at different rates, and therefore not controlled by the RAFT agent. The absence of UV signal for the polymer population of higher molecular weights suggests that the polymer does not have RAFT agent end-groups, and thus that the polymer must have grown by conventional radical polymerisation. However, the GPC chromatogram of CPAB in 2-MeTHF showed complete overlap between the UV peak and the dRI peak and a singular peak (Figure 3.11 B), this shows that for this polymerisation, CRP is unlikely to have occurred. Therefore, for further polymerisations in 2-MeTHF, CPAB was used as the RAFT agent.

[†] Conversion calculated from ¹H NMR.

^u Theoretical M_n calculated relative to RAFT AGENT and monomer concentration, relative to the actual conversion and given in kg mol⁻¹.

^v \bar{D} and M_n (in kg mol⁻¹) obtained by THF-SEC with RI detector against PMMA standards. (Molar ratio RAFT AGENT/AIBN 5:1, 65 °C, 300 rpm stirring rate, 5 mL of solvent)

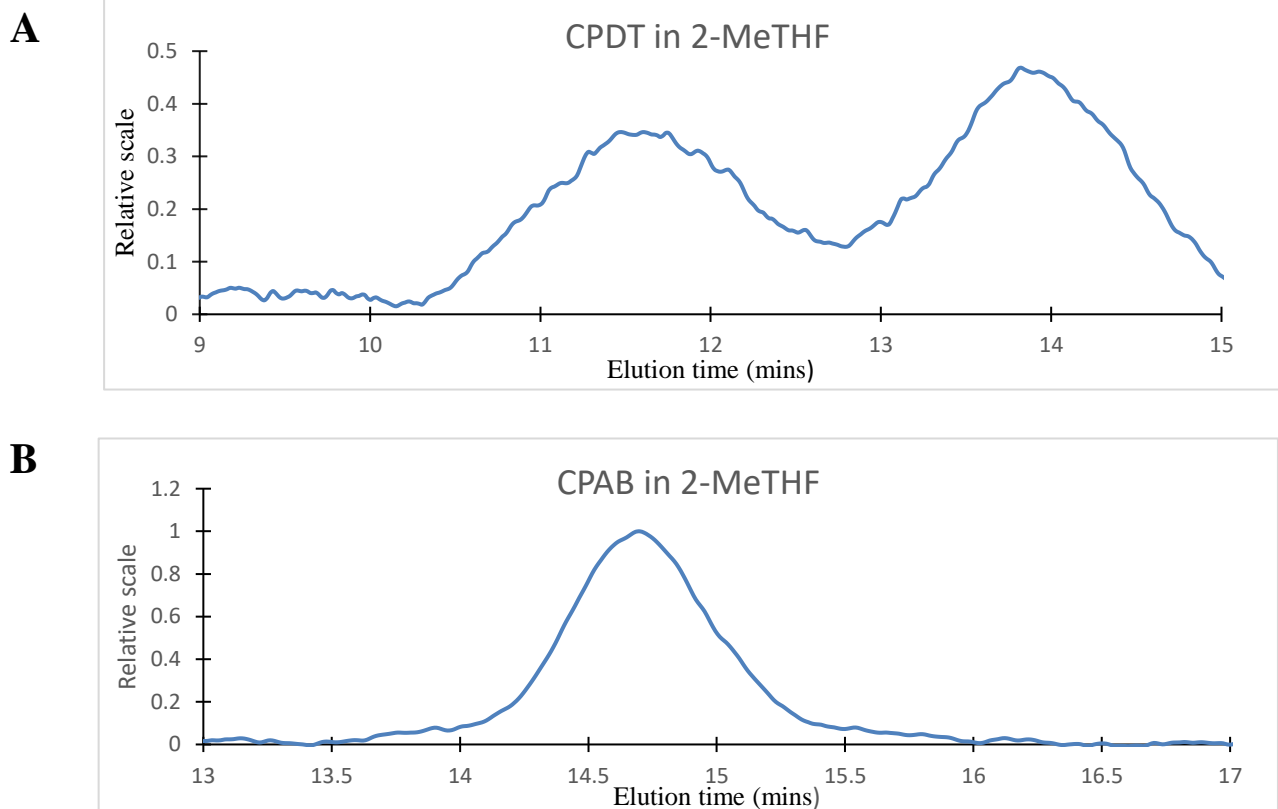


Figure 3.11 the chromatograms from the GPC of (A) the polymerisation of MMA in 2-MeTHF with CPDT as the RAFT agent and (B) the polymerisation of MMA in 2-MeTHF with CPAB as the RAFT agent.

3.7.2 Investigation of Solubility of RAFT agents

The solubility of both RAFT agents was tested in 2-MeTHF and toluene to investigate whether the incompatibility was due to the RAFT agent (CPDT) being insoluble in 2-MeTHF. UV/vis spectra of the RAFT agent dissolved in the solution was measured at 0 hours then again at 24 hours to see if any change in solubility was detected, the results of these are shown (table 3.10).

Table 3.10 The results of the UV at 350 nm for CPDT and 370 nm for CPAB

RAFT agent	Solvent	UV Intensity ^w (0 hours)	UV Intensity ^w (24 hours)
CPDT	2-MeTHF	1.923	1.987
CPDT	toluene	2.318	2.399
CPAB	2-MeTHF	1.413	1.575
CPAB	toluene	1.623	1.710

The results of the UV/Vis spectroscopy confirm that CPAB is soluble in 2-MeTHF and toluene and that CPDT was also shown to be soluble in both solvents, both RAFT agents were also shown to be more soluble in toluene than 2-MeTHF. Therefore, the solubility of the RAFT agent CPDT does not appear to be the cause of the RAFT agent incompatibility with 2-MeTHF. However, as the solubility of the RAFT agent in these solvents was only investigated at room temperature due to time restrictions, this experiment has some limitations. To further understand the solubility of these RAFT agents a UV/Vis study should be carried out at the reaction temperature(65°C).

^w UV/Vis spectra measured between 300-700 nm with a step of 10 nm, using an Epoch 2

3.7.3 Identifying the most important RAFT agent group.

To investigate which part of the RAFT agent was causing the incompatibility issues, two other RAFT agents were used to polymerise MMA in 2-MeTHF at 65°C. The structures of these RAFT agents (figure 3.12), 4-cyano-4-[dodecylsulfanylthiocarbonylsulfonyl] pentatonic acid (CPAD) has the same Z group as CPDT and the same R group as CPAB. 4-cyano-2-propyl benzodithioate (CPBD) has the same Z group as CPAB and the same R group as CPDT. Therefore, this should identify which group on the RAFT agent is the most important for RAFT polymerisations in 2-MeTHF of MMA.

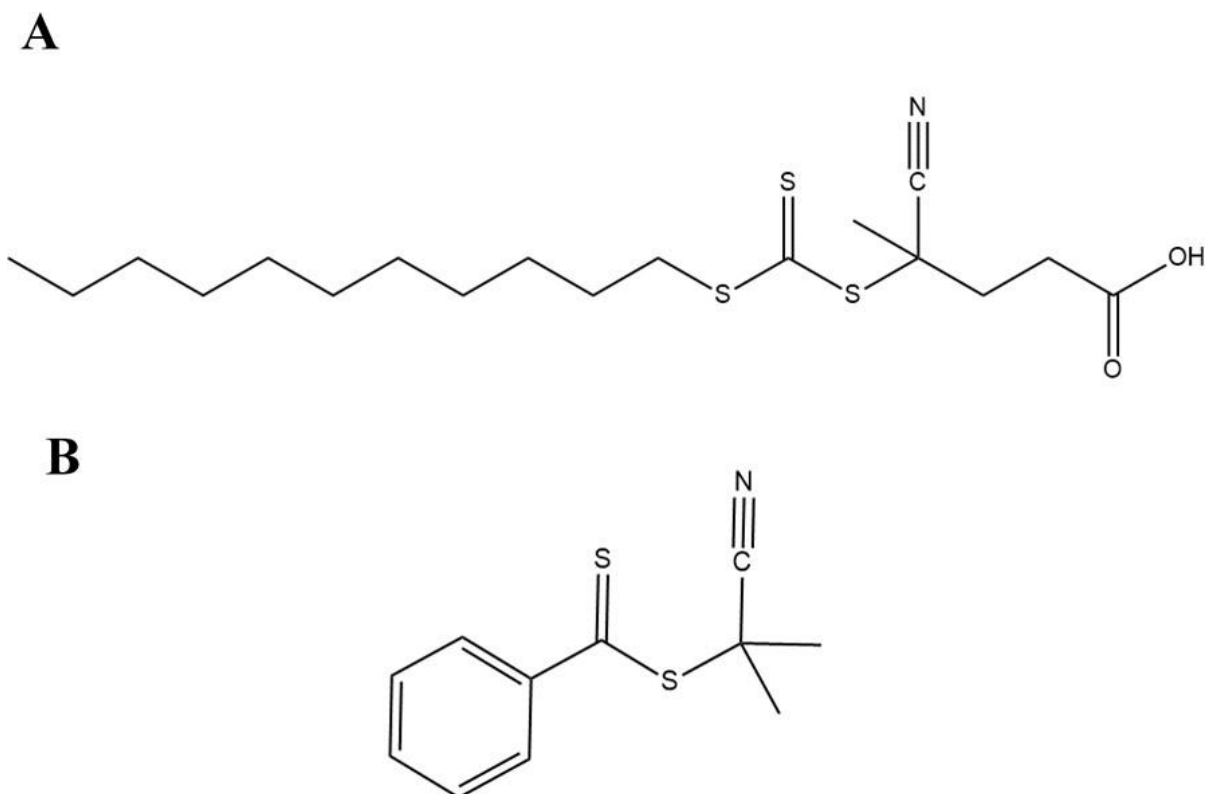


Figure 3.12 The structures of the RAFT agents (A) 4-cyano-4-[dodecylsulfanylthiocarbonylsulfonyl] pentatonic acid (CPAD) and (B) 4-cyano-2-propyl benzodithioate (CPBD).

The polymerisations of MMA in 2-MeTHF were carried out to ensure that only the RAFT agent could affect the polymerisation. The results of these polymerisations are shown (table 3.11).

Table 3.11 The results of the polymerisation of MMA using two different RAFT agents, CPAD and CPBD.

Expt.	RAFT agent	Conv. ^{aa} (%)	$M_{n,th}^{bb}$	M_n^{cc}	\bar{D}^{cc}
BJ56	CPAD	45	12500	19700	1.48
BJ57	CPBD	30	6650	4800	1.16

^{aa} Conversion calculated from ¹H NMR.

^{bb} Theoretical M_n calculated relative to RAFT AGENT and monomer concentration, relative to the actual conversion and given in kg mol⁻¹.

^{cc} \bar{D} and M_n (in kg mol⁻¹) obtained by THF-SEC with RI detector against PMMA standards. (Molar ratio RAFT agent/AIBN 5:1, 65 °C, 300 rpm stirring rate, 5 mL of 2-MeTHF)

The RAFT agent CPBD showed a lower dispersity and had a molecular weight close to the targeted molecular weight, therefore this RAFT agent is better than CPAD for polymerisations of MMA in 2-MeTHF. As CPBD and CPAB both have the same Z group (benzene) and gave better dispersity values in 2-MeTHF than CPDT and CPAD, which have a thiododecyl Z group. It can be suggested that the Z group of the RAFT agent has the greatest importance when using 2-MeTHF as the solvent for polymerisations of MMA at 65°C. This may be due to the slightly more electron-withdrawing nature of the thiododecyl group (Z) compared to the benzene group of CPAB and CPBD. In addition, the polymerisation of MMA with CPBD had a lower conversion than with CPAD, this is due to dithioesters having a longer inhibition period which will make the polymerisation start later (retardation) and therefore the final conversion at the same time point will be lower.^{133,134} A similar effect has been noted with the RAFT polymerisation of MMA in benzene, in which Benaglia *et al.* showed that an electron-withdrawing Z group of a RAFT agent caused a higher conversion but also higher \bar{D} .¹³⁵ Therefore it could be suggested that this effect also has significance for RAFT polymerisation of MMA in 2-MeTHF, however further analysis would be required to definitively prove this.

3.8 Homopolymerisation in 2-MeTHF

3.8.1 High T_g Homopolymers in 2-MeTHF

To ensure that MMA and THGA were able to be polymerised in 2-MeTHF, these were polymerised using CPAB as the RAFT agent as this RAFT agent has been shown to be most effective in the polymerisation of methacrylates in 2-MeTHF.⁸⁹ Terpene-based high T_g monomers IBMA and α -PM were also polymerised (table 3.12), these monomers were analysed to determine if they could also be used as a replacement for MMA in the random and block copolymers, as these monomers have a similar T_g to MMA.

Table 3.12 The results of the high T_g homopolymers.

Expt.	Monomer	Conv. ^{dd} (%)	$M_{n,th}^{ee}$	M_n^{ff}	\bar{D}^{ff}
BJ53	MMA	48	10000	8500	1.13
BJ54	IBMA	19	8000	11000	1.21
BJ55	α -PM	45	19000	17000	1.22

In the ¹H NMR of PIBMA before precipitation (figure 3.13), the appearance of a broad peak at δ 4.45 - 4.70 ppm, confirms polymerisation has occurred; this peak is a result of the repeating proton labelled by the light green dot. In conjunction with a with the reduction of the red doublet peaks at 5.76 and 5.23 ppm, therefore the polymerisation is known to have occurred.

^{dd} Conversion calculated from ¹H NMR.

^{ee} Theoretical M_n calculated relative to RAFT AGENT and monomer concentration, relative to the actual conversion and given in kg mol⁻¹.

^{ff} \bar{D} and M_n (in kg mol⁻¹) obtained by THF-SEC with RI detector against PMMA standards. (Molar ratio RAFT agent/AIBN 5:1, 65 °C, 300 rpm stirring rate, 5 mL of 2-MeTHF)

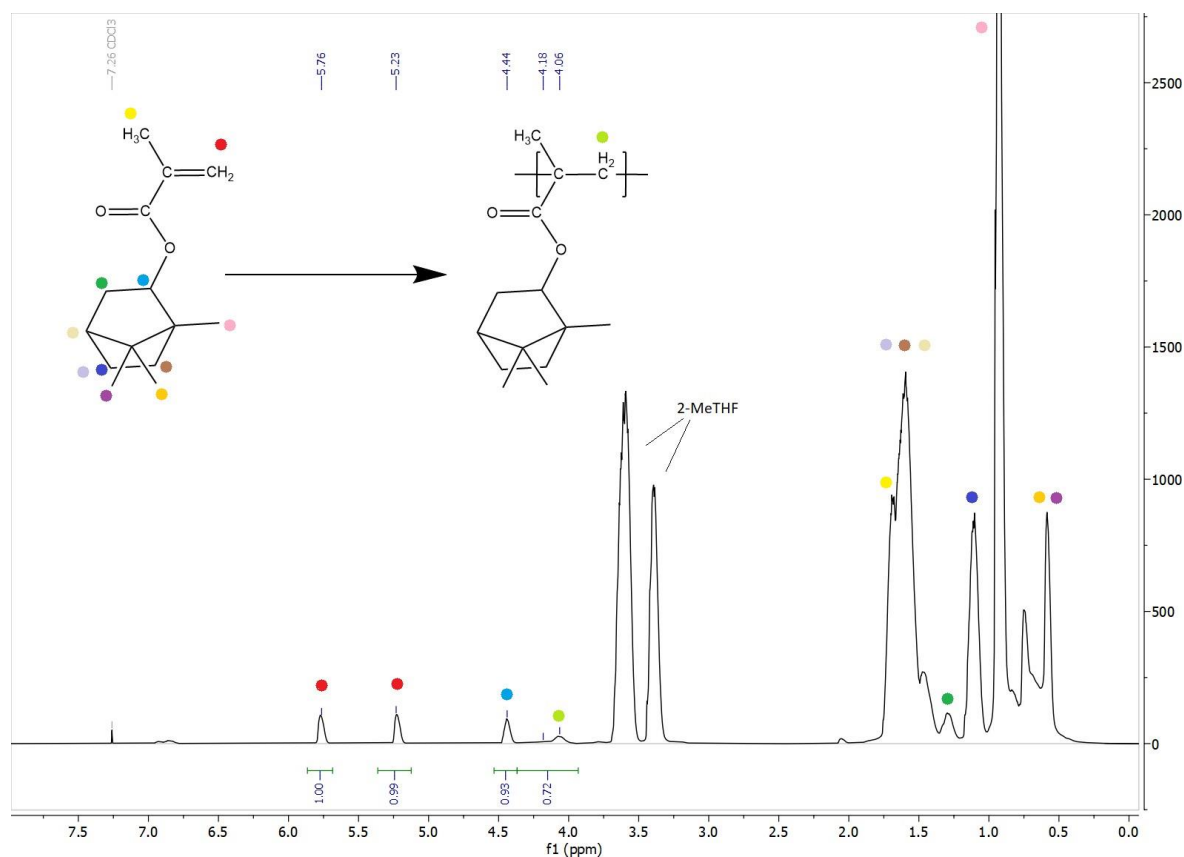


Figure 3.13 ^1H NMR of PIBMA (400 MHz, CDCl_3) – Appendix 7.5

The ^1H NMR of P α -PM (figure 3.14) before precipitation showed the appearance of the peak at 4.18ppm, this confirms that the polymerisation has occurred. This is also in conjunction with the reduction of the red doublet peaks at 5.76 and 5.23ppm, which is the monomer proton.

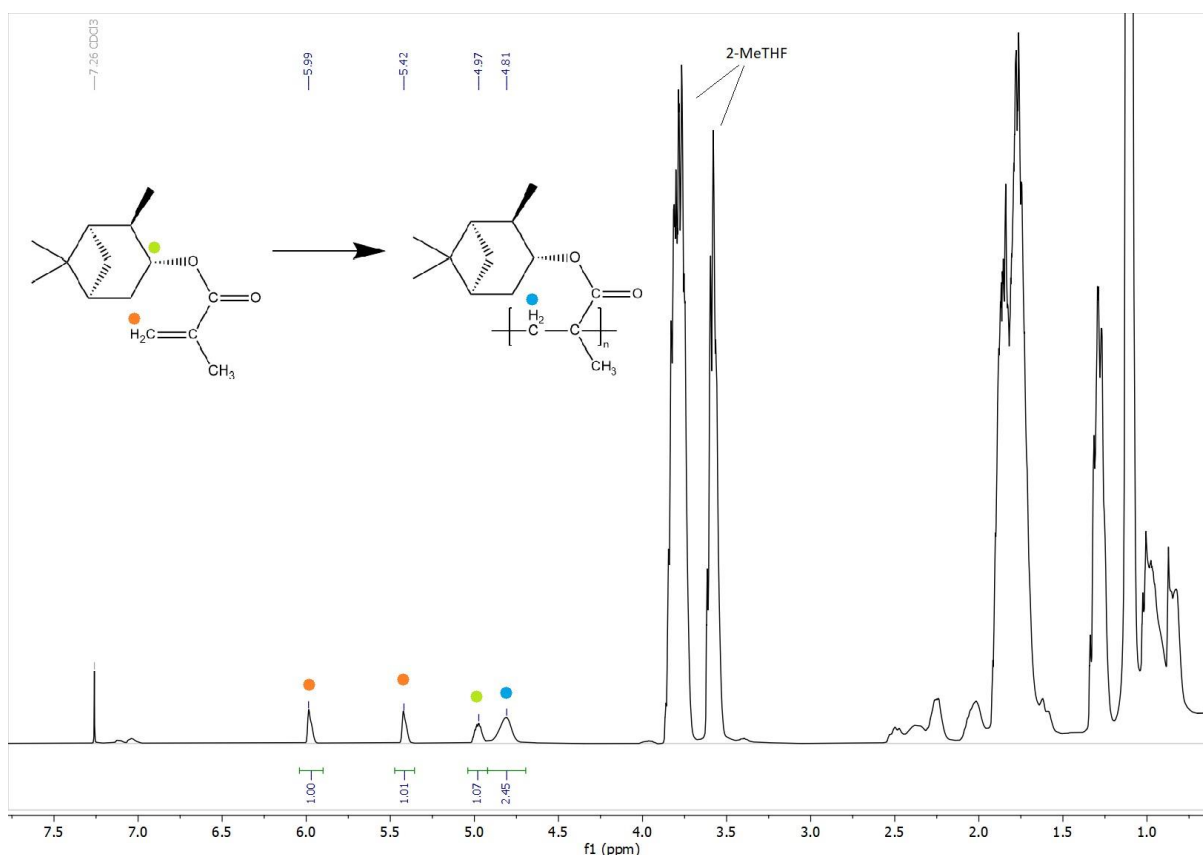


Figure 3.14 ^1H NMR of P α -PM (400 MHz, CDCl_3) – Appendix 7.6

The GPC data showed that the dispersity of PMMA ($\mathcal{D} = 1.13$) was lower than the terpene-based poly(isobornyl methacrylate) ($\mathcal{D} = 1.21$) and poly(α -pinene methacrylate) ($\mathcal{D} = 1.22$), however the value for the dispersity is still within an acceptable limit for RAFT polymerisation for the terpene-based polymers, as the dispersity must be below 1.3.

To find the T_g of the known high T_g polymers DSC and DMA analysis were used (table 3.13).

Table 3.13 T_g values for PMMA, PIBMA and P α -PM

Polymer	T_g (DSC) ^{gg}	T_g (DMA) ^{hh}	M_n
PMMA	105	133.3	8500
PIBMA	104	109.3	11000
P α -PM	104	125.8	17000

The similarity between the DSC T_g values of PMMA and that of the terpene-based PIBMA and P α -PM indicates that these polymers can be used as substitutes for PMMA. The value of the T_g however was lower for IBMA than predicted in literature of up to 200°C,⁶⁶ this is likely due to the smaller chain length of the polymer as this can affect the T_g of a polymer.^{136,137} The T_g value obtained from the DMA is higher than the T_g value from the DSC, the differences that can be observed between the two analyses, are due to the intrinsic difference between the static DSC and the dynamic DMA measurement, resulting in the DSC observed T_g s being lower in absolute values.^{138,139} The DMA of the high T_g homopolymers is shown (figure 3.15).

^{gg} T_g (°C) obtained from DSC with heating range of 0 to 200°C with a heating rate of 10°C min⁻¹ ^{hh} T_g (°C) obtained from DMA with heating range of 20 to 200°C measured at 1 and 10 Hz

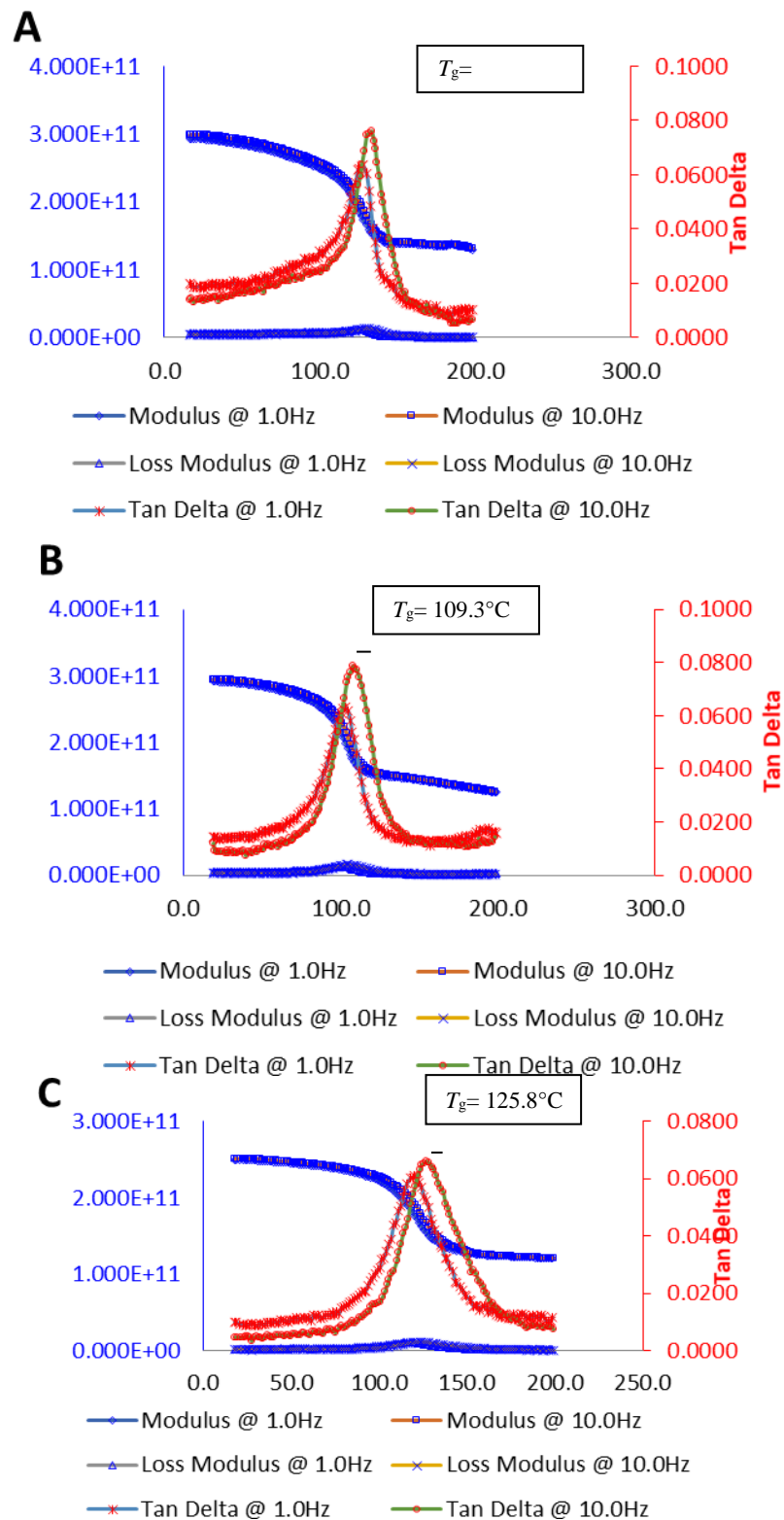


Figure 3.15 The DMA of (A) PMMA, (B) PIBMA and (C) P α -PM.

3.8.2 Homopolymerisation of THGA in 2-MeTHF

THGA was polymerised using 2-MeTHF as the solvent to ensure that this monomer was compatible with the solvent to allow for further polymerisations. The conversion was determined by ^1H NMR was shown to be 93%, which is higher than the conversion obtained in toluene with CPAB of 66% (3.2.2). The results from the GPC showed a high dispersity value of 2.45. This is likely due to branching which was also present in the polymerisation in toluene.³⁴

Thermal analysis of this homopolymer was not obtained due to not enough of the sample available for analysis due to an error in the precipitation of the polymer, however, as the M_n is 9500 kg mol^{-1} and the polymer likely has some branching, it can be assumed that the T_g is similar to the previously obtained T_g value of -62°C , as determined in 3.2.2.

3.9 Random copolymers of High T_g monomers with butyl acrylate in 2-MeTHF

Random copolymers were produced using terpene-based high T_g monomer combined with butyl acrylate to ensure that the terpene-based monomers had similar reactivity to MMA when combined as a random copolymer. The conversion was calculated from the ^1H NMR and the values obtained from the GPC for the molecular weight and dispersity (table 3.14).

Table 3.14 The conversion, actual target molecular weight and the target molecular weight and dispersity of copolymerisation of butyl acrylate with high T_g monomers in 2-MeTHF.

Expt.	High T_g monomer	Low T_g monomer	high T_g monomer conv. ⁱⁱ (%)	low T_g monomer conv. ⁱⁱ (%)	$M_{n,th}^{ij}$	M_n^{kk}	\bar{D}^{kk}
BJ58	MMA	Butyl acrylate	37	20	50000	10000	2.54
BJ59	IBMA	Butyl acrylate	64	10	43000	11000	1.34
BJ60	α -PM	Butyl acrylate	53	20	33000	11000	1.34

ⁱⁱ Conversion calculated from ^1H NMR.

^{ij} Theoretical M_n calculated relative to RAFT AGENT and monomer concentration, relative to the actual conversion and given in kg mol^{-1} .

^{kk} \bar{D} and M_n (in kg mol^{-1}) obtained by THF-SEC with RI detector against PMMA standards. (Molar ratio RAFT AGENT/AIBN 5:1, 65°C , 300 rpm stirring rate, 5 mL of 2-MeTHF)

In all the random copolymers, the conversion of butyl acrylate is lower than the conversion of the high T_g monomers. This may be due to butyl acrylate having a smaller reactivity ratio than the high T_g monomers. In toluene, is for MMA (r_M) and BA (r_B) known to be $r_M = 2.17$ and $r_B = 0.42$.¹²⁷ However, the solvent can affect the reactivity ratio.¹⁴⁰ The results from the ^1H NMR of the random copolymers suggests that in 2-MeTHF the reactivity of α -PM is lower than that of IBMA, as the conversion of P α -PM is lower than that of PIBMA.

The GPC results from the random copolymers showed that the IBMA and α -PM copolymers had low dispersity, however, as the dispersity value was slightly above 1.3, this indicates that some RAFT control has been lost. The high dispersity value for the random copolymer of MMA and butyl acrylate is believed to have been caused by an anomalous result, previous reports have given this copolymer a dispersity of 1.2.¹⁴¹ Due to time constraints, this reaction could not be further explored. The T_g of the random copolymers was investigated using DSC (table 3.15).

Table 3.15 the DSC results for the random copolymers.

High T_g monomer	Low T_g monomer	T_g
MMA	Butyl acrylate	-
IBMA	Butyl acrylate	57.85
α -PM	Butyl acrylate	47.43

The T_g value obtained from the DSC confirms that random copolymers have been produced as the copolymers only had one T_g value. The high T_g of the random copolymers was expected due to the composition of MMA ($T_g=105^\circ\text{C}$) being greater than the composition of THGA ($T_g=-46^\circ\text{C}$) and therefore the polymer chains can pack more tightly and raise the T_g of the random copolymers. The PIBMA-*ran*-PBA has the highest T_g due to this polymer having the lowest conversion of butyl acrylate, 10% compared to 20%. The PMMA-PBA sample could not be run due to an error in the precipitation however, the T_g of PMMA-*ran*-PBA in literature, has been shown to be 33.65°C with a 50:50 molar ratio of MMA to BA.¹⁴²

3.10 Block copolymers of High T_g monomers with butyl acrylate in 2-MeTHF

Block copolymers were produced using terpene based ‘hard’ blocks and butyl acrylate (BA) as the ‘soft’ block. This was carried out to find a terpene-based alternative to the original ‘hard’ block, MMA. Butyl acrylate was used originally to develop the copolymerisation strategies and to help conserve the THGA and ensure that the terpene based ‘hard’ blocks had similar reactivity to MMA when used with a ‘soft’ block such as butyl acrylate. The results from these polymerisations are shown (table 3.16).

Table 3.16 the results of the block copolymers of a high T_g monomer with BA.

Expt.	‘Hard’ block	‘soft’ block	‘hard’ block M_n^{mm}	‘soft’ block conv. ⁿⁿ	$M_{n,\text{th}}^{\text{oo}}$	M_n^{pp}	\bar{D}^{pp}
BJ61	MMA	BA	8500	16.67	1333	19000	1.80
BJ62	IBMA	BA	11000	22.48	1750	16000	2.04
BJ63	α -PM	BA	17000	19.35	1500	21000	1.37

^{ll} T_g ($^\circ\text{C}$) obtained from DSC with heating range of -90 to 200°C with a heating rate of $10^\circ\text{C min}^{-1}$

^{mmm} The M_n of homopolymers previously synthesised, obtained by THF-SEC with RI detector against PMMA standards. Given in kg mol^{-1} .

ⁿⁿ Conversion calculated from ^1H NMR.

^{oo} Theoretical M_n calculated relative to RAFT AGENT and monomer concentration, relative to the actual conversion and given in kg mol^{-1} .

^{pp} \bar{D} and M_n (in kg mol^{-1}) obtained by THF-SEC with RI detector against PMMA standards. (Molar ratio RAFT AGENT/AIBN 5:1, 65°C , 300 rpm stirring rate, 5 mL of 2-MeTHF)

The results from the GPC indicate, as the value for dispersity is above 1.3, that the RAFT polymerisation of the block copolymers was not well controlled. To ensure that this reaction proceeds via a more controlled RAFT polymerisation, further optimisation is required. The ^1H NMR indicated that low conversion of the butyl acrylate monomer had occurred however upon GPC analysis, it showed that the polymer M_n had increased by a larger amount than expected. This could have occurred by some unreacted monomer still being present, as shown by the residual monomer peaks in the ^1H NMR (figure 3.16).

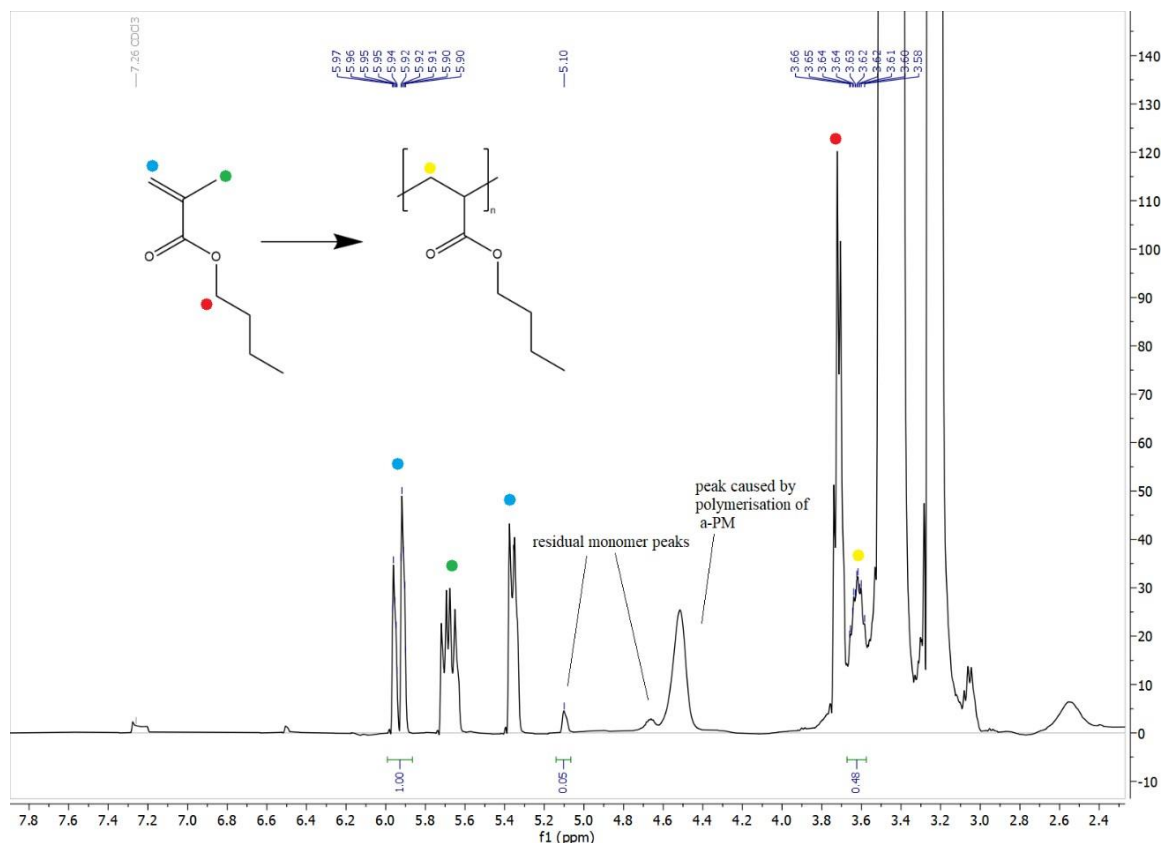


Figure 3.16 the labelled ^1H NMR of $P\alpha\text{-PM-}b\text{-PBA}$ (400 MHz, CDCl_3) – Appendix 7.7

Thermal analysis of these polymers was carried out to determine the T_g value for the block copolymers (table 3.17).

Table 3.17 the T_g of $\text{PMMA-}b\text{-PBA}$, $\text{PIBMA-}b\text{-PBA}$ and $P\alpha\text{-PM-}b\text{-PBA}$

‘Hard’ block	‘soft’ block	T_g
MMA	BA	74.14
IBMA	BA	66.36
$\alpha\text{-PM}$	BA	105.14

These block copolymers only showed T_g value which is believed to be an anomalous result as $\text{PMMA-}b\text{-PBA}$ has been previously shown in literature to exhibit two separate T_g s.^{143,144} This analysis showed that the polymer did not have two separate blocks, which could have been caused by the second block being composed of both butyl acrylate and the ‘high’ T_g monomer, and therefore not having two distinct blocks and this would mean that the polymer would show one value for the T_g . This may have occurred due to an error with the precipitation step of the homopolymer synthesis, allowing some monomer to remain trapped within the homopolymer chains. Therefore, to successfully produce block copolymers of $\text{PMMA-}b\text{-PBA}$, $\text{PIBMA-}b\text{-PBA}$ and $P\alpha\text{-PM-}b\text{-PBA}$, further optimisation is required.

^{qq} T_g ($^{\circ}\text{C}$) obtained from DSC with heating range of -90 to 200°C with a heating rate of $10^{\circ}\text{C min}^{-1}$

3.11 Fully terpene random copolymers in 2-MeTHF

To make a fully-terpene based random copolymer, THGA was combined with IBMA and α -PM in a 1:1 molar ratio. These polymerisations were carried out using 2-MeTHF as the solvent to ensure the polymerisation is as 'green' as possible (table 3.18).

Table 3.18 The results of the fully terpene-based random copolymers.

Expt.	High T_g monomer	High T_g monomer conv. ^{rr} (%)	THGA conv. ^{rr} (%)	$M_{n,th}^{ss}$	M_n^{tt}	\bar{D}^{tt}
BJ72	IBMA	53	47	32000	13000	1.65
BJ73	α -PM	73	57	20800	16000	2.21

The GPC analysis of the fully-terpene based random copolymers shows that both random copolymers showed higher than desired dispersity values of above 1.3. This indicates that the RAFT polymerisation was not controlled. However, the GPC chromatogram showed that the RAFT agent was connected to the polymer as they both eluted at the same time and so is unlikely that the high \bar{D} is due to RAFT agent incompatibility with 2-MeTHF. This conclusion is also supported by the disparity between the targeted M_n and the actual M_n that was recorded by the GPC. To achieve a narrower polydispersity, further optimisation of the reaction is required. However, due to time constrictions this could not be carried out within this project.

Thermal analysis was carried out on the random copolymers to determine the T_g . This was carried out by DSC and the results are shown (table 3.19). The T_g of the PIBMA-*ran*-PTHGA is slightly lower than expected, this is possibly due to a higher degree of branching of the THGA, causing more free volume in the polymer. The T_g value of P α -PM-*ran*-PTHGA is as expected as it has a similar value to the T_g of P α -PM-*ran*-PBA which supports the conclusion that PTHGA is a suitable replacement of the petrochemical-based BA.

Table 3.19 The results from the DSC of the fully-terpene based random copolymers.

High T_g monomer	Low T_g monomer	T_g^{rr}
IBMA	THGA	13.79
α -PM	THGA	43.79

3.12 The reactivity ratios of IBMA and THGA in 2-MeTHF

To determine the reactivity of PIBMA-*ran*-PTHGA copolymers, the reactivity ratio of these monomers was calculated. The random polymerisation of IBMA and THGA was studied at varying monomer compositions, these polymerisations were performed with CPAB as the RAFT agent and with 2-MeTHF as the solvent. The reaction was aimed at low conversion (ca. 10%) to study the propagation step of the polymerisation. The monomer composition and conversions are shown (table 3.20).

^{rr} Conversion calculated from ^1H NMR.

^{ss} Theoretical M_n calculated relative to RAFT AGENT and monomer concentration, relative to the actual conversion and given in kg mol^{-1} .

^{tt} \bar{D} and M_n (in kg mol^{-1}) obtained by THF-SEC with RI detector against PMMA standards. (Molar ratio RAFT AGENT/AIBN 5:1, 65 °C, 300 rpm stirring rate, 5 mL of 2-MeTHF)

^{uu} T_g (°C) obtained from DSC with heating range of -90 to 200°C with a heating rate of 10°C min⁻¹

Table. 3.20 monomer compositions and polymer compositions of the random copolymers of IBMA and THGA used for the reactivity ratio calculations.

IBMA ratio	THGA ratio	IBMA conv. ^{vv} (%)	THGA conv. ^{vv} (%)	Composition of IBMA in polymer. ^{ww} (%)
0.1	0.9	0.649	2.200	22.79
0.2	0.8	0.332	0.990	25.12
0.3	0.7	0.157	1.395	10.11
0.4	0.6	0.847	3.846	18.06
0.5	0.5	3.867	6.542	37.15
0.6	0.4	-	-	-
0.7	0.3	1.959	0	100.00
0.8	0.2	0.424	0	100.00
0.9	0.1	0.704	0	100.00

Using the terminal model and the Mayo-Lewis equation (equation 9), allowed the preference of one monomer to react over the other to be compared. These calculations were performed using Python. The reaction for $f=0.6$ was excluded as the ^1H NMR did not show any peaks for THGA, which was likely caused by an error in the experimental procedure for this reaction. The values were calculated for the reactivity ratio of α -PM and THGA (figure 3.17).

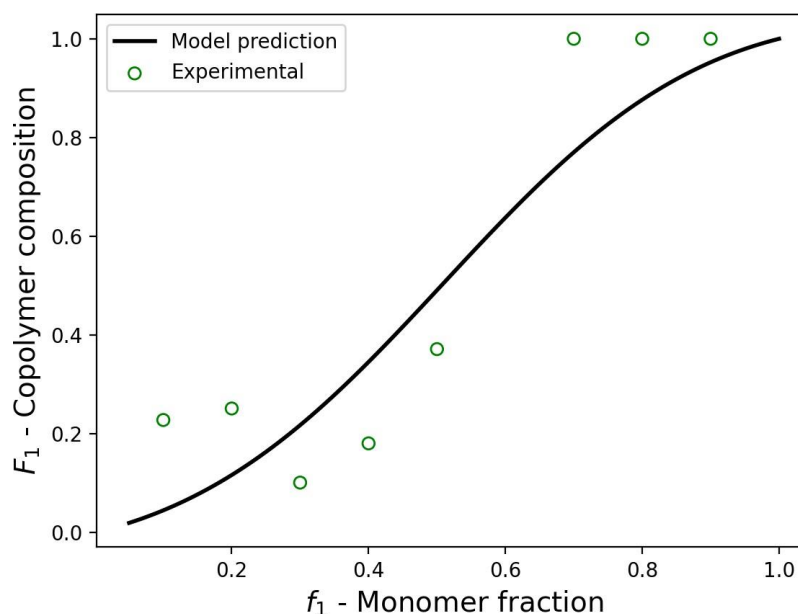


Figure 3.17 The reactivity ratio of IBMA and THGA

The model used to calculate the reactivity ratios as it was unable to adjust. The data collected from the reactivity ratio calculations indicate that this polymerisation occurs in a more block copolymer fashion than a random copolymer. However, to fully conclude that the reactivity ratios are correct, these calculations would likely need to be repeated with longer reaction times to get the conversion of the monomers closer to 10%, to ensure the propagation of the polymer can be studied.

^{vv} Conversion calculated from ^1H NMR.

^{ww} Composition determined by percentage of MMA present in random copolymer. Calculated by ^1H NMR.

3.13 The reactivity ratios of α -PM and THGA in 2-MeTHF

To determine the reactivity of α -PM-*ran*-PTHGA copolymers, the reactivity ratio of these monomers was calculated. The random polymerisation of α -PM and THGA was studied at varying monomer compositions, these polymerisations were performed with CPAB as the RAFT agent and with 2-MeTHF as the solvent. The reaction was aimed at low conversion (ca. 10%) to study the propagation step of the polymerisation. The monomer composition and conversions are shown (table 3.7).

Table. 3.21 monomer compositions and polymer compositions of the random copolymers of α -PM and THGA used for the reactivity ratio calculations.

α -PM ratio	THGA ratio	α -PM conv. ^{xx} (%)	THGA conv. ^{xx} (%)	Composition of THGA in polymer. ^{yy} (%)
0.1	0.9	0.405	9.785	96.03
0.2	0.8	-	-	-
0.3	0.7	0.067	1.801	96.43
0.4	0.6	1.316	10.928	89.25
0.5	0.5	1.220	7.097	85.34
0.6	0.4	0.150	0.794	84.10
0.7	0.3	0.250	0.737	74.68
0.8	0.2	-	-	-
0.9	0.1	0.233	0.442	65.53

Using the terminal model and the Mayo-Lewis equation (equation 9), allowed the preference of one monomer to react over the other to be compared. These calculations were performed using Python. The result from these calculations is shown in figure. The values for $f=0.2$ and $f=0.8$ were excluded as no polymerisation could be determined. The values were calculated for the reactivity ratio of α -PM and THGA (figure 3.18).

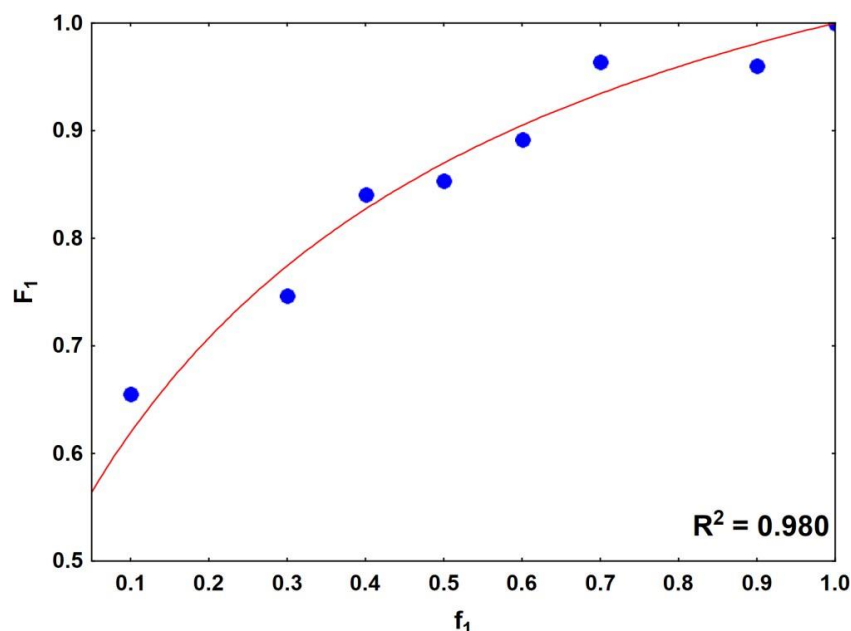


Figure 3.18 The reactivity ratio of α -PM and THGA. The blue circles indicate the experimental data collected and the red line shows the copolymer composition trend.

^{xx} Conversion calculated from ^1H NMR.

^{yy} Composition determined by percentage of MMA present in random copolymer. Calculated by ^1H NMR.

This calculation showed that THGA was acting as monomer 1, as this monomer made up the highest composition of the copolymer. The values obtained gave the reactivity ratio of THGA (r_T) and α -PM (r_A) as $r_T=5.686$ and $r_A=0.000167$. These values show that THGA is the more reactive monomer and as the value of r_T is much higher than 1, this indicates that the THGA is more inclined to react as a homopolymer than to produce a random copolymer. The value of below 1 for r_A indicates that α -PM will contribute a small amount to the overall composition of the copolymer. The R^2 value for this reactivity ratio calculation (figure 3.19) was also calculated.

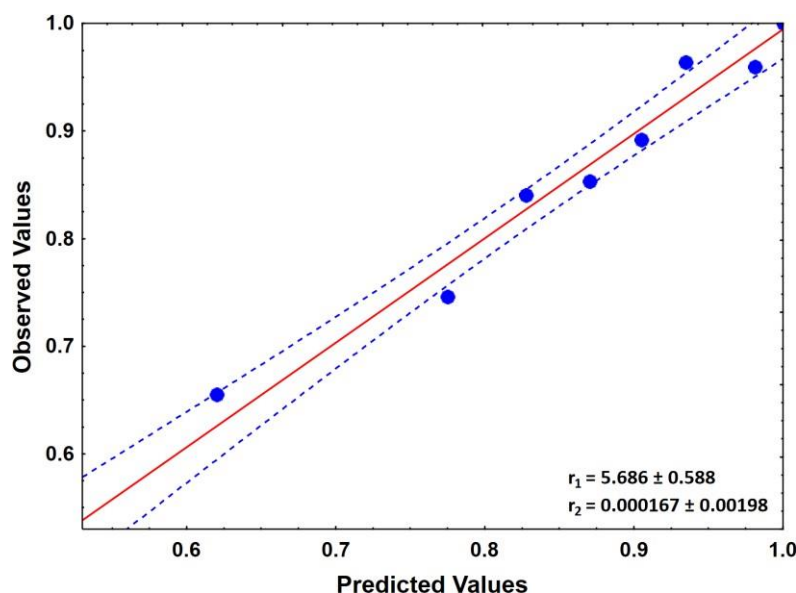


Figure 3.19 The R^2 values calculated for the reactivity ratios of α -PM and THGA. The blue points are the Mayo-Lewis model prediction (predicted values) against the experimental data (observed values). The red line corresponds to the linear regression prediction. The blue dashed lines indicate the regression bands built with a 95% confidence level.

However, to fully conclude that the reactivity ratios are correct, this experiment would likely need to be repeated with longer reaction times to get a higher conversion of the monomers and to ensure all data points can be collected.

3.14 Fully terpene block copolymers in 2-MeTHF

diblock copolymers of a terpene-based ‘hard’ block (IBMA and α -PM) and terpene-based ‘soft’ block THGA were produced. These polymerisations were carried out using 2-MeTHF as the solvent to ensure the polymerisation was as ‘green’ as possible. The results of the ^1H NMR and GPC are shown (table 3.22), the ‘soft’ block was targeted at 80 units of THGA.

Table 3.22 the results from the ^1H NMR and GPC of the fully-terpene block copolymers.

Expt.	‘Hard’ block	‘hard’ block M_n ^{zz}	‘soft’ block	‘soft’ block conv. ^{aaa} (%)	$M_{n,th}$ ^{bbb}	M_n ^{ccc}	\bar{D} ^{ccc}
BJ74	IBMA	11000	THGA	29	5000	16000	1.23
BJ75	α -PM	17000	THGA	30	5000	20000	1.21

^{zz} M_n (in kg mol^{-1}) from previous synthesis of homopolymers, obtained by THF-SEC with RI detector against PMMA standards. (Molar ratio RAFT AGENT/AIBN 5:1, 65 °C, 300 rpm stirring rate, 5 mL of 2-MeTHF) ^{aaa} Conversion calculated from ^1H NMR.

^{bbb} Theoretical M_n calculated relative to RAFT AGENT and monomer concentration, relative to the actual conversion and given in kg mol^{-1} .

^{ccc} \bar{D} and M_n (in kg mol^{-1}) obtained by THF-SEC with RI detector against PMMA standards. (Molar ratio RAFT AGENT/AIBN 5:1, 65 °C, 300 rpm stirring rate, 5 mL of 2-MeTHF)

The GPC data (figure 3.20) for the fully terpene block copolymers shows that a THGA block has been added successfully, as the molecular weight has increased, and showed only one peak. Therefore, the PMMA has been successfully extended as all polymer chains eluted at the same time. The dispersity values also indicate that both block copolymers were successfully RAFT polymerised as $D < 1.3$. The ^1H NMR shows that the conversion is around 30% for both block copolymers.

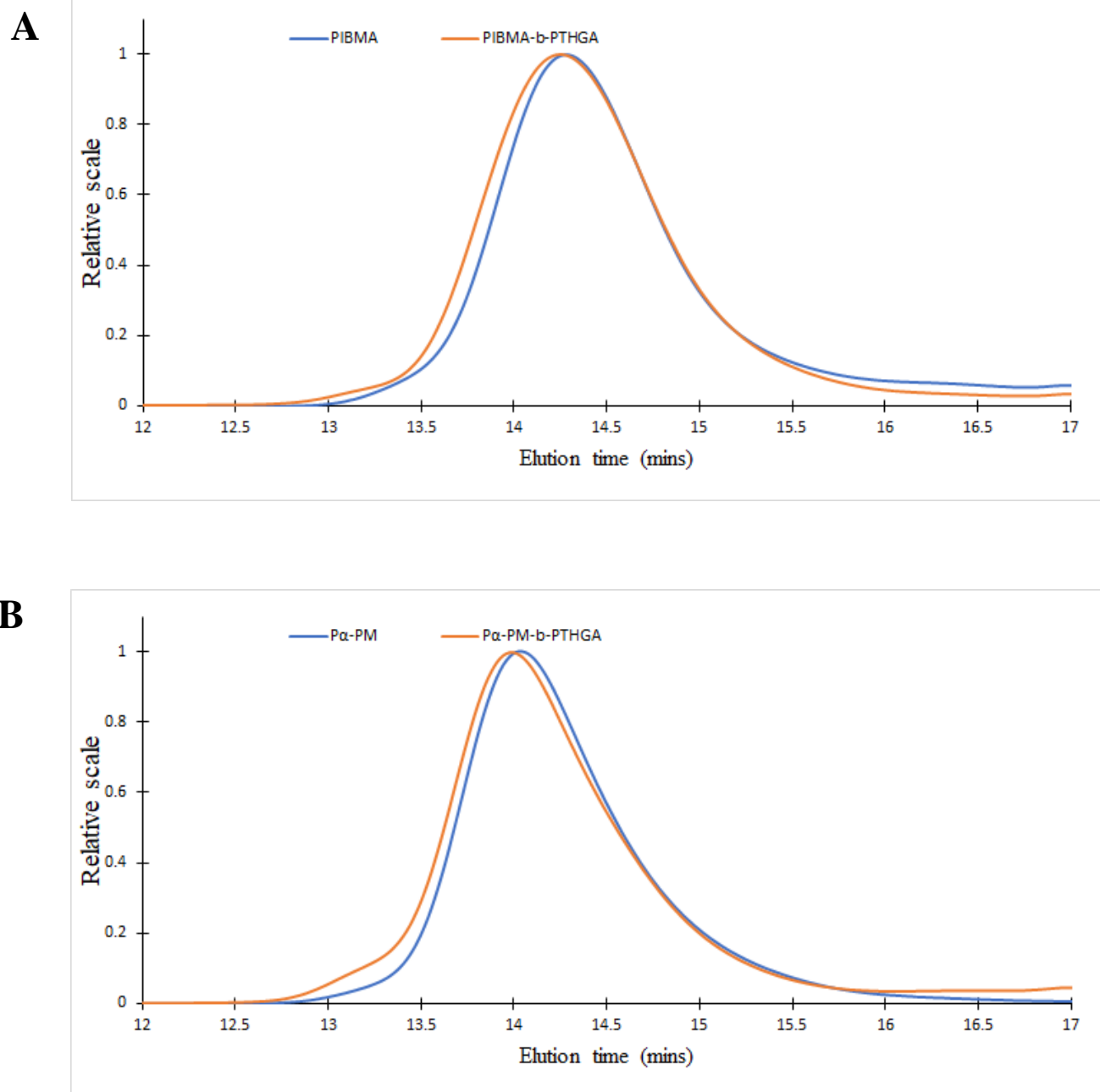


Figure 3.20 the GPC chromatograms for (A) PIMBA and PIMBA-*b*-PTHGA and (B) P α -PM and P α -PM-*b*-PTHGA showing the increase in M_n for the block copolymers indicating the THGA has been successfully added.

Thermal analysis using DSC of these polymers was carried out (table 3.23) which indicated only one T_g value for the polymers. In the case of the P α -PM-*b*-PTHGA polymer, this may be due to the THGA block being smaller than in comparison to the higher T_g block of P α -PM. The T_g of the PIBMA-*b*-PTHGA copolymer is lower than expected, this value indicates the possibility of the PIBMA and PTHGA blocks not being discrete. Therefore, this polymerisation requires optimisation to ensure the T_g of both blocks of the polymer can be identified.

Table 3.23. The results from the DSC of the fully-terpene based block copolymers.

Polymer	T_g^{ddd}
PIBMA- <i>b</i> -PTHGA	26.49
P α -PM- <i>b</i> -PTHGA	114.98

^{ddd} T_g ($^{\circ}\text{C}$) obtained from DSC with heating range of -90 to 200°C with a heating rate of $10^{\circ}\text{C min}^{-1}$

4. Conclusions

Before this project, THGA has only been studied in the block copolymerisation with styrene, therefore, all copolymers produced during this project are novel. In summary, THGA is a suitable terpene-based polymer for the replacement of low T_g polymers and can be used in RAFT polymerisation to produce polymers with a narrow polydispersity and targeted molecular weight.

Initially, terpene derived THGA was successfully synthesised by following a literature method at high yield, this monomer was used in a RAFT screening process to determine the most successful RAFT agent for the homopolymerisation of both MMA and THGA in toluene. The RAFT agents CPDT and CPAB were determined to be the most accurate, however as CPDT showed the best control for MMA, this RAFT agent was used for further polymerisations in toluene. Random copolymers of THGA and MMA were then produced in differing molar ratios to determine the change in T_g , using toluene as the solvent. Due to the difference between the conversion of MMA and THGA, the reactivity ratio of these monomers was then investigated. Diblock copolymers of MMA-THGA were then produced using MMA as the 'hard' block and THGA as the 'soft' block, these polymers showed two separate T_g s, which indicated that a diblock copolymer had been successfully produced.

To improve the greenness of the polymerisations, a different solvent was utilised for all further reactions. 2-MeTHF, which is a bio-based solvent, was screened against two different RAFT agents and two other solvents to show that the polymerisation of MMA in 2-MeTHF was comparable to the RAFT polymerisation of MMA in toluene. This indicated that the RAFT agent CPAB was a good fit for polymerisations in 2-MeTHF however, CPDT which was better in toluene was not compatible. To investigate why this was the case, the solubility of these RAFT agents in 2-MeTHF and toluene was tested at room temperature. The results of this indicated that solubility was not the cause of the incompatibility. The next effect tested was if any solvation effects were present in the polymerisation in 2-MeTHF. The polymerisation of MMA was completed using 2-MeTHF and toluene with both RAFT agents but at a higher temperature of 75°C. This showed that the higher temperature did improve the dispersity and targeted molecular weight for the polymerisation of MMA in 2-MeTHF with CPDT, however, the values were still above the range for a successful RAFT polymerisation. To determine which group of the RAFT agent was the cause of the incompatibility, two other RAFT agents were used. This indicated that the Z group of the RAFT agent was causing the incompatibility, as RAFT agents with an alkyl Z group, did not successfully undergo RAFT polymerisation, this is possibly due to the slight electron-withdrawing nature of alkyl groups.

Using the information provided by the RAFT agent screening in 2-MeTHF, the homopolymerisation of MMA, IBMA, α -PM and THGA were carried out using CPAB as the RAFT agent. These polymerisations were successful and showed that IBMA and α -PM were suitable high T_g terpene-based replacements for MMA. To ensure that these terpene-based alternatives could also be used for random and diblock copolymers, MMA, IBMA and α -PM were combined with the petrochemical monomer butyl acrylate in random and block copolymers. These produced polymers with high dispersity but only one T_g of the block copolymers, therefore this requires further optimisation.

The final stage of the project was to combine THGA with IBMA and α -PM into random and block copolymers. The block copolymers were successfully produced showing a good dispersity value, and accurate M_n , indicating that the RAFT polymerisation was successful. However, these polymers indicated only one T_g value and thus need to be further optimised, possibly with a larger THGA block to ensure two separate T_g values can be determined. The random copolymers showed a high dispersity value and inaccurate M_n , therefore indicating that this requires further optimisation to ensure that the RAFT polymerisation is successful. The P α -PM-ran-PTHGA polymer showed an expected T_g value, and this supports the conclusion that PMMA-PTHGA is a suitable terpene-based alternative for the random copolymers of the petrochemical based PMMA-PBA. The reactivity ratios of IBMA: THGA and α -PM: THGA were then calculated, and to be compared to the values from MMA. The reactivity ratios indicated that when THGA is combined in a copolymer with IBMA the polymer tends towards being blocky. However, when THGA is combined with α -PM in a copolymer, THGA is more likely to form a homopolymer but can also form random copolymers with α -PM, this reactivity ratio showed that THGA was the more reactive monomer. However, these reactivity ratios would likely need to be repeated to ensure that the conclusions determined from these results are correct.

5. Future work

5.1 Optimisation of reaction conditions

The polymerisation of THGA homopolymers in both solvents requires further optimisation to ensure that the polymer has as little branching as possible to give a smaller dispersity of below 1.3, this could be achieved by having a higher molar concentration of THGA in the solvent, as shown by Noppalit et al.³⁴ Similar optimisation is required for the PMMA-*b*-PTHGA as well as the random copolymers produced during this project. The blockcopolymers produced in 3.10 would also need to be repeated to ensure that two separate T_g s can be observed.

The reactivity ratio calculations for α -PM:THGA and IBMA:THGA would also need optimisation to ensure that the values are correct with a higher R^2 value. This would likely involve increasing the reaction times to ensure a higher conversion of monomer closer to 10%.

5.2 Further analysis of polymer

Due to time constraints and scope of the project, further analysis of these polymers could not be carried out. Other analysis techniques that would be useful for determining more properties of the polymers could include more techniques to determine the T_g of the polymers such as rheology, which studies the flow of the matter, thermogravimetric analysis (TGA), which measures weight changes as a function of temperature and time, as well as more DMA analysis.¹⁴⁵ Investigation into the free volume of the THGA polymers may also prove useful in determining the amount of branching in the polymer.¹⁴⁶ This further analysis would provide a better understanding and aid in determining future applications of these polymers.

5.3 Further investigation into RAFT agent compatibility in 2-MeTHF

To further the understanding of the RAFT agent's compatibility in 2-MeTHF, more tests are required to definitively conclude the cause of this, these tests could include introducing other RAFT agents with more electron-withdrawing Z groups to determine if this is the causing factor of the RAFT agent incompatibility with 2-MeTHF. As well as altering the phenyl Z group of CPAB by adding electron-withdrawing groups and electron-donating groups to investigate whether this affects the RAFT control of the polymerisation. Other possible causes of the CPDT being incompatible with 2-MeTHF could be investigated using more solubility studies using UV/Vis with more RAFT agents in a greater range of temperatures. Dynamic light scattering (DLS) could also be used to aid in this hypothesis.

5.4 The use of other green solvents

To greater improve the polymerisation of the fully terpene-based random and block copolymers, further investigation of solvents could prove useful to investigate whether an alternate solvent or supercritical fluid improves the conversion or dispersity of the polymers produced.¹⁰⁶ The use of supercritical CO₂ would be an excellent alternative to investigate due to the high conversion possible when compared to solution polymerisation. As polymerisations in supercritical CO₂ a medium for which dispersion polymerisation can occur. Dispersion polymerisation is a type of heterogeneous polymerisation, the polymer molecules would self-assemble into particles and therefore not require any more purification steps, removing a stage that is required from polymerisation in solution. This would make the polymerisation processes greener as it would remove the methanol required to precipitate the polymer from solution.

5.5 Making THGA in a greener way.

During this project, THGA was produced using a method from literature that required the use of DCM, triethylamine and acryloyl chloride, which are considered toxic. To make the polymerisation process as environmentally sustainable as possible, the acrylation of tetrahydro-geraniol would be required to be carried out by an alternative method. This can be achieved by using the T3P[®] catalyst which promotes the coupling therefore no longer requiring triethylamine. The DCM solvent also should be replaced as DCM is a carcinogen and is now believed to be ozone-depleting.⁹⁰ To replace DCM is more difficult as it is application dependent,⁹² however other less toxic solvents have been shown to act as an alternative to DCM such as lactate esters and Diethoxymethane (DEM or formaldehyde diethylactl).^{147,148} Although these solvents require a higher temperature for solvent removal, therefore making the process slightly less environmentally friendly.¹⁴⁹

6. References

- 1 N. Karak, *Fundamentals of Polymers: Raw Materials to Finish Products*, PHI, 2009.
- 2 B. D. Fairbanks, P. A. Gunatillake and L. Meagher, *Adv. Drug Deliv. Rev.*, 2015, **91**, 141–152.
- 3 H. Namazi, *BioImpacts*, 2017, **7**, 73–74.
- 4 F. S. Bates and G. H. Fredrickson, *Annu. Rev. Phys. Chem.*, 1990, **41**, 525–557.
- 5 K. Nishimori and M. Ouchi, *Chem. Commun.*, 2020, **56**, 3473–3483.
- 6 S. Beck and Ravin Narain, in *Polymer Science and Nanotechnology*, 2020, pp. 21–85.
- 7 J. K. Stille, *J. Chem. Educ.*, 1981, **58**, 862–866.
- 8 S. Capponi and F. Alvarez, , DOI:10.1021/acs.macromol.0c00472.
- 9 A. D. Jenkins, R. F. T. Stepto, P. Kratochvíl and U. W. Suter, *Pure Appl. Chem.*, 1996, **68**, 2287–2311.
- 10 R. B. Grubbs and R. H. Grubbs, *Macromolecules*, 2017, **50**, 6979–6997.
- 11 A. Bossion, K. V. Heifferon, L. Meabe, N. Zivic, D. Taton, J. L. Hedrick, T. E. Long and H. Sardon, *Prog. Polym. Sci.*, 2019, **90**, 164–210.
- 12 A. Calhoun, in *Multilayer Flexible Packaging (Second Edition)*, ed. J. R. Wagner, William Andrew Publishing, 2016, pp. 35–45.
- 13 P. Atkins, J. de Paula and J. Keeler, *Atkins' Physical Chemistry*, Oxford University Press, 11th edn., 2017.
- 14 A. Shrivastava, in *Introduction to Plastics Engineering*, 2018, pp. 17–48.
- 15 D. Braun, *Int. J. Polym. Sci.*, , DOI:10.1155/2009/893234.
- 16 D. McIntyre, *Characterisation*, 2015.
- 17 S. Beyazit, B. Tse Sum Bui, K. Haupt and C. Gonzato, *Prog. Polym. Sci.*, 2016, **62**, 1–21.
- 18 V. Mishra and R. Kumar, *J. Sci. Res. Banaras Hindu Univ.*, 2012, **56**, 141–176.
- 19 C. E. Federico, J. L. Bouvard, C. Combeaud and N. Billon, *Polymer (Guildf.)*, 2018, **139**, 177–187.
- 20 C. L. McCormick and A. B. Lowe, *Acc. Chem. Res.*, 2004, **37**, 312–325.
- 21 J. Chiefari, Y. K. Chong, F. Ercole, J. Krstina, J. Jeffery, T. P. T. Le, R. T. A. Mayadunne, G. F. Meijs, C. L. Moad, G. Moad, E. Rizzardo and S. H. Thang, *Macromolecules*, 1998, **31**, 5559–5562.
- 22 A. D. Jenkins, R. G. Jones and G. Moad, *Pure Appl. Chem.*, 2010, **82**, 483–491.
- 23 S. Perrier, *Macromolecules*, 2017, **50**, 7433–7447.
- 24 J. K. Oh, *J. Polym. Sci. Part A Polym. Chem.*, 2008, **46**, 6983–7001.
- 25 N. J. Warren and S. P. Armes, *J. Am. Chem. Soc.*, 2014, **136**, 10174–10185.
- 26 A. Veloso, W. García, A. Agirre, N. Ballard, F. Ruipérez, J. C. De La Cal and J. M. Asua, *Polym. Chem.*, 2015, **6**, 5437–5450.
- 27 M. Siau, B. S. Hawket and S. Perrier, *J. Polym. Sci. Part A Polym. Chem.*, 2012, **50**, 187–198.
- 28 M. Siau, B. S. Hawket and S. Perrier, *ACS Symp. Ser.*, 2012, **1101**, 13–25.
- 29 T. Properties, 2018, **44**, 1–6.
- 30 E. Penzel, J. Rieger and H. A. Schneider, *Polymer (Guildf.)*, 1997, **38**, 325–337.
- 31 D. A. Links, 2012, 1096–1108.
- 32 S. Rastogi, Y. Yao, D. R. Lippits, G. W. H. Höhne, R. Graf, H. W. Spiess and P. J. Lemstra, *Macromol. Rapid Commun.*, 2009, **30**, 826–839.
- 33 C. T. Lo, Y. Abiko, J. Kosai, Y. Watanabe, K. Nakabayashi and H. Mori, *Polymers (Basel).*, , DOI:10.3390/polym10070721.
- 34 S. Noppalit, A. Simula, L. Billon and J. M. Asua, *Polym. Chem.*, 2020, **11**, 1151–1160.
- 35 A. C. Shi, *Prog. Theor. Phys.*, 2008, 64–70.
- 36 H. SUZUKI and Y. MURAOKA, *Bull. Inst. Chem. Res. Kyoto Univ.*, 1989, **67**, 47–53.
- 37 S. S. Ray and S. Reza, in *Nanostructured Immiscible Polymer Blends*, 2020, pp. 65–80.
- 38 N. P. Balsara, *Curr. Opin. Solid State Mater. Sci.*, 1999, **4**, 553–558.
- 39 H. S. Chan and K. A. Dill, *J. Chem. Phys.*, 1994, **101**, 7007–7026.
- 40 M. Fittipaldi, L. A. Rodriguez and L. R. Grace, *AIP Conf. Proc.*, , DOI:10.1063/1.4918393.
- 41 A. Gandini, *Macromolecules*, 2008, **41**, 9491–9504.
- 42 P. Gallezot, *Chem. Soc. Rev.*, 2012, **41**, 1538–1558.
- 43 K. Yao and C. Tang, *Macromolecules*, 2013, **46**, 1689–1712.
- 44 P. A. Wilbon, F. Chu and C. Tang, *Macromol. Rapid Commun.*, 2013, **34**, 8–37.
- 45 K. Chen and P. S. Baran, *Nature*, 2009, **459**, 824–828.
- 46 J. Omar, M. Olivares, I. Alonso, A. Vallejo, O. Aizpurua-Olaizola and N. Etxebarria, *J. Food Sci.*, 2016, **81**, 867–873.
- 47 M. Semsarilar and S. Perrier, *Nat. Chem.*, 2010, **2**, 811–820.
- 48 K. Satoh, M. Matsuda, K. Nagai and M. Kamigaito, *J. Am. Chem. Soc.*, 2010, **132**, 10003–10005.
- 49 A. Llevot, E. Grau, S. Carlotti, S. Grelier and H. Cramail, *Macromol. Rapid Commun.*, 2016, **37**, 9–28.
- 50 S. Noppalit, A. Simula, L. Billon and J. M. Asua, *Polym. Chem.*, , DOI:10.1039/c9py01667h.

- 51 M. R. Thomsett, T. E. Storr, O. R. Monaghan, R. A. Stockman and S. M. Howdle, *Green Mater.*, 2016, **4**, 115–134.
- 52 C. K. Williams and M. A. Hillmyer, *Polym. Rev.*, 2008, **48**, 1–10.
- 53 L. Averous, *Macromol. Chem. Phys.*, 2009, **210**, 890–890.
- 54 F. L. Hatton, *Polym. Chem.*, 2020, **11**, 220–229.
- 55 B. Maiti, S. Maiti and P. De, *RSC Adv.*, 2016, **6**, 19322–19330.
- 56 B. Maiti, U. Haldar, T. Rajasekhar and P. De, *Chem. - A Eur. J.*, 2017, **23**, 15156–15165.
- 57 J. Zhou, M. Wu, Q. Peng, F. Jiang, H. Pan, B. Wang, S. Liu and Z. Wang, *Polym. Chem.*, 2018, **9**, 2880–2886.
- 58 M. Nasiri and T. M. Reineke, *Polym. Chem.*, 2016, **7**, 5233–5240.
- 59 J. J. Gallager, M. A. Hillmyer and T. M. Reineke, *ACS Sustain. Chem. Eng.*, 2016, **4**, 3379–3387.
- 60 A. L. Holmberg, J. F. Stanzione, R. P. Wool and T. H. Epps, *ACS Sustain. Chem. Eng.*, 2014, **2**, 569–573.
- 61 A. L. Holmberg, N. A. Nguyen, M. G. Karavolias, K. H. Reno, R. P. Wool and T. H. Epps, *Macromolecules*, 2016, **49**, 1286–1295.
- 62 M. F. Sainz, J. A. Souto, D. Regentova, M. K. G. Johansson, S. T. Timhagen, D. J. Irvine, P. Buijsen, C. E. Koning, R. A. Stockman and S. M. Howdle, *Polym. Chem.*, 2016, **7**, 2882–2887.
- 63 A. Agirre, J. Nase, E. Degrandi, C. Creton and J. M. Asua, *Macromolecules*, 2010, **43**, 8924–8932.
- 64 S. S. Baek, S. H. Jang and S. H. Hwang, *J. Ind. Eng. Chem.*, 2017, **53**, 429–434.
- 65 A. A. Waghmare, R. M. Hindupur and H. N. Pati, *Rev. J. Chem.*, 2014, **4**, 53–131.
- 66 J. M. Yu, P. Dubois and R. Jérôme, *Macromolecules*, 1996, **29**, 7316–7322.
- 67 C. Volzone, O. Masini, N. Alejandra, L. Myriam, E. Natalia and M. Isabel, 2001, **214**, 213–218.
- 68 H. T. H. Nguyen, P. Qi, M. Rostagno, A. Feteha and S. A. Miller, *J. Mater. Chem. A*, 2018, **6**, 9298–9331.
- 69 B. Zhang, Y. Ma, D. Chen, J. Xu and W. Yang, *J. Appl. Polym. Sci.*, 2013, **129**, 113–120.
- 70 F. Hajiali, A. Métafiot, L. Benitez-Ek, L. Alloune and M. Marić, *J. Polym. Sci. Part A Polym. Chem.*, 2018, **56**, 2422–2436.
- 71 D. Ramyadevi, K. S. Rajan, B. N. Vedhahari, K. Ruckmani and N. Subramanian, *Colloids Surfaces B Biointerfaces*, 2016, **146**, 260–270.
- 72 S. Il Park, S. I. Lee, S. J. Hong and K. Y. Cho, *Macromol. Res.*, 2007, **15**, 418–423.
- 73 C. Barner-Kowollik, Ed., *Handbook of RAFT Polymerization*, Wiley-VCH Verlag, 2008.
- 74 P. B. Zetterlund, Y. Kagawa and M. Okubo, *Chem. Rev.*, 2008, **108**, 3747–3794.
- 75 G. L. Li, H. Möhwald and D. G. Shchukin, *Chem. Soc. Rev.*, 2013, **42**, 3628–3646.
- 76 M. Zong, K. J. Thurecht and S. M. Howdle, *Chem. Commun.*, 2008, 5942–5944.
- 77 J. M. DeSimone, E. E. Maury, Y. Z. Menceloglu, J. B. McClain, T. J. Romack and J. R. Combes, *Science* (80-), 1994, **265**, 356–359.
- 78 S. C. Thickett and R. G. Gilbert, *Polymer (Guildf.)*, 2007, **48**, 6965–6991.
- 79 P. A. Lovell and F. J. Schork, *Biomacromolecules*, 2020, **21**, 4396–4441.
- 80 P. Pladis and C. Kiparissides, in *Reference Module in Chemistry, Molecular Sciences and Chemical Engineering*, Elsevier, 2014.
- 81 W. Marciniak and D. Janusz, in *Comprehensive Analytical Chemistry*, Elsevier, 86th edn., 2019, pp. 17–40.
- 82 E. Vanzo, *J. Appl. Polym. Sci.*, 1972, **16**, 1867–1868.
- 83 M. Andrew G., in *Techniques and Instrumentation in Analytical Chemistry*, Elsevier, 2001, pp. 305–324.
- 84 M. Fernández-García, J. J. Martínez and E. L. Madruga, *Polymer (Guildf.)*, 1998, **39**, 991–995.
- 85 I. Teasdale, O. Brüggemann and H. Henke, *Polyphosphazenes for Medical Applications*, Walter de Gruyter GmbH & Co KG., 2020.
- 86 B. S. Gupta and M. Afshari, in *Handbook of Properties of Textile and Technical Fibres (Second Edition)*, Woodhead Publishing, 2018, pp. 545–593.
- 87 T. F. McKenna, A. Villanueva and A. M. Santos, *J. Polym. Sci. Part A Polym. Chem.*, 1999, **37**, 571–588.
- 88 W. K. Czerwinski, D. Kunststoff-institut and D.- Darmstadt, *Makromol. Chem., Theory Simul.*, 1993, **2**, 577–585.
- 89 G. Englezou, K. Kortsens, A. A. C. Pacheco, R. Cavanagh, J. C. Lentz, E. Krumins, C. Sanders-Velez, S. M. Howdle, A. J. Nedoma and V. Taresco, *J. Polym. Sci.*, 2020, **58**, 1571–1581.
- 90 P. J. Sánchez-Soto, M. A. Avilés, J. C. Del Río, J. M. Ginés, J. Pascual and J. L. Pérez-Rodríguez, *J. Anal. Appl. Pyrolysis*, 2001, **58–59**, 155–172.
- 91 Guidance on REACH, <https://echa.europa.eu/guidance-documents/guidance-on-reach>, (accessed 13 June 2021).
- 92 F. P. Byrne, S. Jin, G. Paggiola, T. H. M. Petchey, J. H. Clark, T. J. Farmer, A. J. Hunt, C. Robert McElroy and J. Sherwood, *Sustain. Chem. Process.*, 2016, **4**, 1–24.
- 93 J. H. Clark, D. J. Macquarrie and J. Sherwood, *Green Chem.*, 2012, **14**, 90–93.
- 94 P. Kubisa, *Prog. Polym. Sci.*, 2004, **29**, 3–12.
- 95 S. Khandelwal, Y. K. Tailor and M. Kumar, *J. Mol. Liq.*, 2016, **215**, 345–386.
- 96 M. Doble and A. K. Kruthiventi, in *Green Chemistry and Engineering*, Elsevier, 2007, pp. 93–104.
- 97 Bio-based solvents on the rise, <https://www.biobasedpress.eu/2018/07/bio-based-solvents-on-the-rise/>,

(accessed 3 May 2021).

- 98 D. Prat, A. Wells, J. Hayler, H. Sneddon, C. R. McElroy, S. Abou-Shehada and P. J. Dunn, *Green Chem.*, 2015, **18**, 288–296.
- 99 V. Pace, P. Hoyos, L. Castoldi, P. Domínguez De María and A. R. Alcántara, *ChemSusChem*, 2012, **5**, 1369–1379.
- 100 D. Licursi, C. Antonetti, S. Fulignati, M. Giannoni and A. M. Raspolli Galletti, *Catalysts*, , DOI:10.3390/catal8070277.
- 101 V. Antonucci, J. Coleman, J. B. Ferry, N. Johnson, M. Mathe, J. P. Scott and J. Xu, *Org. Process Res. Dev.*, 2011, **15**, 939–941.
- 102 J. J. Bozell, L. Moens, D. C. Elliott, Y. Wang, G. G. Neuenschwander, S. W. Fitzpatrick, R. J. Bilski and J. L. Jarnefeld, *Resour. Conserv. Recycl.*, 2000, **28**, 227–239.
- 103 H. H. Khoo, L. L. Wong, J. Tan, V. Isoni and P. Sharratt, *Resour. Conserv. Recycl.*, 2015, **95**, 174–182.
- 104 B. Kamm, P. R. Gruber and M. Kamm, *Biorefineries-Industrial Process. Prod. Status Quo Futur. Dir.*, 2008, **1–2**, 1–959.
- 105 C. Stewart Slater, M. J. Savelski, T. M. Moroz and M. J. Raymond, *Green Chem. Lett. Rev.*, 2012, **5**, 55–64.
- 106 C. J. Clarke, W. C. Tu, O. Levers, A. Bröhl and J. P. Hallett, *Chem. Rev.*, 2018, **118**, 747–800.
- 107 N. Bensabeh, A. Moreno, A. Roig, O. R. Monaghan, J. C. Ronda, V. Cádiz, M. Galià, S. M. Howdle, G. Lligadas and V. Percec, *Biomacromolecules*, 2019, **20**, 2135–2147.
- 108 F. R. Mayo, F. M. Lewis and M. Lewis, *J. Am. Chem. Soc.*, 1944, **147**, 1594–1601.
- 109 J. T. Lai, D. Filla and R. Shea, *Am. Chem. Soc. Polym. Prepr. Div. Polym. Chem.*, 2002, **43**, 122–123.
- 110 G. Moad, E. Rizzardo and S. H. Thang, *Acc. Chem. Res.*, 2008, **41**, 1133–1142.
- 111 J. F. Baussard, J. L. Habib-Jiwan, A. Laschewsky, M. Mertoglu and J. Storsberg, *Polymer (Guildf.)*, 2004, **45**, 3615–3626.
- 112 M. R. Wood, D. J. Duncalf, P. Findlay, S. P. Rannard and S. Perrier, *Aust. J. Chem.*, 2007, **60**, 772–778.
- 113 D. Sugumaran, K. Juhanni and A. Karim, *eProceedings Chem.*, 2017, **2**, 1–11.
- 114 R. Greiner and F. R. Schwarzl, *Rheol. Acta*, 1984, 378–395.
- 115 H. Teng, K. Koike, D. Zhou, Z. Satoh, Y. Koike and Y. Okamoto, *J. Polym. Sci. Part A Polym. Chem.*, 2009, **47**, 315–317.
- 116 M. Mohammadi, H. fazli, M. karevan and J. Davoodi, *Eur. Polym. J.*, 2017, **91**, 121–133.
- 117 P. Zhang, J. Xin and J. Zhang, *ACS Sustain. Chem. Eng.*, 2014, **2**, 181–187.
- 118 F. Della Monica and A. W. Kleij, *Polym. Chem.*, 2020, **11**, 5109–5127.
- 119 R. L. Atkinson, O. R. Monaghan, M. Elsmore, P. D. Topham, D. T. W. Toolan, M. J. Derry, V. Taresco, R. A. Stockman, D. S. A. De Focatiis, D. J. Irvine and S. M. Howdle, *Polym. Chem.*, 2021, 34–50.
- 120 N. M. Ahmad, F. Heatley and P. A. Lovell, *Macromolecules*, 1998, **31**, 2822–2827.
- 121 N. Ballard, S. Hamzehlou and J. M. Asua, *Macromolecules*, 2016, **49**, 5418–5426.
- 122 M. Chenal, L. Bouteiller and J. Rieger, *Polym. Chem.*, 2013, **4**, 752–762.
- 123 S. Noppalit, A. Simula, N. Ballard, X. Callies, J. M. Asua and L. Billon, *Biomacromolecules*, , DOI:10.1021/acs.biomac.9b00185.
- 124 X. Luo, S. Xie, J. Liu, H. Hu, J. Jiang, W. Huang, H. Gao, D. Zhou, Z. Lü and D. Yan, *Polym. Chem.*, 2014, **5**, 1305–1312.
- 125 H. Daimon, H. Okitsu and J. Kumanotani, *Polym. J.*, 1975, **7**, 460–466.
- 126 F. M. Lewis, C. Walling, W. Cummings, E. R. Briggs and F. R. Mayo, *J. Am. Chem. Soc.*, 1948, **70**, 4277.
- 127 A. S. Brar and S. Kaur, *Polym. J.*, 2005, **37**, 316–323.
- 128 K. Matyjaszewski, M. J. Ziegler, S. V. Arehart, D. Greszta and T. Pakula, *J. Phys. Org. Chem.*, 2000, **13**, 775–786.
- 129 D. Zhang, *Am. Stat.*, 2017, **71**, 310–316.
- 130 J. P. Barrett, 2016, **28**, 19–20.
- 131 L. Saunders, R. Russell and D. Crabb, *Investig. Ophthalmol. Vis. Sci.*, 2012, **53**, 6830–6832.
- 132 A. Pellis, F. P. Byrne, J. Sherwood, M. Vastano, J. W. Comerford and T. J. Farmer, *Green Chem.*, 2019, **21**, 1686–1694.
- 133 C. Barner-Kowollik, M. Buback, B. Charleux, M. L. Coote, M. Drache, T. Fukada, A. Goto, B. Klumperman, A. B. Lowe, J. B. Mcleary, G. Moad, M. J. Monteiro, R. D. Sanderson, M. P. Tonge and P. Vana, *J. Polym. Sci. Part A Polym. Chem.*, 2006, **44**, 5809–5831.
- 134 S. R. S. Ting, T. P. Davis and P. B. Zetterlund, *Macromolecules*, 2011, **44**, 4187–4193.
- 135 M. Benaglia, E. Rizzardo, A. Alberti and M. Guerra, *Macromolecules*, 2005, **38**, 3129–3140.
- 136 K. O'Driscoll and R. Amin Sanayei, *Macromolecules*, 1991, **24**, 4479–4480.
- 137 K. Satoh, H. Sugiyama and M. Kamigaito, *Green Chem.*, 2006, **8**, 878–88.
- 138 G. Laye, S. B. Warrington, G. R. Heal, D. M. Price, R. Wilson and P. Haines, *Principles of thermal analysis and calorimetry*, Royal Society of Chemistry, 2002.
- 139 D. M. O'Brien, R. L. Atkinson, R. Cavanagh, A. A. C. Pacheco, R. Larder, K. Kortsen, E. Krumins, A. J.

Haddleton, C. Alexander, R. A. Stockman, S. M. Howdle and V. Taresco, *Eur. Polym. J.*, , DOI:10.1016/j.eurpolymj.2020.109516.

140 A. Kaim and P. Oracz, *Polymer (Guildf)*., 1999, **40**, 6925–6932.

141 L. Emiliani, The University of Hesinki, 2014.

142 M. Fernández-Garcia, R. Cuervo-Rodriguez and E. L. Madruga, *J. Polym. Sci. Part B Polym. Phys.*, 1999, **37**, 2512–2520.

143 D. A. Shipp, J. L. Wang and K. Matyjaszewski, *Macromolecules*, 1998, **31**, 8005–8008.

144 M. N. Nguyen, Q. T. Pham, V. D. Le, T. B. V. Nguyen, C. Bressy and A. Margailan, *Asian J. Chem.*, 2018, **30**, 1125–1130.

145 N. P. Cheremisinoff, *Polymer Characterization: Laboratory Techniques and Analysis*, William Andrew Publishing, 1996.

146 P. M. Budd, N. B. McKeown and D. Fritsch, *J. Mater. Chem.*, 2005, **15**, 1977–1986.

147 N. W. Boaz and B. Venepalli, *Org. Process Res. Dev.*, 2001, **5**, 127–131.

148 L. Lomba, E. Zuriaga and B. Giner, *Curr. Opin. Green Sustain. Chem.*, 2019, **18**, 51–56.

149 Fisher Scientific, Solvent alternatives for green chemistry.

7. Appendix

7.1 NMR of THGA

¹H NMR (400 MHz, CDCl₃, 25°C) δ (ppm): 6.40 (dd, *J* = 17.3, 1.5 Hz, 1H, H1), 6.13 (q, *J* = 17.3, 10.4 Hz, 1H, H2), 5.82 (dd, *J* = 10.4, 1.5 Hz, 1H, 1'H), 4.20 (s, 2H, H5), 1.78 – 1.65 (m, 1H, H11), 1.64 – 1.42 (m, 3H, H6,7), 1.37 – 1.26 (m, 4H, H9,10), 1.20 – 1.08 (m, 4H, H6,8), 0.99 – 0.80 (m, 9H, H12,13,14).

¹³C NMR (101 MHz, CDCl₃, 25°C) δ (ppm): 166.2 (C3), 130.2 (C1), 128.7 (C2), 63.1 (C5), 39.2 (C10), 37.1 (C8), 35.5 (C6), 29.8 (C7), 27.9 (C11), 24.6 (C9), 22.6 (C12), 22.5 (C13), 19.4 (C14).

7.2 NMR of PMMA

¹H NMR (400 MHz, CDCl₃, 25°C) δ (ppm) : 6.18 (s, 1H), 5.63(s, 1H), 3.83 (s, 3H), 3.68 (s, 5H).

7.3 NMR of PTHGA

¹H NMR (400 MHz, CDCl₃, 25°C) δ: δ (ppm): 6.47 (dd, *J* = 17.3, 1.5 Hz, 1H), 6.19 (dd, *J* = 17.3, 10.4 Hz, 1H), 5.87 (dd, *J* = 10.4, 1.5 Hz, 1H), 4.27 (m, 2H), 4.14 (s, 7H),), 1.78 – 1.65 (m, 1H), 1.64 – 1.42 (m, 3H), 1.37– 1.26 (m, 4H), 1.20 – 1.08 (m, 4H), 0.99 – 0.80 (m, 9H).

7.4 NMR of PMMA-*ran*-PTHGA

¹H NMR (400 MHz, CDCl₃, 25°C) δ (ppm): 6.47 (dd, *J* = 17.3, 1.5 Hz, 1H), 6.19 (dd, *J* = 17.3, 10.4 Hz, 1H), 6.18(s, 1H), 5.87 (dd, *J* = 10.4, 1.5 Hz, 1H), 5.68 (s, 1H), 4.29 (m, 2H), 4.16 (s, 1H), 3.83 (s, 3H), 3.69 (s, 7H).

7.5 NMR of PIBMA

¹H NMR (400 MHz, CDCl₃, 25°C) δ (ppm): 6.09 – 5.96 (m, 1H), 5.48 (p, *J* = 1.7 Hz, 1H), 4.69 (dd, *J* = 7.7, 3.4 Hz, 1H), 4.30 (s, 1H), 3.98 – 3.79 (m, 11H), 3.67 (td, *J* = 8.0, 6.4 Hz, 6H).

7.6 NMR of Pα-PM

¹H NMR (400 MHz, CDCl₃, 25°C) δ (ppm): 5.99 (s 1H), 5.42 (s 1H), 4.97 (s 3H), 4.81 (s 1H).